VOLUME 36 SEPTEMBER 1958 NUMBER 9

Canadian Journal of Physics

Published by THE NATIONAL RESEARCH COUNCIL

OTTAWA CANADA

CANADIAN JOURNAL OF PHYSICS

(Formerly Section A, Canadian Journal of Research)

Under the authority of the Chairman of the Committee of the Privy Council on Scientific and Industrial Research, the National Research Council issues THE CANADIAN JOURNAL OF PHYSICS and five other journals devoted to the publication, in English or French, of the results of original scientific research. Matters of general policy concerning these journals are the responsibility of a joint Editorial Board consisting of: members representing the National Research Council of Canada; the Editors of the Journals; and members representing the Royal Society of Canada and four other scientific societies.

Manuscripts for publication should be submitted to Dr. H. E. Duckworth, Editor, Canadian Journal of Physics, Hamilton College, McMaster University, Hamilton, Ontario.

(For instructions on preparation of copy, see **Notes to Contributors** (inside back cover).)

Proof, correspondence concerning proof, and orders for reprints should be sent to the Manager, Editorial Office (Research Journals), Division of Administration and Awards, National Research Council, Ottawa 2, Canada.

Subscriptions, renewals, requests for single or back numbers, and all remittances should be sent to Division of Administration and Awards, National Research Council, Ottawa 2, Canada. Remittances should be made payable to the Receiver General of Canada, credit National Research Council.

The journals published, frequency of publication, and prices are:

Canadian Journal of Biochemistry and Physiology	Monthly	$3.00 a year
Canadian Journal of Botany	Bimonthly	$4.00 a year
Canadian Journal of Chemistry	Monthly	$5.00 a year
Canadian Journal of Microbiology	Bimonthly	$3.00 a year
Canadian Journal of Physics	Monthly	$4.00 a year
Canadian Journal of Zoology	Bimonthly	$3.00 a year

The price of regular single numbers of all journals is 75 cents.

CORRECTION

Canadian Journal of Physics, Vol. 36. On p. 803 the following illustration should appear above (*c*) and (*d*) in Fig. 2.

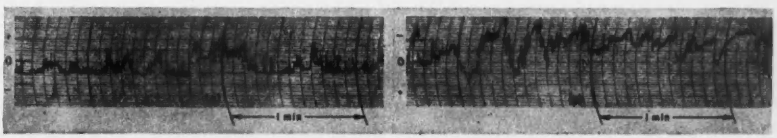

Canadian Journal of Physics

Issued by THE NATIONAL RESEARCH COUNCIL OF CANADA

VOLUME 36 SEPTEMBER 1958 NUMBER 9

LOW TEMPERATURE BEHAVIOR OF DEBYE CHARACTERISTIC TEMPERATURES[1]

G. K. HORTON[2] AND H. SCHIFF

ABSTRACT

The low temperature behavior of the characteristic Debye temperature is investigated using the six- and nine-direction Houston approximation and by way of illustration, the lattice dynamics of Born and Begbie (nearest neighbors only). We study the values of Θ_0 and B_2 for Cu, Au, Ag, Al, and Pb in the formula $\Theta_T = \Theta_0 [1 - B_2(T/\Theta_0)^2 \ldots]$. The existence in Pb of a shallow maximum before the usual minimum, found earlier by Bhatia and Horton, is confirmed. The method is quite general and may be used for non-metals and with other theoretical models.

The low temperature behavior of the characteristic Debye temperature was worked out in detail by Bhatia and Horton (1955).* Their method determined the values of the α_n's in the expansion of the frequency distribution function (Blackman 1955),

$$G(\omega) = V \sum_n \alpha_n \omega^{2n}. \tag{1}$$

The equivalent Debye temperature Θ_T at a temperature T is then given by

$$\Theta_T = \Theta_0 \sum_n B_{2n} \left(\frac{T}{\Theta_0}\right)^{2n}, \qquad (T \ll \Theta_0) \tag{2}$$

$$\text{where} \quad B_0 = 1, \quad B_2 = -(20\pi^2/21)(\alpha_2/\alpha_1)\left(\frac{k}{\hbar}\Theta_0\right)^2, \text{ etc.} \tag{3}$$

$$\text{and} \quad \Theta_0 = \left(\frac{9N_0}{\alpha_1}\right)^{1/3} \frac{\hbar}{k}. \tag{4}$$

The values of the α_n's may be obtained by using Houston's approximation (Houston 1948). This was done by Bhatia and Horton, who used Bhatia's lattice dynamical model (Bhatia 1955) to find the value of B_2 for a number of face-centered and one-body-centered cubic metal. They showed that the

[1]Manuscript received May 14, 1958.
Contribution from the University of Alberta, Edmonton, Alberta, Canada.

[2]Now at Solid State Section, Division of Pure Physics, National Research Council, Ottawa, Canada.

*Similar results may be found in Salter (1956).

steepness of the drop of the Θ_T vs. T curve for a given crystal could be understood in this way, in fact that for some crystals the drop was much steeper than for others; indeed it was found that for Pb, using room-temperature values of the elastic constants since no 0° K values were available, the Θ_T vs. T curve went through a shallow maximum before the usual minimum.

The effect of using a different lattice dynamical model, again using Houston's method, was investigated by Horton and Schiff (1956). They showed how the substitution of either the conventional two-neighbor central force model (Leighton 1948) or the nearest-neighbor non-central force model (Begbie and Born 1947) in place of the Bhatia model altered the conclusions of Bhatia and Horton; qualitatively they were unchanged. It seems certain that none of these models provides a particularly good description of any actual metal, but the broad similarity of many of the results obtained using different models suggests strongly that a further study of any one of them may throw light on the low-temperature behavior of crystals.

In this paper we report the effect on these earlier low-temperature results of using the various refinements of Houston's method that have been studied recently by Betts, Bhatia, and Wyman (1956) and by Betts (1958). We have chosen the Born and Begbie model for the present calculations, both because of its simplicity and because it appears more appropriate for the low-temperature description of metals than the equally simple central force theory (Horton and Schiff 1958). The results of our calculation are summarized in Table I.

TABLE I

THE VALUES OF THE PARAMETERS Θ_0 AND B_2 OCCURRING IN FORMULA (2) FOR THE LOW-TEMPERATURE DEBYE Θ_T

Metal	$-\sigma = 2-(c_{11}-c_{12})/c_{44}$	$\Theta_0^{(3)}$	$\Theta_0^{(6)}$	$\Theta_0^{(9)}$	$B_2^{(3)}$	$B_2^{(6)}$	$B_2^{(9)}$
Al	0.311*	427.71	428.14	428.13	17.35	15.77	15.82
Au	1.30†	155.43	162.77	162.19	6.327	4.480	5.155
Ag	1.33†	218.50	228.37	227.62	5.545	9.347	9.445
Cu	1.37‡	329.72	345.64	344.43	1.950	8.817	8.684
Pb	1.50§	82.98	89.98	89.38	−19.03	−3.647	−3.925

NOTE: The 0° K elastic constants were used in the following three references.

*Sutton (1953).

†Neighbours and Alers (1958). We would like to thank Dr. Alers for communicating his results to us before publication.

‡Gaffney and Overton (1954).

§The results for Pb were obtained using room-temperature values of the elastic constants. In order to make a rough estimate of the effect of 0° K constants we proceed as follows. Let us assume a *linear* temperature dependence, the *same for all the c's*. Further let the slope be chosen so as to yield the correct experimental $\Theta_0 = 94.5°$ K (Keesom and Pearlman 1956), using the six-term Houston formula, which is known to give a result accurate to better than 1%. It is then easy to show that the values of the B_2's are *unchanged*.

The parameter σ is a measure of the anisotropy of the metal, while $\Theta_0^{(3)}$, $\Theta_0^{(6)}$, $\Theta_0^{(9)}$, and the corresponding B_2's were obtained using the Houston three-, six-, and nine-direction approximations respectively, which may be found in the papers referred to earlier. The characteristic temperatures $\Theta_0^{(9)}$ agree to 0.1% with those evaluated by the method of Budzinski and Schiff (1957). The correctness of the B_2's may be gauged from the convergence exhibited in Table I. (The B_2's are made up of positive and negative contributions,

in contrast to Θ_0, which consists of positive contributions only. Consequently their convergence is correspondingly slower.) The Θ_0's could also be obtained from the numerical tables compiled by de Launay (1956). These tables cannot be used to look up the B_2's, though tables for the B_2's have been announced by Marcus and Kennedy (1958) for certain lattice dynamical models. The low-temperature behavior for the central force model has also been discussed by Leighton (1948).

The accuracy of the present approximations would seem to be sufficient to establish beyond reasonable doubt that the value of B_2 for Pb using this model and room-temperature elastic constants is indeed negative although it is now so small that it will be difficult to distinguish it experimentally from zero. A much larger *positive* value of B_2 has been reported by Dolecek (1955), but it does not seem to us that the experimental accuracy justifies a unique interpretation of his results. In particular Dolecek's values for γ and Θ_0 are higher than those estimated from other measurements (Keesom and Pearlman 1956); it is perhaps significant that with a lower value of γ, Dolecek's results would imply a lower value of both Θ_0 and B_2.

When using the three-direction Houston formula, different models were found to give similar results. This may be modified when a more realistic lattice dynamical model becomes available. One might hope, however, that the present models may not be too different from a correct model and hence that the results even for the Born and Begbie nearest-neighbor model may have some physical significance.

We would like to stress that our procedure is available for any model and may be applied to non-metals. The convergence seems sufficiently good to justify it for the analysis of the experimental results and to find the higher B's. In many cases the six-direction formula will give good results when the crystal is reasonably isotropic. For non-cubic crystals, to which our procedure is equally applicable, one can replace the Houston method by those developed by Betts, Bhatia, and Horton (1956).

ACKNOWLEDGMENTS

We should like to thank Messrs. P. Buckley, A. Cseuz, and J. Huston for help with the calculations. We should also like to thank Dr. Betts for making his nine-direction formula available to us in advance of publication. The $\Theta_0^{(9)}$ form part of a larger table to be published by him. It is a pleasure to acknowledge the financial assistance of the University of Alberta General Research Committee and the National Research Council of Canada.

REFERENCES

Begbie, G. H. and Born, M. 1947. Proc. Roy. Soc. A, **188**, 179.
Betts, D. D., Bhatia, A. B., and Horton, G. K. 1956. Phys. Rev. **104**, 42.
Betts, D. D., Bhatia, A. B., and Wyman, M. 1956. Phys. Rev. **104**, 37. Formula (2.48).
Betts, D. D. 1958. Private communication.
Bhatia, A. B. and Horton, G. K. 1955. Phys. Rev. **98**, 1715.
Bhatia, A. B. 1955. Phys. Rev. **97**, 363.
Blackman, M. 1955. Encyclopaedia of Physics, Vol. 7 (1) (Springer-Verlag, Berlin), p. 325.
Budzinski, E. and Schiff, H. 1957. Can. J. Phys. **35**, 507.

DE LAUNAY, J. 1956. Solid state physics, Vol. 2, (Academic Press Inc., New York), pp. 219–303.
DOLEČEK, R. L. 1955. Proceedings of the Low Temperature Conference, Paris. p. 300.
GAFFNEY, J. and OVERTON, W. C. 1954. Phys. Rev., **95**, 602.
HORTON, G. K. and SCHIFF, H. 1956. Phys. Rev. **104**, 32.
HORTON, G. K. and SCHIFF, H. 1958. Proc. Roy. Soc. In press.
HOUSTON, W. V. 1948. Revs. Modern Phys. **20**, 161.
KEESOM, P. H. and PEARLMAN, N. 1956. *In* Kittel, C. Introduction to solid state physics (J. Wiley and Sons, New York), p. 132.
LEIGHTON, R. B. 1948. Revs. Modern Phys. **20**, 165.
MARCUS, P. M. and KENNEDY, A. 1958. Bull. Am. Phys. Soc. II, **3**, 226.
NEIGHBOURS, J. R. and ALERS, G. A. 1958. Phys. Rev. In press.
SALTER, L. 1956. Unpublished Oxford dissertation.
SUTTON, P. M. 1953. Phys. Rev. **91**, 816.

THE FREEZING POINTS OF HIGH PURITY METALS AS PRECISION TEMPERATURE STANDARDS

IV. INDIUM: THERMAL ANALYSES ON THREE GRADES OF CADMIUM[1]

E. H. McLaren

ABSTRACT

An investigation of the freezing and melting temperatures of a sample of high purity indium (Cominco 99.999+ %) has been made. Plateaux of essentially constant ($< \pm$ 0.0001° C) temperature with durations for over 1 hour are readily obtained on the cooling curves of induced freezes on this metal. The standard deviation of the plateau temperature (liquidus point) from a series of 24 induced freezes was ±0.0001° C. The pressure effect on the freezing temperature of indium was found to be 0.0049° C for 1 atm. Alloy melting ranges were measured following different types of freezing.

An extensive intercomparison of liquidus points and alloy melting ranges has been made on a sample of 99.99% cadmium and two samples of 99.999+ % cadmium from different suppliers. The liquidus points of the high purity samples were indistinguishable using precision resistance thermometry but one sample melted over a slightly smaller range of temperature than the other. Both these samples showed minor arrests on melting curves after induced freezing and detailed analyses of the melting contours after various types of freezing indicated some evidence of characteristic structure inside a range of 0.002° C.

INTRODUCTION

A study of the liquid–solid transformation temperatures in a sample of high purity indium and comparative thermal analyses on three grades of high purity cadmium have been made. This work is part of a continuing investigation of the liquidus temperatures and alloy melting ranges of high purity metals to determine the suitability of metal freezing points as precision temperature standards and the usefulness of precision resistance thermometry to discriminate among high purity metals.

EXPERIMENTAL

Indium

The high purity indium was obtained from the Consolidated Mining and Smelting Company, Trail, B.C., Canada, and Table I shows a typical analysis of this material and an estimate of the expected depression of the liquidus point from that of the pure element. A 1.2-kg sample was used under a dry nitrogen atmosphere.

(*a*) *Thermal Analysis*

Following the techniques developed earlier to investigate the freezing and melting temperatures in high purity zinc, cadmium, and tin (McLaren 1957*a*, *b*, 1958), a similar series of thermal analyses was made on this indium sample.

[1]Manuscript received May 26, 1958.
Contribution from the Division of Applied Physics, National Research Council, Ottawa, Canada.
Issued as N.R.C. No. 4817.

TABLE I

TYPICAL IMPURITY CONTENT OF COMINCO* HIGH PURITY INDIUM

Impurity	Impurity content, p.p.m.	Estimated liquidus depression (° C)	Phase diagram
Zn	N.d.†	—	
Cd	1	0.0001	Valentiner (1943)
Pb	2	0.0001	Valentiner and Haberstroh (1938)
Bi	N.d.	—	
Ag	<1	<0.0005	Hellner (1951)
Cu	1	0.0003	Weibke and Eggens (1934)
		Total <0.0010	

*See Turner, Mitchell, and Bryan (1957).
†N.d.—not detected by routine spectrochemical analysis.

In this paper normal freezing refers to undisturbed natural solidification while induced freezing relates to a technique that is used to shorten the recalescent period. The latter is effected by freezing a thin mantle of metal on the axial thermometer-well after nucleation has commenced; this releases sufficient latent heat to raise the melt temperature to the liquidus temperature.

Figure 1 shows freezing curves that were obtained using three different freezing techniques, curves I, II, and III arising from very fast normal, very

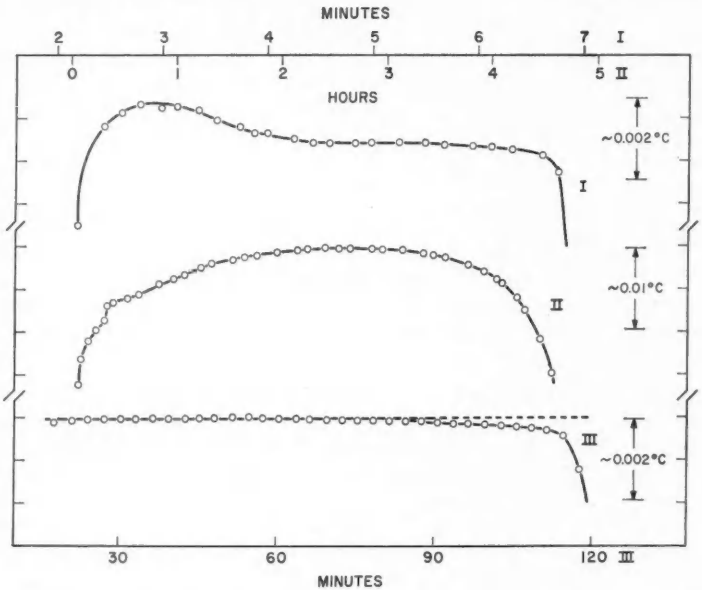

FIG. 1. Typical freezing curves on high purity indium: I, very fast normal; II, very slow normal; III, slow induced.

slow normal, and slow induced freezing respectively. The time scales on these plots begin at the end of the supercool which for the indium sample in the experimental arrangement used here amounted to about 0.07° C. These freezing curves are similar to those obtained with high purity zinc and cadmium; the plateaux developed on induced freezing vary less than 0.0001° C for periods depending on the gross rate of cooling of the furnace block; nucleation and recalescence, however, are measurably slower than in zinc and cadmium. Because of the slower recalescence in indium, temperature measurements may be made during the rise from supercool even on very fast freezes (see curve I, Fig. 1) and the sections of essentially constant temperature on the thermal curves of very slow normal freezes (curve II, Fig. 1) have very much shorter durations than are obtained on similar freezes of zinc and cadmium. To assist the melt to the liquidus point quickly on induced freezing it was found expedient to nucleate the freeze at a more rapid cooling rate than was required subsequently to obtain a slow induced freeze.

The tendency to a retarded recalescence in indium is most likely due to its smaller latent heat of fusion compared with those of zinc and cadmium.

The plateaux of nearly constant temperature that are obtained on slow induced freezes on this high purity indium provide an excellent index for a temperature standard and, as do the plateaux on slow induced freezes of zinc and cadmium, probably arise from extended liquidus arrests caused by coring as the sample solidifies.

Prior to determining the reproducibility of the plateau freezing temperature of this sample, we made extensive measurements of the alloy melting ranges following various types of freezing to gauge the thermal effects of the dis-

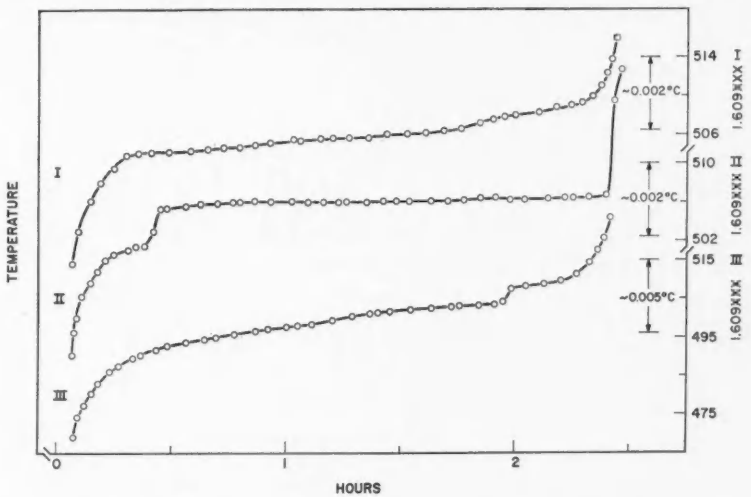

FIG. 2. Typical melting curves on high purity indium after: I, very fast normal freeze; II, slow induced freeze; III, very slow normal freeze.

solved impurities. Figure 2 shows the thermal curves obtained on remelting the ingot immediately after the corresponding freezes of Fig. 1. The melting curves after the very fast and the slow induced freezes (curves I and II, Fig. 2) show melting occurring over a few thousandths of a degree only, but after slow normal freezing significant melting takes place over a range of about 0.01° C (curve III, Fig. 2). The minor arrest on the remelting curve after induced freezing is probably due to a sharp segregation of impurities during the freeze; this segregation would account for the extremely flat major arrest on this melting curve. In contrast, the melting curve after the very slow normal freeze reveals that the impurities were received by the new solid during the slow recalescence over a broad range of temperatures and the small step near the liquidus break is the only evidence of heavy coring in the ingot.

Figure 3 shows derived inverse plots of melting curves obtained after five different types of freezing; Table II outlines the transformation conditions that existed for the group. In order to obtain a large number of points along

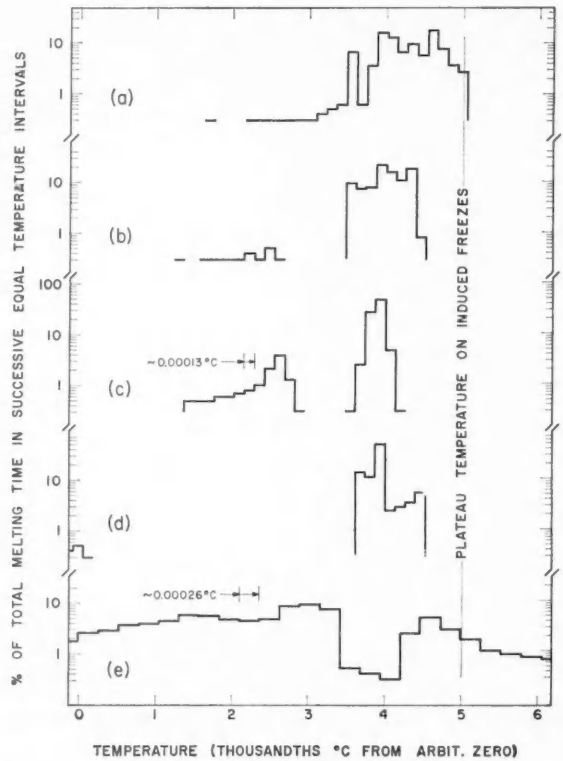

FIG. 3. Inverse melting curves on high purity indium after freezes of type (*a*) very fast normal, (*b*) fast normal, (*c*) slow induced, (*d*) slow normal, and (*e*) very slow normal.

each melting curve a shortened measurement technique was used with NR resistance balances at 2-ma current, single daily measurements at the triple

TABLE II

TRANSFORMATION CONDITIONS FOR THE MELTING CURVES OF FIG. 3

Type of freeze	Freezing curve	Freezing duration (minutes)	Solid anneal (minutes)	Melting* duration (minutes)	Melting curve (Fig. 3)	Total duration liquid to liquid (minutes)
Very fast	Fig. 1, I	7	66	147	(*a*)	220
Fast normal	—	55	95	155	(*b*)	305
Slow induced	Fig. 1, III	130	107	148	(*c*)	385
Slow normal	—	130	111	154	(*d*)	395
Very slow normal	—	310	45	145	(*e*)	500

*Total melting times of Fig. 3.

point of water, and approximate corrections for pressure over the melt.† For these reasons the difference indicated in Fig. 3 between the plateau temperature (liquidus point) obtained on induced freezes and the melting temperatures may be in error by as much as 0.0005° C. On the other hand relative errors along a particular curve due to slowly changing gas pressures over the melt would be less than 0.0001° C.

The histograms in Fig. 3 show a strong dependence on the thermal history of the sample. The width at the 1% level‡ for the main arrests varies from about 0.0005° C after induced freezing (curve (*c*)) to over 0.004° C after very slow normal freezing (curve (*e*)). The wider alloy melting range after the very slow unassisted freeze shows that significant amounts of solid are laid down over a wider spread in impurity concentration that was due to the slow recalescence and also probably due to some impurity diffusion in the solid during the long time interval in which the sample is held near its liquidus temperature.

These differences in melting ranges following different rates and types of freezing emphasize the importance of using similar thermal treatments when comparing samples on the basis of their alloy melting ranges.

(*b*) *Pressure Effect on the Freezing Temperature*

The effects of external pressure on the plateau freezing temperature of indium were experimentally determined and the results are shown in Fig. 4. The increase in the freezing temperature of indium with 1-atm gas pressure over the melt was 0.0049° C. An immersion of about 8 cm (of the mid-point of the sensing element of a Meyers thermometer) was required before the measured temperatures agreed within 0.0001° C of the variation deduced

†NR balances mean the average of the resistance balances obtained with the thermometer connected in the Normal and Reversed positions on the Mueller–Wheatstone bridge.

‡The width at the 1% level is an arbitrary melting range parameter and is simply the melting width at the 1% level on the histograms that are derived by determining the fraction of the total melting time spent in given temperature intervals from the direct time–temperature curves (McLaren 1958).

from the Clausius–Clapeyron relation. This latter variation is shown on the solid line on curve I and was calculated using the above measured gross pressure effect and a liquid density at the freezing point of 7.03 g/cc as determined by Williams and Miller (1950).

(*c*) *Reproducibility of Plateau Freezing Temperature*

Figure 5 shows results that were obtained on the reproducibility of the

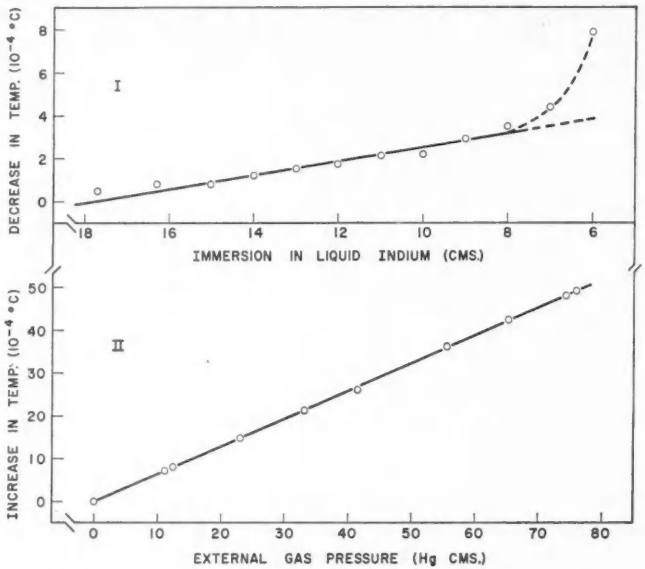

FIG. 4. Pressure effects on the plateau freezing temperature of indium.

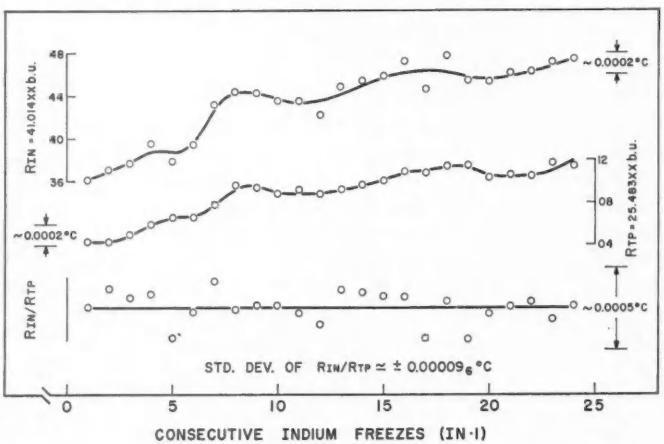

FIG. 5. Reproducibility of the plateau freezing temperature of high purity indium.

plateau freezing temperature (liquidus point) of this indium sample taken from a series of slow induced freezes carried out during a 3-week interval. R_{In} is the resistance of the thermometer at the plateau freezing temperature corrected to 1-atm gas pressure over the melt. The mid-point of the sensing element of the Meyers thermometer was immersed about 15 cm in the melt. R_{TP} is the average of the thermometer resistance at the triple point of water before and after the appropriate indium freeze. Both R_{In} and R_{TP} are zero current resistances corrected to unity bridge ratio and true bridge zero expressed in bridge units of resistance (McLaren 1957*a*).

A single water triple point cell was used throughout the investigation; one ice mantle covered the work on freezes 1–8 inclusive and another mantle was used for the remainder of the work. Prior to these measurements the thermometer was annealed at about 450° C to remove as much as possible of the added resistance due to accidental cold-working of the platinum, and additional overnight anneals were made after freeze numbers 8, 12, 15, and 19 respectively in order to maintain the thermometer in an annealed state.

The standard deviation of the ratio R_{In}/R_{TP} for the 24 induced freezes on this high purity indium was equivalent to $\pm 0.00009_6$° C.

Cadmium

Earlier work (McLaren 1957*b*) had shown that the liquidus point (321.032°C) of a sample of New Jersey Super Pure cadmium had a reproducibility and stability comparable with that of any precision-fixed point on the International Temperature Scale. Two additional samples of high purity cadmium have been provided by the Consolidated Mining and Smelting Company, one a sample of special high purity and the other a sample of normal high grade Tadanac cadmium. Extensive thermal analyses have been made on the three samples. This work soon resolved into an attempt to distinguish between the two samples of highest purity on the basis of either alloy-melting ranges following various freezing techniques or liquidus temperatures measured on induced freezes. Table III lists the samples and gives the available information on their impurity contents as supplied by the sources. Estimated depressions of the liquidus points from that of the pure element are <0.0013° C and

TABLE III

IMPURITY CONTENTS OF CADMIUM SAMPLES

Sample	Source and grade	Analysis	Impurity content* (p.p.m.)							
			Pb	Cu	Tl	Ag	Zn	Fe	Mg	Al
Cd.3	New Jersey Zinc Company, Super Pure	Typical	N.d.	V.f.	—	—	N.d.	N.d.	V.f.	V.f.
Cd.4	Consolidating Mining and Smelting Company, High purity No. 9521	Cd.4	1	<1	<1	N.d.	—	—	—	—
Cd.5	Consolidated Mining and Smelting Company, Tadanac	Typical	60	20	20	—	>50	—	—	—

*N.d.—not detectable in qualitative spectrochemical analysis. V.f.—"may be very faintly visible in the spectrogram but may represent electrode or atmospheric contamination rather than impurities in the metal"; E. A. Anderson, New Jersey Zinc Company, Palmerton, Pa., U.S.A.

$<0.046°$ C respectively for the impurity contents listed for samples Cd.4 and Cd.5. Sample Cd.3 was loaded in September, 1955, and has been used frequently for fixed point work since that time, while sample Cd.4 was loaded in November, 1957, especially for this comparison.

(*a*) *Thermal Analyses*

The three samples were allowed to transform under a variety of freezing conditions in order to make comparisons of the freezing curves and subsequent remelting curves.

Figure 6 shows the results of very fast freezing on the three samples; these freezes were made by extracting the pyrex tubes holding the crucibles of cadmium out of the furnaces and allowing the transformations to take place in the air. Although sample Cd.5 may be easily distinguished from the purer samples, it is immediately apparent that samples Cd.3 and Cd.4 have nearly the same impurity contents.

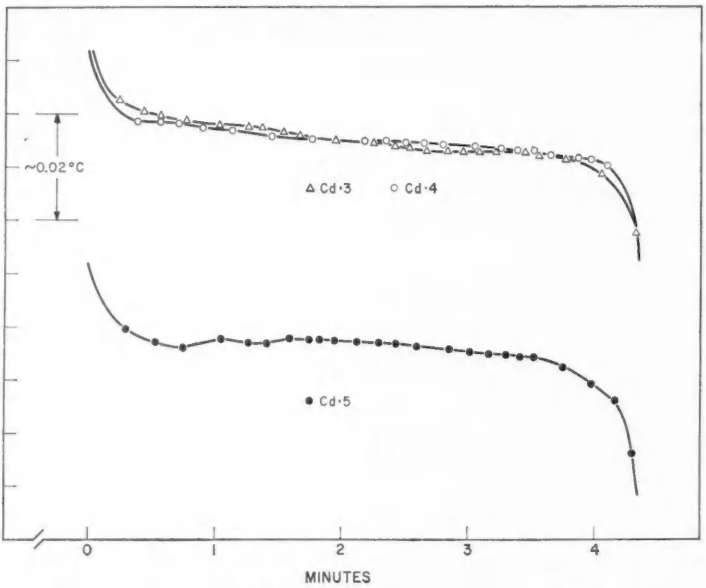

FIG. 6. Very fast normal freezes on three cadmium samples.

Figure 7 shows freezing curves obtained from fast normal freezes on all samples; the freezes were made by allowing the samples to transform freely with the furnace power supplies turned off. The thermometer indicated a supercooling of about 0.03° C in samples Cd.3 and Cd.4 and less than 0.01° C in sample Cd.5. Although these freezes and additional similar freezes showed distinctive differences in the shapes of the curves during recalescence for Cd.3 and Cd.4, it would be difficult to attribute this entirely to differences in

impurity contents of the two samples since the initial rate of nucleation of the solid phase is probably affected by the condition of the walls of the graphite crucibles and the degree of supercooling. This crucible factor might not be identical for both samples because sample Cd.3 had been used frequently during a 2-year interval prior to these measurements.

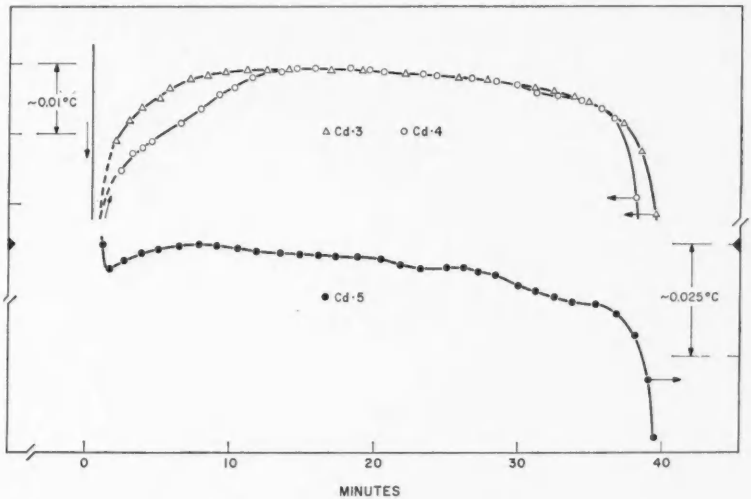

FIG. 7. Fast normal freezes on three cadmium samples.

For these reasons it has been more profitable to investigate melting ranges after various types of freezing to discriminate among samples of high purity metals, and Fig. 8 shows melting curves that were obtained immediately after the corresponding freezes of Fig. 7. Samples Cd.3 and Cd.4 melt over a temperature range of a few thousandths of a degree and there is evidence of structures on both their melting curves: melting can be detected over a temperature range greater than one degree for sample Cd.5.

Figure 9 shows induced freezes on the three samples. The plateau freezing temperatures for samples Cd.3 and Cd.4 are indistinguishable on these freezes while a plateau of nearly constant temperature was not obtained for sample Cd.5. This failure to develop a plateau is probably a consequence of the larger impurity content of sample Cd.5; the slope of the liquidus for this alloy, over the range of compositions initially frozen out, must be large enough for freezing to take place over a measurable range of temperature even when the sample is assisted to the liquidus point by the induced freezing technique.

Figure 10 shows derived inverse plots of the melting curves obtained after these induced freezes. It now becomes possible to make some distinction between sample Cd.3 and Cd.4. Although the melting ranges at the 1% level of the total melting time for the high purity cores of both samples are about

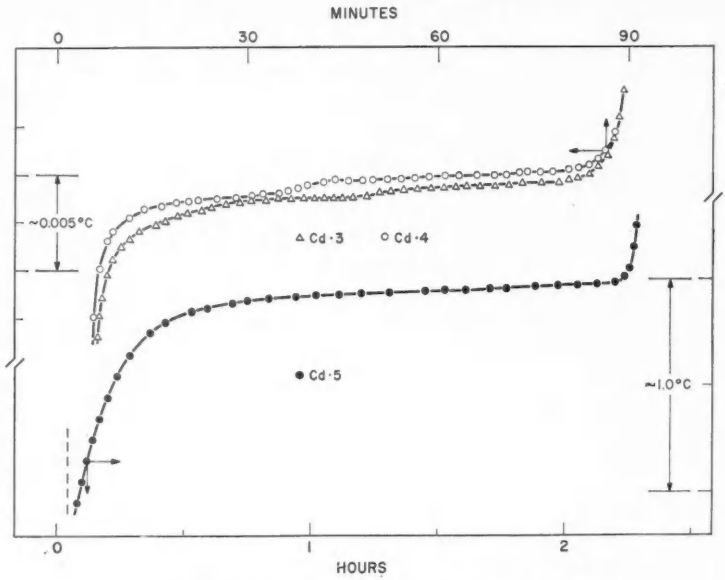

FIG. 8. Melting curves after the fast normal freezes of Fig. 7.

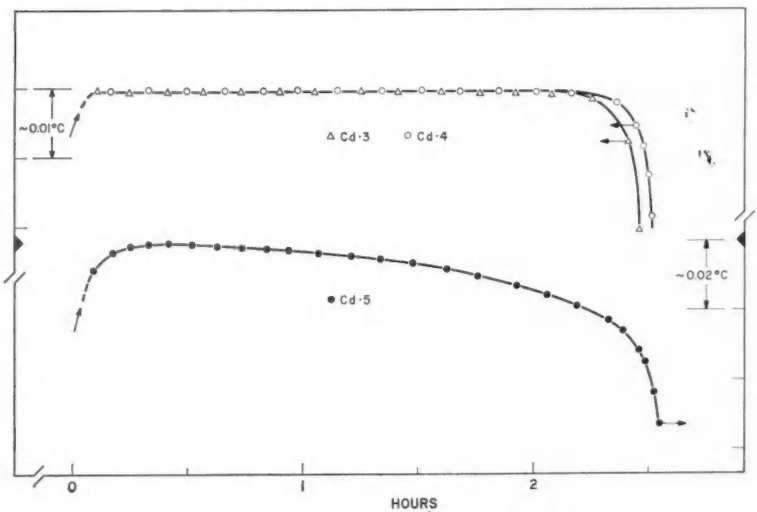

FIG. 9. Slow induced freezes on three cadmium samples.

0.003° C it is clearly evident on comparing the histograms that substantial amounts of melting takes place over a larger temperature range in Cd.3 than in Cd.4. Both samples show minor arrests lying close to the main arrests. For completeness the inverse plot of the melting curve after the induced freeze on Cd.5 is also shown in Fig. 10.

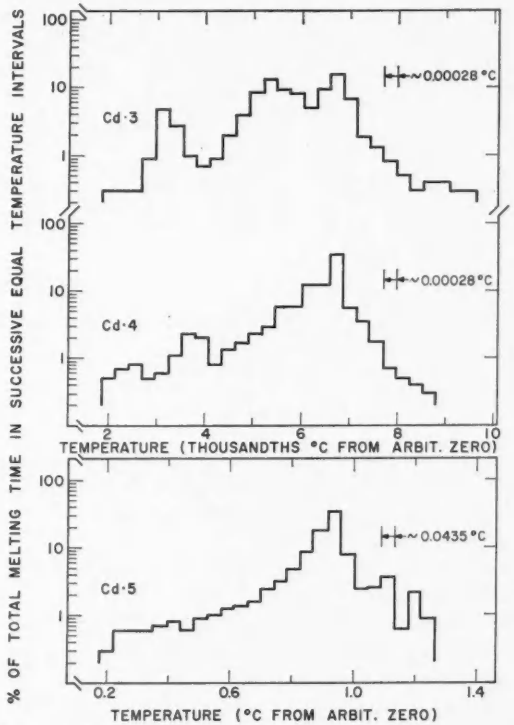

FIG. 10. Inverse melting curves after the slow induced freezes of Fig. 9.

Since the foregoing work showed that the thermal curves for Cd.3 and Cd.4 were nearly identical under similar thermal treatments, further efforts were made to try to reveal distinctive differences in these samples by carefully examining melting contours after a variety of freezing conditions. Table IV summarizes transformation conditions and melting range estimates made on the widths at the 1% level on inverse plots of several series of direct melting curves; estimates of the melting ranges of the least pure sample, Cd.5, are also included in this table. Series 1 to 5 are similar to types of transformations already discussed but series 6 and 7 require further explanation. Curves II of Fig. 11 show composite inverse plots of the five melting curves in series 1 to 5 for each sample which were fitted at the temperature intervals in which the

TABLE IV

TRANSFORMATION CONDITIONS AND ALLOY-MELTING RANGES FOR THE THREE CADMIUM SAMPLES ESTIMATED FROM INVERSE PLOTS OF THE DIRECT MELTING CURVES DERIVED FROM THE FRACTION OF THE TOTAL MELTING TIME SPENT IN TEMPERATURE INTERVALS I, II, III, AND IV HAVING MAGNITUDES OF 0.00028° C, 0.00014° C, 0.02° C, AND 0.01° C RESPECTIVELY

				Melting range at the 1% level of the total melting time					
	Prior freeze			I		II		III	IV
Series	Type	Duration (minutes)	Melting duration (minutes)	Cd.3 (° C)	Cd.4 (° C)	Cd.3 (° C)	Cd.4 (° C)	Cd.5 (° C)	Cd.5 (° C)
1	(Normal	5	80	0.0038	0.0033	0.0028	0.0025		
2	2NR)	5	120	0.0032	0.0024	0.0024	0.0020	0.20	0.13
3	(Normal	40	65	0.0041	0.0034	0.0029	0.0026		
4	2NR)	40	130	0.0044	0.0033	0.0029	0.0026	0.18	0.15
5	(Induced	160	90	0.0046*	0.0043*	0.0042*	0.0038*		
	2NR)	160	90	0.0032†	0.0033†	0.0028†	0.0024†	0.30	0.18
6	(Composite series 1–5)	—	—		—	0.0028†	0.0025	—	—
7	(Normal 2N)	5	120	0.0038‡	0.0029	0.0021§	0.0021	—	—

*Complete samples.
†High purity cores.
‡Temperature interval 0.00022° C.
§Temperature interval 0.00011° C.

greatest amount of melting occurred; the melting ranges from these average plots are listed as series 6 in Table IV. Curves I of Fig. 11 (series 7) were determined using 2N bridge balances only; resistance was estimated to the nearest micro-ohm (~0.000011° C).*

The results in Table IV re-emphasize the importance of using similar thermal treatments and temperature analyses when comparing the alloy melting ranges of different samples with the resistance thermometer.

Inspection of Fig. 11 shows that although the melting contours of the two samples are very similar sample Cd.4 appears to melt over a slightly narrower range of temperature than sample Cd.3. The close correlation of curve I to curve II for a particular sample indicates that the 2N technique may be successfully used to compare melting contours of samples with narrow melting ranges provided the resistance thermometer is used in an experimental arrangement favoring a nearly constant temperature distribution over the connecting lead resistances. Table V gives a comparison of the incremented percentages of the total melting time spent in given temperature ranges from the plots of

*The 2N technique allowed two measurements to be made each minute compared to about one measurement in 2 minutes using 2NR techniques. The 2N technique is open to criticism because any significant slow change in the lead resistance to the thermometer would tend to smear any structure on the melting contour; however, in practice it has been frequently observed that a Meyers standard thermometer immersed in a zinc ingot on a very slow induced freeze will maintain 2N balances (2R as well) to 10 micro-ohms for periods of at least 2 hours. Stability of this order in the lead resistances of a Meyers thermometer is undoubtedly due to the thermometer's being deep-bedded in the heavily insulated furnace and to the use of heavy conductors connecting the thermometer leads to the Mueller bridge, all apparatus being maintained in an air-conditioned laboratory.

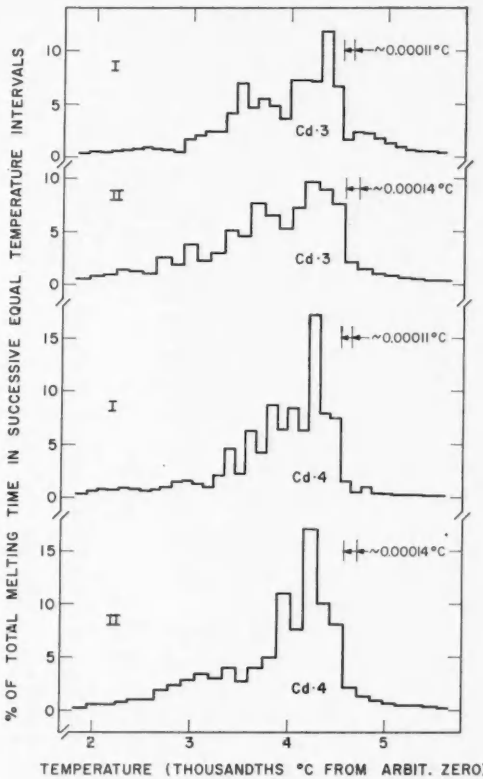

FIG. 11. Inverse melting curves: I, after very fast normal freezes, and II, fitted composite of five melting curves for samples Cd.3 and Cd.4.

Fig. 11; the sensibly higher fraction of sample Cd.4 that melted in a range of 0.001° C probably arises from a slightly different impurity content than is present in sample Cd.3.

(*b*) *Comparison of Liquidus Points*

A careful intercomparison of the plateau temperatures developed on slow induced freezes of the cadmium samples was carried out using two furnaces and the measuring sequence that was used earlier (McLaren 1958) to compare the liquidus points of samples of high purity zinc. The resistances at the cadmium plateau temperatures were corrected to 1-atm nitrogen pressure over the melts. Measurements were made with the mid-point of the sensing coil of a single Meyers thermometer immersed about 15 cm in the cadmium. One ice mantle on a single water triple point cell was used to baseline all measurements. Fig. 12 gives results of comparing the plateau temperatures of samples Cd.3

TABLE V

PERCENTAGE OF THE TOTAL TIME SPENT IN GIVEN MELTING RANGES DERIVED FROM THE HISTOGRAMS I AND II OF FIG. 11

I (2N)				II (2NR)			
Melting range (10^{-4} °C)	(*a*) Cd.4 (%)	(*b*) Cd.3 (%)	*a*/*b*	Melting range (10^{-4} °C)	(*a*) Cd.4 (%)	(*b*) Cd.3 (%)	*a*/*b*
1.1	17	12	1.4	1.4	17	10	1.7
2.2	25	19	1.3	2.8	27	19	1.4
3.3	32	26	1.2	4.2	35	26	1.3
4.4	38	33	1.2	5.6	43	34	1.3
5.4	47	40	1.2	6.9	54	39	1.4
6.5	53	43	1.2	8.3	59	45	1.3
7.6	62	48	1.3	9.7	63	53	1.2
8.7	66	53	1.2	11.1	66	58	1.1
9.8	72	58	1.2	12.5	70	63	1.1
10.9	74	65	1.1	13.9	73	66	1.1
12.0	79	69	1.1	15.3	76	68	1.1
13.1	81	70	1.1	16.7	79	72	1.1
14.1	82	72	1.1	18.1	81	74	1.1
15.2	83	75	1.1	19.4	83	76	1.1
16.3	84	76	1.1	20.8	85	78	1.1
17.4	86	78	1.1	22.2	86	80	1.1
18.5	87	79	1.1	23.6	87	81	1.1
19.6	88	81	1.1	25.0	88	82	1.1
20.7	89	83	1.1	26.4	89	83	1.1
21.8	89	84	1.1	27.8	90	84	1.1
22.8	90	85	1.1				

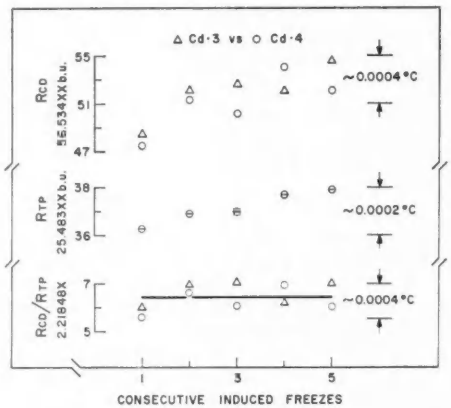

FIG. 12. Intercomparison of plateau temperatures of samples Cd.3 and Cd.4.

and Cd.4 with five determinations made on each sample. The intercomparisons are summarized in Table VI.

TABLE VI

INTERCOMPARISON OF CADMIUM PLATEAU TEMPERATURES

Sample	No. of freezes	Ratio R_{Cd}/R_{TP}		Reproducibility (equivalent 10^{-4} °C)		Plateau temp. rel. to Cd.3 (° C)
		Mean	$10^8 \times$ Min. dev.	Min. dev.	Spread	
Cd.3	5	2.21848667	±43	±1.2	2.9	
Cd.4	5	8627	±42	±1.2	3.7	−0.00011
Cd.3, Cd.4	10	8647	±46	±1.3	4.0	
Cd.3	1	2.21848697				
Cd.5	1	0535				−0.023

DISCUSSION

The high reproducibility of the liquidus point of high purity indium is comparable with that of any fixed point on the International Temperature Scale and experimentally this freezing point is incomparably easier to realize than is the attainment of a precision Steam Point. For this reason the indium point (156.611° C Int. 1948) should receive serious consideration as a precision alternative to the Boiling Point of Water on the International Temperature Scale.

The extreme difficulty encountered in attempting to distinguish between cadmium samples Cd.3 and Cd.4, even though one sample (Cd.3) had been used for over 2 years as a laboratory secondary standard prior to these measurements, illustrates the high stability and ready attainment of the liquidus point of high purity cadmium.

Two distinct advantages of the liquidus points of high purity metals as precision temperature fixed points are: corrections can be easily and accurately made for pressure effects on the freezing temperatures, and alloy melting ranges can be occasionally measured to guard against decreases in purity and associated changes in the liquidus points. For the 6 years during which studies have been made in this laboratory on the transformation temperatures of samples of high purity Zn, Cd, Sn, and In, no evidence of contamination of any melt has been observed; in fact the liquidus points of these metals, with the triple point of water, have provided a means for examining under high precision the stability of the temperature coefficients of the resistance thermometers. In addition the liquidus points of high purity metals are eminently suitable for use in comparing the temperature scales realized in different laboratories: it is no longer necessary to base such comparisons on transported resistance thermometers whose temperature coefficients are known to change as a result of cold-working during transit.

Further work is contemplated on the freezing temperatures of high purity tin, lead, and bismuth. Earlier investigations on samples of 99.99% tin from two different sources had revealed highly reproducible plateau temperatures on particular samples (McLaren 1957*b*) but a difference of about 0.008° C between the liquidus points of the samples; 99.999+ % tin has now been

procured and thermal analyses and annealing studies will be made on this metal. The highly reactive alkali metals with thallium and gallium are the remaining metals that have freezing temperatures in the range 0° C to 420° C; and although the freezing points of the former do not appear particularly promising as temperature standards, precision thermal analyses on high purity samples of these metals may provide useful metallurgical information. It is also hoped to examine zone-refined samples of metals since this might reveal the limit at which impurity differences can no longer be detected by precision thermal analysis.

The structures that are developed on the melting contours of these high purity metals fall into two types. The minor arrests seen in Fig. 3 (*c*) and Fig. 10 (Cd.3, Cd.4) are almost certainly due to the segregation of impurities that are nearly insoluble in the solid solvent. The structures shown inside the melting contours of the high purity cores in Fig. 11 may be partly due to more soluble impurities, but what the "natural melting range" of the pure element would be and whether or not any isotope fractionation occurs for specific freezing conditions that could be detected on the melting contour is not known. Theoretical considerations by MacDonald and Lovejoy (1955) on the effects of differences in zero point energies on the melting points of the zinc isotopes suggested that significant fractionation on freezing for the heavy elements would be unlikely. However it would be desirable to have mass analyses made on sectioned ingots following different types of freezes to verify these theoretical expectations especially in view of the well-established fractionation of D and O^{18} in normal water on freezing (Teis and Florensky 1941) and the very interesting results reported by Alieva (1958) on differences in isotopic composition among samples of high purity zinc.

CONCLUSIONS

This investigation has shown that it is possible to develop sections of very steady temperature that are reproducible to the order of $\pm 0.0001°$ C on induced freezes of high purity indium. The forms of the thermal curves obtained on high purity indium are similar to those obtained with high purity zinc and cadmium.

No measurable difference was found between the liquidus points of the two samples of cadmium with highest purity but close inspection of melting contours showed that one sample melted over a slightly smaller range of temperatures than the other.

ACKNOWLEDGMENT

It is a pleasure to acknowledge the valuable contribution of Mr. E. G. Murdock, who assisted in all phases of the experimental work.

REFERENCES

ALIEVA, PH. Z. 1958. Comité International des Poids et Mesures, Procès-Verbaux des Séances de 1958, **26**, Annexe T11.

HELLNER, E. 1951. Z. Metallk. **42**, 17.

MACDONALD, D. K. C. and LOVEJOY, D. R. 1955. Private communication.

McLAREN, E. H. 1957*a*. Can. J. Phys. **35**, 78.
——— 1957*b*. Can. J. Phys. **35**, 1086.
——— 1958. Can. J. Phys. **36**, 585.
TEIS, R. V. and FLORENSKY, K. P. 1941. Compt. rend. acad. sci. U. R. S. S. **32**, 199.
TURNER, G. H., MITCHELL, C. J., and BRYAN, J. M. 1957. Analysis by instrumental methods. Report by the Research and Development Division, The Consolidated Mining and Smelting Company of Canada Limited, Trail, B.C.
VALENTINER, S. 1943. Z. Metallk. **35**, 250.
VALENTINER, S. and HABERSTROH, A. 1938. Z. Physik. **110**, 727.
WEIBKE, F. and EGGERS, H. 1934. Z. anorg. u. allgem. Chem. **220**, 293.
WILLIAMS, D. D. and MILLER, R. R. 1950. J. Am. Chem. Soc. **72**, 3821.

CONDENSATION COEFFICIENTS OF SILVER, GOLD, AND COPPER IN VACUUM DEPOSITION[1]

S. CHANDRA AND G. D. SCOTT

ABSTRACT

A beam of atoms striking a substrate will in general not condense completely, but some of the incident atoms will re-evaporate. The condensation coefficient—defined as the ratio of the number of atoms condensing to the total number incident on the substrate—has been determined for silver at substrate temperatures from − 30° C to 170° C, and for gold and copper at temperatures from 25° C to 165° C. For silver at room temperature the condensation coefficient is found to be 0.936, which indicates 6.4% of the incident atoms are re-evaporated or diffusely reflected. By a simple graphical analysis of the results it is shown that the temperature below which complete condensation occurs is 200° K for silver, 230° K for gold, and 180° K for copper.

INTRODUCTION

In 1915 Wood showed that mercury atoms condense completely onto a glass substrate only at temperatures below −140° C. Similarly, for zinc, mercury, and cadmium, Knudsen (1916) found that the temperatures below which complete condensation of the atoms takes place are between −183° C and −78° C. These authors also showed that in each case, above a certain substrate temperature, there is no condensation of the metal. In their experiments, the stream density, i.e., the number of atoms striking a unit area of a substrate normal to the forward direction in 1 second, was constant, and they did not attempt to find the effect of the stream density on the condensation temperature. However, Cockcroft (1928) has shown that the temperature above which cadmium atoms fail to condense on the substrate of polished copper or silver disks depends on the stream density of the atoms.

Frenkel (1923) has given a theoretical discussion related to these phenomena. For the condensation of metal atoms on a substrate, he assumed (*a*) that the metal atoms after striking the surface move over it as atoms of a two-dimensional gas for a short time, called the mean free time, and then re-evaporate, and (*b*) that these atoms while moving on the surface may collide with one another to form pairs which have a greater mean free time than a single atom. The pairs, or "doublet atoms," act as nuclei of condensation for the atoms of the two-dimensional gas. Frenkel showed that if t_0 is the period of oscillation of an atom normal to the surface of a substrate about a point where its potential energy is u_0, then its mean free time t is given by

$$t = t_0 \exp (u_0/kT),$$

where k is the Boltzmann constant and T is the absolute temperature of the substrate. The above expression shows that, as T increases, t decreases, i.e., the probability of re-evaporation of an atom is greater from a hot substrate

[1]Manuscript received June 9, 1958.
Contribution from the Department of Physics, University of Toronto, Toronto, Ontario.

than at lower temperatures. The condensation coefficient of a metal defined as the ratio of the number of atoms condensing on a substrate to the total number striking it will therefore decrease as the temperature of the substrate increases.

Devienne (1953) made a study of the effect of the substrate temperature on the condensation coefficients of antimony, silver, and gold by the use of their radioactive isotopes. His tables for antimony show a decrease in the condensation coefficient of the metal with an increase in substrate temperature. For silver and gold Devienne was not able to obtain "very precise results" because of the low activity of the isotopes. However, repeated experiments on substrates of glass and copper at room temperature indicated that the condensation coefficient is not precisely equal to unity but fairly close to this value, "ranging between 0.9 and 1." He also observes that when the temperature of the condensing plate is raised, the coefficient decreases, but "it appears that the effect is only great enough to be noticeable at temperatures above 300° C."

The re-evaporation or restitution of silver atoms incident on a substrate during vacuum deposition has also been established qualitatively by the "reflection" experiments of Aziz and Scott (1956). In the present work the condensation coefficients were accurately determined for silver with substrate temperatures from −30° C to 175° C and for gold and copper with substrate temperatures from 25° C to 160° C. The measurements consisted of finding the thicknesses of the deposit on one substrate which received the atoms directly evaporated from the source and on a second substrate which collected the re-evaporated atoms from the first. The two substrates are referred to as the reflector and collector respectively.

EXPERIMENTAL

The evaporations were carried out in a 12-in. evaporating unit equipped with a liquid-air trap. Carefully cleaned microscope slides served as the reflector and the collector. The two slides were placed in a holder so that they were parallel, 1 cm apart, and inclined at 45° to the direction of the incident beam as in Fig. 1. The slides were mounted inside a double-walled cylindrical radiation shield which provided a constant-temperature chamber within the evaporating unit. A cooling coil of copper tubing and an electrical heating element inside the shield were used to obtain the desired temperature. For temperatures down to −30° C, alcohol cooled by an external bath of dry ice and alcohol was circulated through the coil. The substrate temperature was determined by two chromel–alumel thermocouples, one below and the other above the slides.

The metals were evaporated directly from a "boat-type" tungsten filament. The stream density of the atomic beam was kept approximately the same in all runs with a given metal by maintaining a constant voltage across the filament. The rate of deposition at the reflector for silver was about 45 Å of thickness per second, which corresponds to a beam intensity of 6×10^{15} atoms cm^{-2} sec^{-1}.

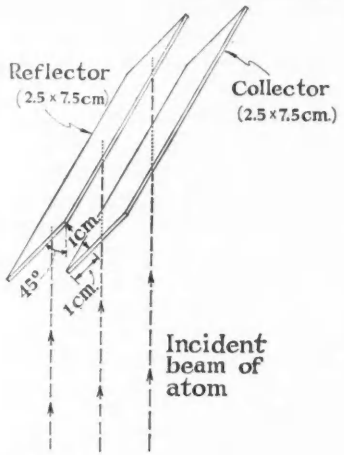

FIG. 1. Arrangement of the two microscope slides as reflector and collector.

The thicknesses of the deposited films were measured at the center of the reflector and near the edge of the collector. The method employed for the thickness measurements was that of multiple beam interferometry as developed by Scott, McLauchlan, and Sennett (1950). The typical variation of thickness of the film on the collector slide with distance from its edge is shown in Fig. 2. Because the reflector and the collector overlapped by 1 cm along the sides, the film was of nearly constant thickness for about 3 mm from the edge. It was this constant thickness which was used to determine the condensation coefficients.

The main function of the glass slides was to provide mechanical support for the films. Under the conditions of these experiments a continuous film of the metal is formed on the reflector for a thickness of about 100 Å. The total deposit on the reflector was usually in the range 1000 to 4000 Å. Since the deposit on the collector was found to be proportional to the deposit on the reflector, it can be concluded that the restitution (i.e., re-evaporation) measured is primarily a characteristic of the metal film itself and is not influenced significantly by the nature of the substrate.

A preliminary test was carried out to confirm the expected absence of specular reflection of the beam of evaporated atoms. The result showed that specular reflection, if present, must be less than 0.1%.

The possibility that atoms "reflected" once might be "reflected" a second time at the collector was considered. If this effect were present to a significant extent, a correction to the measured thicknesses would be required in order to calculate the condensation coefficient. No correction was deemed necessary since after the first reflection the atoms will lose a large fraction of their initial kinetic energy and the probability of a second reflection will be much smaller.

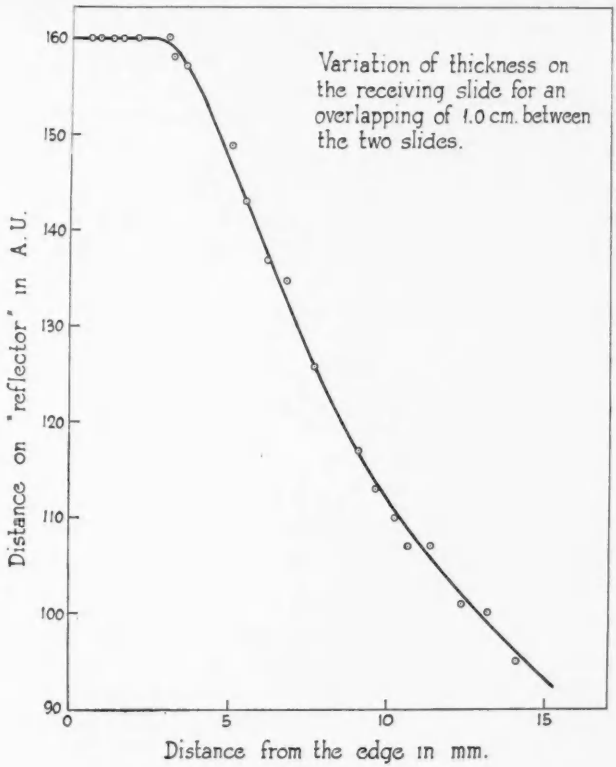

FIG. 2. Variation in thickness across collector slide.

Geometrical Correction

To calculate the condensation coefficient from the observed thicknesses of the deposits on the reflector and the collector, it is necessary to make a correction for the particular geometry used. The required correction factor is the ratio of the deposit actually collected to that which would be collected if the reflector were an infinite plane uniformly "illuminated" by the incident atomic beam. For the geometrical arrangement used (Fig. 1), the factor was calculated to be 0.773.

OBSERVATIONS

The results for silver, gold, and copper are given in Table I. The measured thickness, D, on the reflector, and the corrected thickness, d, on the collector, are listed at various substrate temperatures. The condensation coefficient is found from the ratio $D/(D+d)$. It can be noted that in all three cases the

condensation coefficient decreases with increase of temperature as implied by the Frenkel theory: e.g., the values for silver at $-28°$ C and 171° C are 0.982 and 0.879 respectively. At room temperature the condensation coefficient is 0.936, which is within the range of 0.9 to 1.0 given by Devienne.

The temperature, T_0, at which complete condensation occurs was determined by trial in order to give a straight line plot between $\ln(D/d)$ and $1/(T-T_0)$. The final plots for each of the metals are shown in Fig. 3. The values of T_0 are 200° K for silver, 230° K for gold, and 180° K for copper.

Experiments were carried out with aluminum but no restitution was found. Even for a thickness of 5000 Å on the reflector no deposit appeared on the

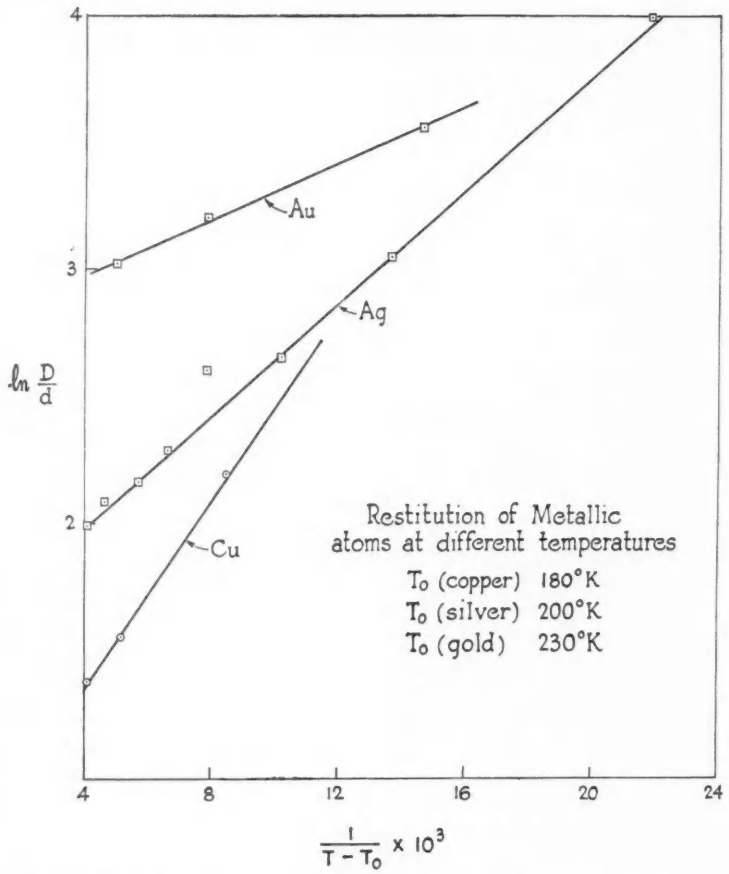

FIG. 3. Final plot to obtain the temperature T_0—the temperature below which complete condensation occurs.

TABLE I

CONDENSATION COEFFICIENTS OF SILVER, GOLD, AND COPPER

Metal	Substrate temperature, °K	Thickness D on reflector, Å	Corrected thickness d on collector, Å	Condensation coefficient, $D/(D+d)$
Silver	245	4990	91	0.982
	273	4920	233	0.955
	298	2090	142	0.936
	328	4230	311	0.931
	351	5496	558	0.908
	376	5360	615	0.898
	419	4843	598	0.890
	444	4945	677	0.879
Gold	298	3387	98	0.972
	357	2940	119	0.961
	430	2817	137	0.954
Copper	298	1020	115	0.899
	373	1100	233	0.825
	430	920	233	0.797

collector with substrate temperatures as high as 175° C. Since deposits less than 5 Å in average thickness can readily be detected, the restitution of aluminum atoms must be less than 0.1% at temperatures up to 175° C.

ACKNOWLEDGMENTS

The authors wish to express sincere thanks to Mr. G. T. Woodward for technical assistance. The financial aid provided to one of them (S.C.) by the Garnet W. McKee – Lachlan Gilchrist Scholarship during the session 1956–57 and by the Advisory Committee on Scientific Research, University of Toronto, during the summers of 1956 and 1957 is gratefully acknowledged.

REFERENCES

AZIZ, R. A. and SCOTT, G. D. 1956. Can. J. Phys. **34**, 731.
COCKROFT, J. D. 1928. Proc. Roy. Soc. A, **119**, 293.
DEVIENNE, F. M. 1953. Vacuum, **3**, 392.
SCOTT, G. D., MCLAUCHLAN, T. A., and SENNETT, R. S. 1950. J. App. Phys. **21**, 843.
WOOD, R. W. 1915. Phil. Mag. **30**, 300.

MEASUREMENTS OF ABSOLUTE PAIR PRODUCTION CROSS SECTIONS AT LOW ENERGIES[1]

S. STANDIL AND V. SHKOLNIK[2]

ABSTRACT

Using an improved analysis in conjunction with a relative method for the measurement of absolute pair production cross sections, the pair production cross sections per atom of lead have been measured for the gamma rays emitted by Co^{60} and Sb^{124}. The Z-dependence of this cross section was measured for the Co^{60} radiation using targets of Al, Fe, Cu, Mo, Ag, Sn, and Pb. The results obtained are generally in agreement with other experimental determinations and are, along with those of other investigators, represented graphically.

INTRODUCTION

Several authors have measured the pair production cross section in lead for gamma-ray energies between the pair creation threshold at 1.022 Mev and at 3 Mev (Hahn *et al.* 1952; Schmid and Huber 1955; Jenkins 1956; Standil and Moore 1956; Shkolnik and Standil 1957). In addition, exact theoretical calculations exist for lead at gamma-ray energies of 1.53 and 2.66 Mev (Jaeger and Hulme 1936), and crude extrapolations based on these results have been made (Cleland, Townsend, and Hughes 1951; Hahn, Baldinger, and Huber 1952). The accuracy of such extrapolations between threshold and 1.5 Mev is $\sim 20\%$, and experimental results are usually compared with the values obtained from the Bethe–Heitler formula (Bethe and Heitler 1934), which is not valid in these cases. Establishment of an experimental pair production cross section vs. energy curve over this energy range thus seemed desirable.

Using three targets (Fe, Cd, and Pb), Hahn, Baldinger, and Huber (1952) measured the Z-dependence of the pair production cross section, and Dayton (1953) has published similar results obtained with four different targets (Al, Cu, Sn, and Pb). We have also made this kind of determination using our experimental method and seven different metal targets (Al, Fe, Cu, Mo, Ag, Sn, and Pb).

THE EXPERIMENTAL METHOD AND TREATMENT OF DATA

The experimental arrangement, shown in Fig. 1, and the general method have already been described (Shkolnik and Standil 1957) and in the present measurements only minor changes in the geometry were made. The pair production cross section per atom of target, σ, was given by

$$\sigma = \left(\frac{4\pi r^2}{N_{12}^S}\right)\left(\frac{N_{12}^T}{N}\right)\left(\frac{S}{Q}\right), \tag{1}$$

[1]Manuscript received April 8, 1958.
Contribution from the Department of Physics, University of Manitoba, Winnipeg, Manitoba. This work was supported by the National Research Council of Canada.
[2]On leave from the University of Belgrade, Yugoslavia.

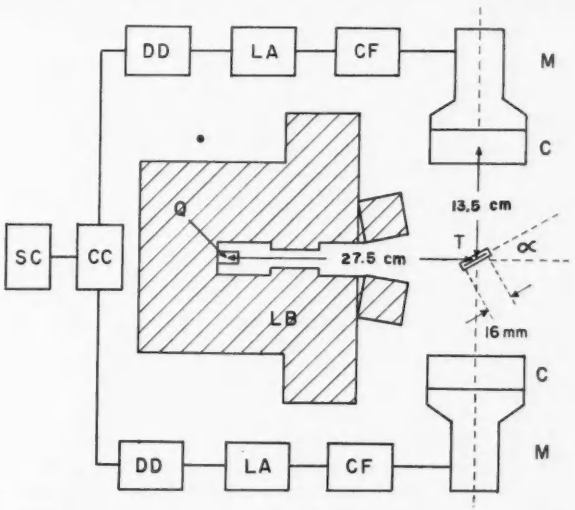

FIG. 1. The experimental arrangement (not to scale). T—target; LB—lead; Q—Co^{60} source (~150 mc); M—photomultiplier (DuMont 6364); C—sodium iodide crystal (3.5 in. diameter by 2.0 in.); CF—cathode follower; LA—linear amplifier; DD—differential discriminator; CC—coincidence circuit (resolving time 0.35 μsecond); SC—scaler.

where r = source-to-target distance,

N_{12}^{S} = corrected coincidence counting rate (annihilation quanta) of the reference (noncalibrated) Na^{22} source placed in the target position,

N_{12}^{T} = corrected coincidence counting rate due to positron annihilations in the target,

N = number of target atoms,

S = number of reference source Na^{22} positrons annihilated per second, and

Q = number of gamma rays emitted per second by the source.

N_{12}^{S} was corrected for absorption of the annihilation quanta in the Na^{22} container, the corrections for one- and three-quantum annihilations being negligible; N_{12}^{T} was corrected for absorption of the primary beam and the annihilation quanta in the metal target and its envelope. Here too the effects of one- and three-quantum annihilations are negligible (Hulme and Jaeger 1936; Bell and Graham 1953).

The corrections for absorption in the lucite container of the Na^{22} reference source and the graphite envelope of the target were determined by using known absorption coefficients and estimating the average paths in these absorbers. The correction for the effect of finite size was determined by measuring the probability of detecting annihilations as a function of the perpendicular distance of their occurrence from the counter axis and averaging

this over the particular geometry. A point source of Na^{22} was utilized in these auxilliary measurements.

The optimum orientation of the target with respect to the incident beam and the counter axis, i.e., the position with minimum absorption, was found experimentally ($\alpha = 30°$) by rotating the target about its vertical axis and detecting the coincidence rate for a given target. Neglecting the edge effects, this permits a more accurate correction procedure than that previously used. The coincidence counting rate for a given target, n_{12}^T, may be written as

$$n_{12}^T = Cme^{-Bm}, \tag{2}$$

where m = target mass,

B = an "effective" absorption coefficient per unit target mass, and

$$C = \left(\frac{dn_{12}^T}{dm}\right)_{m=0}. \tag{3}$$

C is the coincidence counting rate due to positron annihilations per unit target mass, computed for an infinitely thin target, i.e., no absorption is involved. The experimental data for the coincidence counting rates and the corresponding target masses substituted into equation (2) and subjected to a least squares fit gave C and its error for all targets. The term (N_{12}^T/N) in expression (1) is then given by

$$\frac{N_{12}^T}{N} = C\frac{A}{N_0}, \tag{4}$$

where A is the mass number of the target material and N_0 is Avogadro's number. The thickness-to-diameter ratio of the target did not exceed the value 0.1 in any case, hence the edge effects were in fact negligible. A typical least squares fit of equation (2) to the experimental data is shown in Fig. 2 for the case of the Co^{60} gamma rays and lead targets.

The determination of the S/Q term of equation (1) was straightforward and as discussed in our previous paper. Because of the complex spectra of Co^{60} and Sb^{124}, these measurements were made using the highest-energy gamma rays in each case (1.33 Mev for Co^{60} and 2.09 Mev for Sb^{124}).

THE RESULTS

The sum of cross sections per atom of lead for the equal intensity (1.17 and 1.33 Mev) Co^{60} lines was found to be

$$\sum\sigma(k)_{\text{exp}} = (0.274\pm0.025) \text{ barns.}$$

This is in better agreement with the experimental values of Hahn, Baldinger, and Huber (1952), (0.272±0.030) barns, and Schmid and Huber (1955), (0.274±0.008) barns, than with an extrapolation based on the Jaeger and Hulme (1936) calculation, which gives $\sum\sigma(k)$ as (0.300±0.050) barns.

Using the data recently published for the complex gamma-ray spectrum of

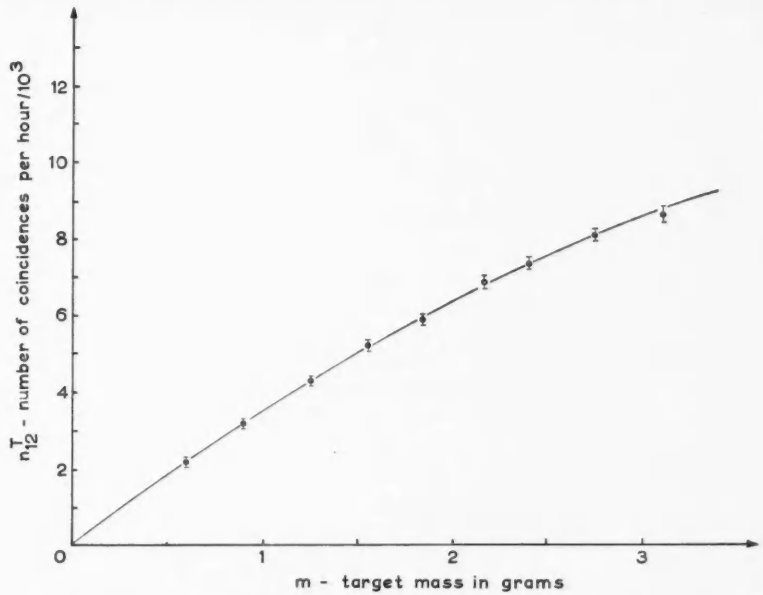

FIG. 2. Observed coincidence counting rate vs. target mass for Co^{60} on lead targets. The solid line is the least squares fit of equation (2) to these data.

Sb^{124} (Dzhelepov *et al.* 1957) the sum of the cross sections for all lines above the pair production threshold was found to be

$$\sum \sigma(k) \frac{Q(k)}{Q(2.09)} = (9.14 \pm 0.40) \text{ barn/atom},$$

where the factor multiplying $\sigma(k)$ gives the intensity of the line with energy k Mev relative to the intensity of the 2.09 Mev line. The result based on extrapolation of the Jaeger and Hulme calculations gives for the above sum of weighted cross sections the value of (9.60±0.20) barn/atom.

Our data previously published for the gamma radiation from Zn^{65} on lead targets have been subjected to the treatment herein described. This gives a value for the cross section of (13.4±1.0) millibarns per atom, which is 3% lower than the result previously reported. The difference is due to an original overestimate of the average path in the target.

The data for the gamma rays from Na^{24} (Standil and Moore 1956) have been similarly treated and this yields a final value for the pair production cross section in Pb at 2.76 Mev of (3.43±0.70) barn/atom, in agreement with the result of Schmid and Huber (1955). The large error of this result is inherent in the method then employed.

Fig. 3 shows these results, together with those of other authors, joined by a

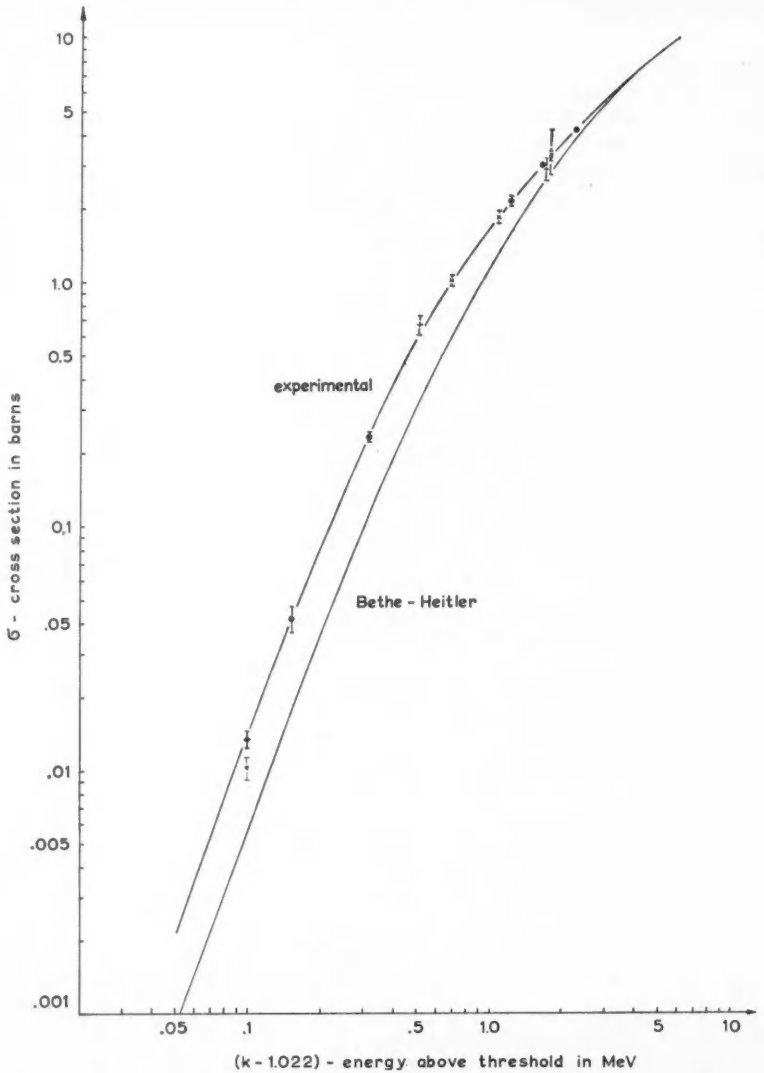

FIG. 3. Pair production cross section in lead vs. energy above threshold. The explanation of symbols for experimental points is as follows: ■—Shkolnik and Standil (1957) (1.12 Mev, Zn^{65}); ▼—Jenkins (1956) (1.12 Mev, Zn^{65}); ○—Hahn *et al.* (1952), Schmid and Huber (1955), and this experiment (1.17 and 1.33 Mev from Co^{60}); +—Jaeger and Hulme (1936) (calculated); ×—this experiment (1.70 and 2.09 Mev, Sb^{124}); ●—Hahn *et al.* (1952) (2.20, 2.62, 3.20 Mev, Th (C+C″)); □—Schmid and Huber (1955) (2.76 Mev Na^{24}); ▲—Standil and Moore (1956) (2.76 Mev, Na^{24}).

smooth curve and thus represents the variation of the experimental pair production cross section in lead with energy above the pair threshold. The values of $\sigma(k)$ for the complex radiation of Sb^{124}, Co^{60}, and Th($C+C''$) have been estimated from a knowledge of the sum of weighted cross sections and the general shape of the curve in Fig. 3 as determined by other points. The cross section for $Z = 82$, obtained from the Bethe–Heitler formula, is also plotted for comparison.

Z-DEPENDENCE MEASUREMENTS

The Z-dependence of the pair production cross section and radiation emitted by Co^{60} was measured using thin targets (Al, Fe, Cu, Mo, Ag, Sn, and Pb) of equal diameter. For each element at least seven target masses were employed and the observed coincidence counting rate vs. mass curves least-squares fitted with equation (2). These measurements being of a relative nature, no corrections for absorption in the same target container were necessary. The results obtained are in agreement with a Z-dependence of σ, given by

$$\sigma \sim aZ^2+bZ^4, \tag{5}$$

or

$$\frac{\sigma}{aZ^2} \sim 1+dZ^2. \tag{6}$$

A plot of σ/aZ^2 vs. Z^2 is shown in Fig. 4. The slope of this line gives a value of d which is compared with the results of the data of other authors in Table I.

TABLE I

VALUES OF THE FACTOR d FOR THE RADIATION FROM Co^{60}

Author	$d.10^4$
Hahn, Baldinger, and Huber (1952)	1.66±0.30*
Dayton (1953)	1.59±0.13*
Schmid and Huber (1954)	1.55±0.10
West (1956)	1.81±0.30*
Present experiment	1.53±0.03

*The errors in these values have been estimated by the present authors.

CONCLUSIONS

An experimental pair production cross section vs. energy curve for Pb has been determined and the Z-dependence of this cross section for the Co^{60} radiation has been found. The present measurements are in good agreement with those of other authors with the exception of Jenkins (1956), as is seen from Fig. 3. We note too that most experimental values for these cross sections agree with those obtained by extrapolation of the Jaeger and Hulme calculations. The use of Figs. 3 and 4 enables the determination of the pair production cross section for the Co^{60} radiation in any absorber.

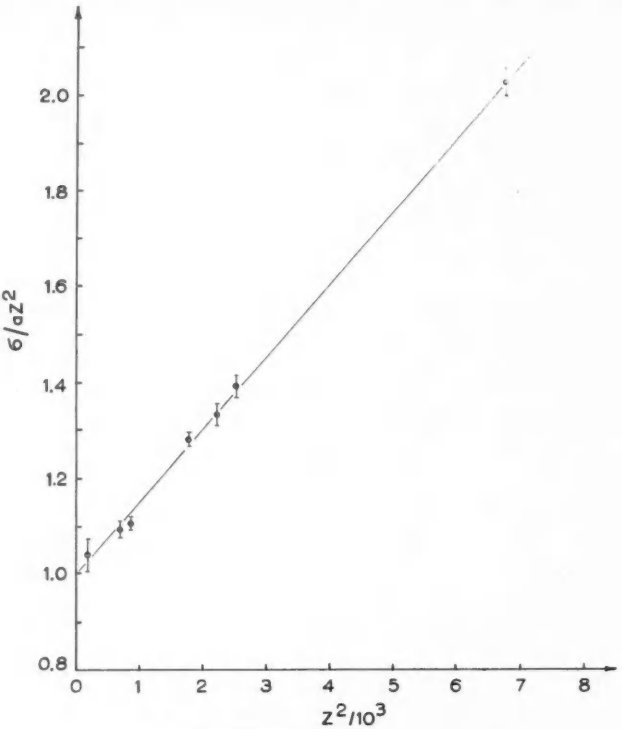

FIG. 4. σ/aZ^2 vs. Z^2 for Co^{60} radiation.

REFERENCES

BELL, R. E. and GRAHAM, R. L. 1953. Phys. Rev. **90**, 644.
BETHE, H. and HEITLER, W. 1934. Proc. Roy. Soc., A, **146**, 83.
CLELAND, M. R., TOWNSEND, J., and HUGHES, A. L. 1951. Phys. Rev. **84**, 298.
DAYTON, I. E. 1953. Phys. Rev. **89**, 544.
DZHELEPOV, B. S., ZHUKOVSKY, N. N., NEDOVESOV, V. G., UCHEVATKIN, I. F., and CHUMIN, V. G. 1957. Nuclear Phys. **2**, 408.
HAHN, B., BALDINGER, E., and HUBER, P. 1952. Helv. Phys. Acta, **25**, 505.
HULME, H. R. and JAEGER, J. C. 1936. Proc. Cambridge Phil. Soc. **32**, 158.
JAEGER, J. C. and HULME, H. R. 1936. Proc. Roy. Soc., A, **153**, 443.
JENKINS, T. 1956. Bull. Amer. Phys. Soc. **1**, 167.
SCHMID, P. and HUBER, P. 1954. Helv. Phys. Acta, **27**, 152.
——— 1955. Helv. Phys. Acta, **28**, 369.
SHKOLNIK, V. and STANDIL, S. 1957. Can. J. Phys. **35**, 1156.
STANDIL, S. and MOORE, R. D. 1956. Can. J. Phys. **34**, 1126.
WEST, H. I., JR. 1956. Phys. Rev. **101**, 915.

ZEEMAN SPLITTING OF DONOR STATES IN GERMANIUM[1]

R. R. HAERING[2]

ABSTRACT

The linear Zeeman effect of the $2p\ m = \pm 1$ donor states is calculated in the effective mass approximation. The resulting level splitting is independent of the longitudinal mass characterizing the ellipsoidal conduction band energy surfaces. This result is valid as long as the Zeeman splitting of the $m = \pm 1$ states is small compared to the energy difference between the $2p\ m = 0$ and the $2p\ m = \pm 1$ states. The Zeeman pattern to be expected in germanium is plotted as a function of the angle between the magnetic field and the (100) direction.

1. INTRODUCTION

The effective mass theory of impurity states has been very successful in explaining the nature of "shallow" impurity states in silicon and in germanium (Kohn 1957*a*).* This theory is expected to yield a good description of impurity states when the electron orbits are very large compared to the dimensions of a unit cell of the crystal. In this limit, the perturbation due to an isolated impurity is simply a coulomb potential modified by the static dielectric constant of the crystal in question (Kohn 1957*b*, 1958). Such a description of the impurity perturbation breaks down in the cell in which the impurity ion is located (Luttinger and Kohn 1955), since the dielectric constant loses its meaning at such short distances. This correction modifies mainly the *s*-like states, which have a nonvanishing amplitude at the impurity center. We expect, however, that the effective mass theory will give an adequate description of the *p*-like states in germanium.†

In the following discussion, we shall calculate the Zeeman splitting of the $2p\ m = \pm 1$ states of donor impurities in germanium. We shall consider only the splitting due to the orbital angular momentum. Since the Zeeman effect is measured experimentally by means of optical (infrared) transitions, the splitting due to the electron spin will cancel in the observed energy differences.

In germanium, the constant energy surfaces for the low-lying energies in the conduction band may be assumed to be a set of four ellipsoids oriented along the (111) directions. Consequently, the kinetic energy operator in the effective mass equation has ellipsoidal symmetry and the impurity eigenstates may be labelled by a magnetic quantum number which refers to the axis of symmetry. This quantum number corresponds to the *ml* quantum number in the hydrogen atom. However, because of the lower degree of symmetry of the effective kinetic energy operator of the impurity atom, eigenstates which differ only in the value of the above quantum number m are no longer degenerate

[1]Manuscript received April 22, 1958.
Contribution from the Department of Mathematical Physics, University of Birmingham, Birmingham, England.
[2]Now at the Department of Physics, Hamilton College, McMaster University, Hamilton, Ontario, Canada.
*This review article also contains many other relevant references.
†$2p$-like states are states which approach hydrogenic $2p$ functions in the limit $(m_l)/(m_l) \to 1$.

in energy. For instance, the $2p\ m = 0$ level has a lower energy than the $2p\ m = \pm 1$ level. The degeneracy between $+m$ and $-m$ remains, however. We shall see later that the above facts result in a considerable simplification of the calculation of the Zeeman effect.

We shall find that the Zeeman splitting depends only on the transverse mass m_t, which characterizes the ellipsoid in question. Furthermore, the level splitting depends only on the component of the magnetic field parallel to the axis of rotational symmetry (the z-principal axis) of the ellipsoid, and hence vanishes when the field is applied perpendicular to this direction. These results are a consequence of the nondegeneracy of the $2p\ m = 0$ and $2p\ m = \pm 1$ states and may be expected to break down when the Zeeman splitting of the $2p\ m = \pm 1$ states becomes comparable to the energy difference between the unperturbed $2p\ m = 0$ and $2p\ m = \pm 1$ states.

2. FORMULATION OF THE PROBLEM

In the one-electron approximation, the wavefunction of a bound donor electron in germanium satisfies the following equation:

$$\left[-\frac{\hbar^2}{2m}\nabla^2 + V(r) + U(r)\right]\Phi^i = E_i\Phi^i. \tag{1}$$

In equation (1) $V(r)$ is the periodic lattice potential and $U(r)$ is the additional potential due to the replacement of one germanium atom by a (singly ionized) donor ion. We shall assume this potential to be given by:

$$U(r) = -\frac{e^2}{\kappa r},$$

where κ is the static dielectric constant of germanium ($\kappa \simeq 16.0$).

The effective mass theory may be derived by expanding Φ^i (i denotes the different stationary states) in terms of the Bloch functions $\Psi_{n\mathbf{k}}$:

$$\Phi^i = \sum_m \int_{\text{zone}} d^3k A_m^i(\mathbf{k})\Psi_{m\mathbf{k}}. \tag{2}$$

If the impurity state in question has a large orbit and if its energy lies much nearer to the minimum energy of the nth conduction band than to any other band, one may show that equation (2) becomes

$$\Phi^i = \int_{\text{all } k} d^3k A_n^i(\mathbf{k})\Psi_{n\mathbf{k}} \tag{3}$$

and the coefficient A_n^i satisfies the so-called effective mass equation:

$$\left\{\epsilon_n(0) - E_i + \frac{\hbar^2}{2m_t}(k_x^2 + k_y^2) + \frac{\hbar^2}{2m_l}k_z^2\right\}A_n^i(\mathbf{k}) = \frac{4\pi e^2}{\kappa}(2\pi)^{-3}\int_{\text{all } k'} d^3k' \cdot \frac{A_n^i(\mathbf{k}')}{|\mathbf{k}-\mathbf{k}'|^2}. \tag{4}$$

Here we have specialized to the case of an ellipsoidal energy surface whose

minimum is at $\mathbf{k} = 0$. In germanium we actually have four ellipsoids at the zone boundaries oriented in the (111) directions. In the effective mass approximation, the functions (3) belonging to different ellipsoids do not mix, however. Equation (4) is then valid for each of these ellipsoids if we measure $\mathbf{k}$ from the conduction band minima instead of from $\mathbf{k} = 0$. We may transform equation (4) by introducing:

$$F_n^t(\mathbf{r}) = (2\pi)^{-3/2} \int_{\text{all } k} d^3k \, e^{i\mathbf{k}\cdot\mathbf{r}} A_n^t(\mathbf{k}). \tag{5}$$

The factor $(2\pi)^{-3/2}$ is convenient so that the functions F_n^t are normalized when Φ^t is normalized. From here on, all functions F^t and A^t will refer to the nth band (in our case the lowest conduction band of germanium), so that we shall omit the index n labelling this band. With the aid of the relation (5), equation (4) may be transformed to become:

$$\left\{ -\frac{\hbar^2}{2m_t}\left(\frac{d^2}{dx^2}+\frac{d^2}{dy^2}\right) - \frac{\hbar^2}{2m_l}\frac{d^2}{dz^2} - \frac{e^2}{\kappa r}\right\} F^t = \epsilon_t F^t, \tag{6}$$

where $\epsilon_t = E_t - \epsilon_n(0)$.

3. THE ZEEMAN EFFECT

When a magnetic field is applied, we must add to the Hamiltonian in equation (1) an extra term

$$\mathscr{H}' = -\frac{e}{2mc}\mathbf{H}\cdot(\mathbf{r}\times\mathbf{p}). \tag{7}$$

Terms quadratic in H can be ignored since we are calculating the linear Zeeman effect. In order to obtain the Zeeman splitting, we shall need the matrix elements of $\mathscr{H}'$ between the unperturbed states Φ^t, i.e. we shall need

$$(\Phi^t, \mathscr{H}'\Phi^{t'}). \tag{8}$$

Here Φ^t is the total eigenfunction of the impurity state with energy E_t. It is convenient to express the matrix element (8) in terms of a matrix element between the modulating functions F^t and $F^{t'}$. One finds:

$$(\Phi^t, \mathscr{H}'\Phi^{t'}) = -\frac{e}{2c}\left(F^t, \left\{H_x\left(\frac{yp_z}{m_l}-\frac{zp_y}{m_t}\right)+H_y\left(\frac{zp_x}{m_t}-\frac{xp_z}{m_l}\right)+H_z\left(\frac{xp_y}{m_t}-\frac{yp_x}{m_t}\right)\right\}F^{t'}\right). \tag{9}$$

The proof of this result, which is rather plausible on the basis of the similarity between equations (1) and (6), is outlined in the Appendix.

In equation (9), the x, y, and z axes are the principal axes of the ellipsoid in question. Let us now consider the $2p$ $m = \pm 1$ states. The modulating functions for these states have the form

$$F^{\pm} \sim f(z^2, \rho)e^{\pm i\phi}, \tag{10}$$

where $\rho = (x^2+y^2)^{\frac{1}{2}}$. The important feature of these functions is that they are

even in the variable z. On the other hand, the parts of the matrix element (9) proportional to H_x and H_y are odd functions of z. Hence (9) simplifies to:

$$(11)\quad \left(\Phi^{\pm}, -\frac{e}{2mc}\mathbf{H}\cdot(\mathbf{r}\times\mathbf{p})\Phi^{\pm}\right) = -\frac{eH_z}{2m_t c}\,(F^{\pm}, (xp_y - yp_x)F^{\pm})$$
$$= -\frac{eH\cos\beta}{2m_t c}\left(F^{\pm}, -i\hbar\frac{\partial}{\partial\phi}F^{\pm}\right).$$

Here β is the angle between the magnetic field and the z-principal axis. We now note that the operator $-i\hbar\dfrac{\partial}{\partial\phi}$ has no off-diagonal matrix elements between the functions (10) and that

$$\left(F^{+}, -i\hbar\frac{\partial}{\partial\phi}F^{+}\right) = +\hbar; \qquad \left(F^{-}, -i\hbar\frac{\partial}{\partial\phi}F^{-}\right) = -\hbar.$$

When these results are used, we obtain the following expression for the shift of the energy levels:

$$(12)\qquad \Delta E_{m=\pm 1} = \mp\frac{e\hbar H}{2m_t c}\cos\beta.$$

Note that this result is independent of the longitudinal mass ml and that only the component of the magnetic field along the z-principal axis is effective in splitting the levels. This is a consequence of the nondegeneracy of the $m = 0$ level. If this state were degenerate with the $m = \pm 1$ states (as it is for spherical $E(k)$ surfaces), then the terms involving H_x and H_y would also contribute. Furthermore, the perturbation (9) would connect the degenerate states $m = 0$ and $m = \pm 1$, so that the above simple treatment would not be valid. We may thus expect the above result to be reliable as long as the splitting ΔE is small compared to the energy difference between the unperturbed $2p\ m = 0$ and $2p\ m = \pm 1$ states. In germanium this means that (Kohn 1957*a*):

$$\Delta E \ll 3\times 10^{-3}\ \text{ev}.$$

We may estimate a characteristic splitting from equation (12) by putting: $m_t = 0.08m_0$; $H = 10^4$ gauss; $\cos\beta = 1$. One readily finds that

$$\Delta E_{H=10^4} \sim 7\times 10^{-4}\ \text{ev}.$$

It is also an easy matter to compute the expected Zeeman pattern for an arbitrary direction of the magnetic field. The result is plotted in Fig. 1 as a function of the angle θ between the magnetic field and the (100) direction. The magnetic field is taken to lie in a (110) plane. In terms of this angle θ, the Zeeman pattern due to the four ellipsoids in germanium is given by:

$$\Delta E = \pm\frac{e\hbar H}{2m_t c}\cos(\theta\pm 55°) \qquad \text{and} \qquad \Delta E = \pm\frac{e\hbar H}{2m_t c}\cdot\frac{\cos\theta}{\sqrt{3}}.$$

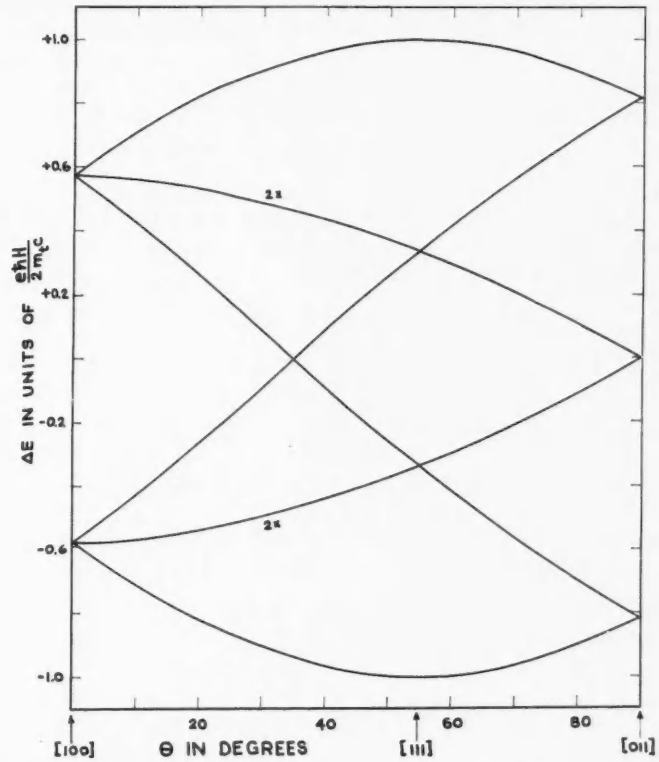

FIG. 1. Zeeman splitting of the $2p$ $m = \pm 1$ donor states in germanium as a function of the angle between the magnetic field and the (100) direction. One of the three pairs of lines is doubly degenerate for all angles θ.

4. DISCUSSION

The calculation outlined above corresponds to the strong field Zeeman effect in the atomic case, since we have assumed the spin-orbit energy to be negligible. We may estimate this energy by using the analogy with the hydrogen atom. We find that the $2p$ level is shifted by an amount of the order of

$$\frac{E_{2p}}{(137\kappa)^2},$$

which is completely negligible compared to a typical shift due to the magnetic field. Hence, if the above estimate is reliable, we are justified in neglecting the spin-orbit energy except in very weak fields.

It is interesting to note that the Zeeman pattern in Fig. 1 does not depend

on whether the conduction band in germanium consists of four or of eight ellipsoids. Hence a measurement of the Zeeman effect will not yield additional information regarding this question. However, the Zeeman effect could yield an independent estimate of the transverse mass, if the effective mass theory provides a valid description of this effect.

ACKNOWLEDGMENTS

The author would like to thank Professor W. Kohn for suggesting this problem. Thanks also go to Professor R. E. Peierls and to Dr. T. D. Shultz for stimulating discussions. The financial support of the National Research Council of Canada is gratefully acknowledged.

APPENDIX

Consider a typical term in the matrix element (9).

$$M = (\Phi^{i}, yp_x\Phi^{i'}). \tag{A1}$$

On substitution of the relation (3) this becomes:

$$M = \int\int d^3k d^3k' A_n^{*i}(\mathbf{k}) A_n^{i'}(\mathbf{k}') \cdot (\Psi_{n\mathbf{k}}, yp_x\Psi_{n\mathbf{k}'}). \tag{A2}$$

We may evaluate the matrix element of yp_x between Bloch states by expanding the periodic parts of these functions to lowest order in $\mathbf{k}$.

$$\Psi_{n\mathbf{k}} = e^{i\mathbf{k}\cdot\mathbf{r}} u_{n\mathbf{k}} \simeq e^{i\mathbf{k}\cdot\mathbf{r}} \left\{ u_{n_0} + \sum_{\substack{n' \\ n' \neq n}} \frac{\hbar\mathbf{k}\cdot\mathbf{p}_{n'n}}{m\omega_{nn'}} \cdot u_{n'_0} \right\}, \tag{A3}$$

where:

$$\mathbf{p}_{n'n} \neq \frac{(2\pi)^3}{\Omega} \int_{\Omega} u^*_{n'_0} [-i\hbar\nabla] u_{n_0} d\tau$$

and $\omega_{n'n} = \epsilon_{n'}(0) - \epsilon_n(0)$ is the energy difference between the n' th and the nth band at $\mathbf{k} = 0$.

If (A3) is substituted in (A2) one finds to lowest order:

$$M = \int d^3k A_n^{*i}(\mathbf{k}) \left\{ + \frac{i\hbar m}{m_t} k_x \frac{\partial}{\partial k_y} \right\} A_n^{i'}(\mathbf{k}). \tag{A4}$$

Here x, y, and z refer to the principal axes of the ellipsoid. We have made use of the f-sum rule and of the relations

$$\frac{\partial^2 \epsilon_n}{\partial k_\alpha \partial k_\beta} = \delta_{\alpha\beta} \frac{\hbar^2}{m_{\alpha\alpha}}$$

where: $m_{xx} = m_{yy} = m_t$; $m_{zz} = m_l$. If we now introduce the functions F_n^i defined by (5), equation (A4) becomes:

$$M = \frac{m}{m_t} \int d^3r F_n^{*i} \left\{ -i\hbar y \frac{\partial}{\partial x} \right\} F_n^{i'} \tag{A5}$$

$$= \frac{m}{m_t} (F^i, yp_x F^{i'}).$$

Similar results are valid for the terms zp_y, yp_z, etc. When these results are added, equation (9) follows.

REFERENCES

KOHN, W. 1957*a*. Solid state physics, Vol. 5 (Academic Press Inc., New York), p. 257.
——— 1957*b*. Phys. Rev. **105**, 509.
——— 1958. To be published in Phys. Rev.
LUTTINGER, J. M. and KOHN, W. 1955. Phys. Rev. **97**, 883.

SOME GEOPHYSICAL APPLICATIONS OF THE ELASTICITY THEORY OF DISLOCATIONS[1]

J. A. STEKETEE

ABSTRACT

In this paper some aspects of the elasticity theory of dislocations (E.T.D.) which may be of geophysical significance are discussed. The central position of *A*- and *B*-nuclei of strain in this theory is emphasized. Applications to cracks and seismological models are indicated. Some limitations of the E.T.D. for applications to geophysics appear in the discussion of strain energy. Finally the displacement field at the surface of a semi-infinite elastic medium which contains a particular *B*-nucleus at depth *c* is discussed. Although the considerations in this paper are in several respects incomplete and of a preliminary character it is expected that the reader may recognize the analogy of the E.T.D. with potential theory and will appreciate the power of the theory to unify several isolated problems on cracks and seismological models and to suggest further applications which are of geophysical interest.

1. INTRODUCTION

It is the purpose of the following lines to discuss some aspects of the theory of dislocations which may be of significance for geophysical problems. The geophysical questions we have in mind are (i) problems connected with fault-plane studies of earthquakes and with such phenomena as the San-Andreas fault in California, (ii) problems connected with fracture zones in the crust and mantle which are believed to play a significant role in the structure of island arcs and certain mountain ranges as proposed in the orogenetic theories of J. T. Wilson (1954, 1957) and A. E. Scheidegger (1953, 1958).

It is clear that each one of the groups of problems mentioned is so vast and complex that one can hardly expect to obtain all the answers from one simple theory. Also it will be noticed that the considerations in this paper are in several respects incomplete and of a preliminary character.

On the other hand it is found that the theory of dislocations is in so close agreement with some of the images and models used in seismology and in more qualitative geophysical discussions that it seems reasonable to expect some information concerning these problems from a study of dislocation theory.

It should be made clear at this stage that the term dislocation theory may lead to confusion. While the author is unaware of theories of dislocations in certain branches of the medical sciences, it is convenient to distinguish in physics and mathematical physics between two different meanings.

The first, which is at present no doubt the more significant one, indicates a field of solid state physics where one is concerned with certain types of irregularities in crystals. This field has developed considerably since 1934

[1]Manuscript received May 20, 1958.
Contribution from the Department of Applied Mathematics, University of Toronto, Toronto 5, Ontario.

and a vast and rapidly expanding literature exists dealing with problems of slip in crystals, solidification, work-hardening, etc. (cf. Friedel 1956). More recently also attention is being paid to the connections with the phenomenological theories of rheology (plasticity, non-linear elasticity, etc. (cf. Grammel 1956)).

The second, more restricted meaning indicates a branch of the mathematical theory of elasticity, which has been developed in the beginning of this century by a number of Italian mathematicians—scientists of whom especially V. Volterra (1907) and C. Somigliana (1908, 1914–15) should be mentioned. While the original investigators used the word "distorsioni", the term "dislocation" in this connection was introduced by A. E. H. Love (1944). The early investigators were chiefly concerned with states of stress in multiply connected bodies (cf. Volterra 1907) but it can be seen easily that this theory of dislocations performs for the Navier equations of elasticity the same task which the theory of surface distributions of poles and dipoles performs for the Laplace equation. To distinguish the second meaning from the solid state physics it may be convenient to call it the elasticity theory of dislocations (E.T.D.).

While this separation in two theories seems useful for our purpose it should not be imagined that the theories were developed independently; on the contrary, the progress in solid state physics was, and still is to some extent, dependent on the results of the E.T.D.

In this paper we shall be concerned only with the E.T.D. There are, no doubt, in the dislocation theory of solid state physics several ideas and suggestions which may also find application in geophysics. However, a large number of the problems arise from explicit consideration of the crystal lattice, and this type of problem seems to be of little direct importance in geophysics, where the length scales are so large compared with the atomic distances in a crystal that the continuum assumptions need not be questioned.

It is expected that the E.T.D. may be useful in geophysics for several reasons: (i) it will provide quantitative answers to some questions, (ii) it unifies certain methods and results already in use, (iii) it introduces the clarity which is characteristic of a mathematical model.

To obtain this clarity, however, a price has to be paid; to make the situation amenable to mathematical treatment simplifications have to be made, and as is usual in mathematical physics only those features can be retained which are believed to be of major importance. For our case this means that we shall omit the curvature of the earth, its gravity, temperature, magnetism, and non-homogeneity and shall concern ourselves with an infinite or semi-infinite homogeneous and isotropic medium where the laws of the classical theory of elasticity hold. While it is no doubt true that in this way several of the interesting features are discarded it has to be admitted that we gain in simplicity and clarity so that we shall be able to investigate certain features with great precision.

A further restriction we impose is that only static problems will be considered. This implies that, for example, the waves and other transient features

associated with earthquakes will not be discussed. The formulae we use can be generalized to the dynamic case but the complexity of the mathematical expressions increases considerably and it seemed therefore reasonable to consider first the more elementary static case. It should be pointed out that the solutions in the dynamical case are in general composed of at least two parts, the *P*- and *S*-waves. In the static case these two parts merge and become undistinguishable. It is therefore necessary to take a certain amount of care in extrapolating results obtained here to the dynamic case. In particular it should be noticed that there are in the following pages several cases where results obtained for static situations are confronted with seismological material. The conclusions drawn in such cases can only be considered as tentative. Dynamical calculations will be necessary to confirm these conclusions.

The further content of this paper is divided in eight sections. In Section 2 we discuss the general theory in some detail and point out the significance of the *A*- and *B*-nuclei for the theory of dislocations. We further draw attention to the fact that the models used by seismologists fit in a natural way in the framework of the elasticity theory of dislocations. Section 3 deals with Galerkin vectors. We prove the equivalence of the static nuclei *B* and *D* and extend the use of the Galerkin vector slightly further. In Section 4 we recompute the displacement field and stress field of a Griffith crack to show that this crack may be considered as a special type of dislocation. In Section 5 some properties of *B*- and *C*-nuclei are investigated. An additional argument is given in support of certain conclusions of Honda while a feature emerges which may throw some light on experiments of Press.

In Section 6 the strain energy of the dislocation is discussed and the fundamental theorem of Colonnetti is proved. Some of the restrictions of the theory of dislocations in its present form are pointed out. In Section 7 the displacement field at the surface of a semi-infinite medium which contains a certain *B*-nucleus at depth c is discussed. In Section 8 some general remarks on the elasticity theory of dislocations are made.

2. FUNDAMENTAL CONSIDERATIONS

Geologists and geophysicists distinguish faults usually in thrust faults, transcurrent faults, and normal faults (cf. Anderson 1942). The distinction depends on the orientation and the displacements of the fault faces with respect to the surface of the earth. The essential elements these faults all possess are the two faces of the fault which were created originally by fracture of the material. After the fracture, or while the fracture propagated, the fault faces suffered, in addition, a displacement with respect to each other. It is usually assumed that largely the same process takes place in the focus of an earthquake (Byerly 1955; Scheidegger 1957).

In the E.T.D. the following situation is considered; in an infinite or finite elastic body, which may be unstrained and at rest, the following largely fictitious process is performed: imagine an open surface Σ which may be situated entirely in the interior of the body. A cut is made over Σ, and the two faces of the cut, which we denote as Σ^+ and Σ^-, are deformed in different

ways by applying some force distributions to them. If these force distributions are in static equilibrium the deformed state shall again be an equilibrium state and the situation created in this manner we call a dislocation over Σ.

If the body is already strained to begin with, the process here described has to be extended in this way that, while the cut is made, forces equal to the original forces acting across Σ have to be introduced on the two faces of the cut to maintain the original equilibrium state.

It is clear that this process is largely identical with the geological process which is supposed to have taken place at a fault. In particular if the time in which the whole process took place is very small, so that inertia effects become of importance, it corresponds roughly with an earthquake.

To make the description more exact we denote the components of the elastic displacement vector by u_i $(i = 1, 2, 3)$ and the components of the stress tensor by τ_{ij} where

$$\tau_{ij} = \lambda\delta_{ij}\, u_{k,k}+\mu(u_{i,j}+u_{j,i}), \tag{2.1}$$

λ and μ are Lamé's constants, δ_{ij} is the Kronecker symbol, and $u_{i,j} = \partial u_i/\partial x_j$ where x_j $(j = 1, 2, 3)$ is a Cartesian coordinate.

Following Sokolnikoff and Specht (1946) we denote the force per unit area on a surface element as

$$\overset{\nu}{T}_i = \tau_{ij}\nu_j, \tag{2.2}$$

where ν_j's $(j = 1, 2, 3)$ denote the direction cosines of the normal to the surface element.

The dislocation is then determined by the shape of the surface Σ and by the discontinuity Δu_i in the components of the displacement vector across the cut, that is

$$\Delta u_i = u_i{}^+ - u_i{}^-, \tag{2.3}$$

where $u_i{}^+$ is the displacement vector for a point P^+, originally being in P on Σ but now situated on Σ^+, and where $u_i{}^-$ is the displacement vector for the corresponding point P^-, which is now on Σ^-. It is clear that the edge σ of Σ shall be a singularity in general; Δu_i is not necessarily zero at the edge, and in that case the displacement components are not uniquely determined there.

We shall restrict the deformations of Σ^+ and Σ^- to infinitesimal deformations. The requirement that the final state of the body with a dislocation over Σ is an equilibrium state can then simply be written as

$$\Delta\overset{\nu}{T}_i = \overset{\nu}{T}_i{}^+ + \overset{\nu}{T}_i{}^- = 0, \tag{2.4}$$

where the forces are taken in the direction of the outside (or inside) normals to both Σ^+ and Σ^-. It should be noted that the outside normal to Σ^+ is inside normal to Σ^- and vice versa. We shall, following some other authors (cf. Eshelby 1951–52), distinguish between two types of dislocations:

(i) Volterra dislocations (also called dislocations of Volterra–Weingarten),

(ii) Somigliana dislocations.

In the first case the discontinuity in the displacement components is prescribed to be

$$\Delta u_i = u_i^+ - u_i^- = U_i + \Omega_{ij} x_j, \qquad \Omega_{ij} = -\Omega_{ji}, \tag{2.5}$$

where U_i and Ω_{ij} are constants. The relation (2.5), which is the well-known Weingarten relation, states that the discontinuity Δu_i across Σ should be of the type of a rigid body displacement. In solid state physics one usually considers the case $\Omega_{ij} = 0$, and U_i is then called the Burgers vector.

In the case of a Somigliana dislocation Δu_i can have any form, provided the forces which maintain the dislocation do not violate the relations (2.4). For a Volterra dislocation, the relations (2.4) are automatically satisfied since a rigid body displacement does not generate any strains and stresses.

In case the body was unstrained to begin with, it will be strained once the dislocation is made, as there is a force distribution acting upon Σ^+ and Σ^- to keep the faces in their deformed position.*

The formulae for the displacement field in an infinite elastic medium strained by a dislocation over a surface Σ was obtained by Volterra (1907). It may be useful to outline how this relation is obtained.

We begin with the reciprocal theorem of Betti, which is a relation between two possible but different displacement fields and stress fields for a particular elastic body. Both displacement fields are supposed to satisfy the equilibrium equations and the theorem can then be written in our notation as

$$\int\int_S \{u_i^{(1)} \overset{\nu}{T}_i^{(2)} - u_i^{(2)} \overset{\nu}{T}_i^{(1)}\} dS = 0, \tag{2.6}$$

where the superscripts inside parentheses refer to the two different displacement and stress fields.

One of the two displacement fields is now taken to be the field described by the Somigliana tensor $u_i^k(P, Q)$ (Steketee 1958).† This displacement field is generated in an infinite elastic medium by a force $\mathbf{F} = 8\pi\mu \mathbf{e}_k$ in Q. If, as we have supposed, the medium is finite, the forces to be supplied on S to obtain the displacement field $u_i^k(P, Q)$ inside the body can be computed in a straightforward fashion. Furthermore it becomes necessary to distinguish the case where Q is outside or inside the body. In the last case a reciprocal theorem is obtained (Love 1944, pp. 245–246), which is, in our notation,

$$u_k(Q) = \frac{1}{8\pi\mu} \int\int_S \{u_i^k(P, Q) \overset{\nu}{T}_i(P) - u_i(P) \overset{\nu}{T}_i^k(P, Q)\} dS. \tag{2.7}$$

*It should be remarked that the process of producing a dislocation has been intentionally simplified here. One finds in the literature several additional rules which make the operation physically more realistic; at the edge of Σ, material may be removed if certain edges are in the way, while it is also usual to add that the faces are again welded together. While these rules may be useful for experiments, they are of no significance for the theory. For the theory it is important that the relations (2.4) are satisfied but whether this is done by a force distribution or by welding cannot be seen in the formulae. As the force distributions more clearly reveal that the body must be strained, the possibility of a welding operation has not been mentioned.

†We shall refer to this paper on several occasions and indicate it further as (St.58). If we refer to a particular formula this will be indicated behind the reference.

If we apply this theorem to an elastic body which is stressed by a dislocation over Σ while the outer surface S is left free from forces, it is clear that the integration has to be extended over Σ^+ and Σ^- in addition to the outer surface S of the body. If we reverse the normal to one of the two faces Σ^+ or Σ^- and keep in mind that (2.4) is satisfied we obtain easily the expression

$$u_k(Q) = \frac{-1}{8\pi\mu}\int\int_S u_i \overset{r}{T}{}_i^k \, dS + \frac{1}{8\pi\mu}\int\int_\Sigma \Delta u_i \overset{r}{T}{}_i^k \, d\Sigma, \tag{2.8}$$

which expresses the displacement components in a point Q in the body in the discontinuity Δu_i across Σ and the displacements of the outer surface S. The first integral vanishes if we assume that S recedes to infinity requiring at the same time that Q is not at infinity, and Σ has no points at infinity either. In this way we arrive at the formula of Volterra,

$$u_k(Q) = \frac{1}{8\pi\mu}\int\int_\Sigma \Delta u_i \, \tau_{ij}^k \, (P, Q) \, \nu_j \, d\Sigma. \tag{2.9}$$

The discontinuity Δu_i has not been prescribed and the relation therefore holds for both Volterra and Somigliana dislocations. In the case of a Volterra dislocation it is usual to substitute (2.5) in (2.9) and write the expression as the sum of six "distorsions élémentaires" (St.58—2.7). In particular, if the 3 Ω_{ij}'s vanish it can be shown (cf. Burgers 1939) that the displacement field does not depend on the actual shape of Σ but only on the shape of the edge σ of Σ. This theorem, which is analogous to a result for uniform dipole distributions over a surface in potential theory, is of great importance in solid state physics.

If we repeat the derivation once again but starting from an initial state in which the body is already strained, the same result (2.9) is obtained, provided no additional forces are applied on S when the dislocation is made. This indicates that the displacement field associated with a dislocation over Σ is independent of the initial state of stress and strain. This result, which is of interest for applications to geophysics, will be discussed further in Section 6.

In the derivation of (2.9) $\tau_{ij}^k(P, Q)$ was considered as the ij-component of the stress tensor generated by a force $8\pi\mu\mathbf{e}_k$ in Q. It was shown in the preceding paper (St.58), and can be traced back to a paper of Love (1903–04), that $\tau_{ij}^k(P, Q)$ may be considered for fixed i and j and up to a dimensional constant with dimension $\Delta u_i/\mu$ as the k-component of the displacement vector in Q generated by a combination of strain nuclei in P; in the case $i = j$ this is a combination of a center of compression and an additional double force without moment in the i-direction; in the case $i \neq j$ it is a combination of two coplanar, mutually perpendicular double forces with moments. If we denote by a sphere a center of compression or expansion which is a combination of three equal, mutually perpendicular double forces without moments, the two combinations may be schematically represented as they are in Fig. 1, (A) and (B). It will be convenient to refer to the two combinations as an A- and B-nucleus. It follows that the displacement component $u_k(Q)$ in (2.9) may be considered as the resultant effect of a distribution of A- and B-nuclei over Σ. The magni-

tude of the contribution of a particular combination of nuclei in a point P on Σ to the displacement components in Q depends both on the local values of

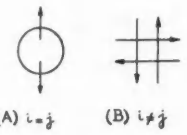

FIG. 1.

Δu_i and the orientation of the surface element $d\Sigma$ with respect to Q and the direction considered in Q. To clarify this further, consider a surface element $d\Sigma$ of Σ with normal in the x_3-direction. Its contribution to the displacements in Q is

$$du_k(Q) = \frac{1}{8\pi\mu}(\Delta u_1 \tau^k_{13} + \Delta u_2 \tau^k_{23} + \Delta u_3 \tau^k_{33})\, d\Sigma. \tag{2.10}$$

It is clear that Δu_1 and Δu_2, which are in directions perpendicular to the normal, may be called the slip, while Δu_3 represents the discontinuity in displacement of the two faces $d\Sigma^+$ and $d\Sigma^-$ in the direction of their normal. The effect of the slip can be described by nuclei of type B while the effect of the normal discontinuity is described by a nucleus A.

Owing to the transformation properties of $\tau^k_{ij}(P, Q)$ the same explanation holds from point to point on Σ; the effect of a normal discontinuity is represented by a type A nucleus, a slip discontinuity is represented by a type B nucleus. It is then also clear that the effect of a slip fault in our model is represented by a distribution of B-nuclei over the fault plane.

If Δu_i, which varies already from point to point on Σ, varies also with time, the effect is similar to changing the strength or intensity of the nuclei on Σ with time. In that case we are no longer justified in using the static nuclei derived from the Somigliana tensor but we have to use the dynamical strain nuclei discussed by Love (1903–04; 1944, pp. 304–307). With the introduction of these dynamical nuclei we also introduce the two types of elastic waves and the situation created in this way is essentially the model of an earthquake. It has to be pointed out that a detailed investigation of the dynamical case has still to be undertaken; while the generalizations mentioned here seem reasonable it is not impossible that in the general case also other terms appear which have to vanish in the static case as a result of the relation (2.4).

It is, however, interesting to see how the theory of dislocations confirms the methods used for describing the mechanism in the focus of earthquakes. The focus of an earthquake is small compared with the dimensions of the earth so that the focus is usually taken to be a point or, if more detailed information is wanted, it is enclosed in a small sphere, the focal sphere. To describe what happens in the focus several mechanisms have been investigated, all built up from certain strain nuclei (cf. Nakano 1923). It is usually agreed

that the three types in Fig. 2 approximate the phenomena observed most closely.

FIG. 2.

It is clear that type B is the dynamical counterpart of nucleus B in Fig. 1, which is necessary to describe a slip fault. It was mentioned by Honda (1957) that the displacement fields of nucleus D and B in Fig. 2 are the same. A very simple proof for this equivalence, but valid only for the case of static nuclei, will be given in the next section.

There has been some uncertainty among seismologists (Honda 1957; Hodgson 1957) whether the nuclei D and B or the nucleus C in Fig. 2 is the most significant. Some remarks about this problem can be found in Section 5 of this paper.

Among other theories for the mechanism of earthquakes there is a theory of Ishimoto (1932) (cf. also Byerly 1942) which suggests that the sudden motion of magma, ejected from a cavity into the rocks of least resistance, is the origin of an earthquake. It seems possible that the results obtained here might provide a test for this theory; if the magma suddenly forces itself into cracks and crevasses in the wall of the cavity, and if indeed this should be the major feature of the earthquake, it is clear that the mechanism is essentially described by dynamic A-nuclei. The seismograms should show the features of such a nucleus which can be easily investigated with the formulae of Love for a dynamic strain nucleus.

3. GALERKIN VECTORS

It was shown in the preceding paper (St.58) that the expressions we have to consider can be put in a very compact form if Galerkin vectors are used. The Galerkin vector $\mathbf{\Gamma} = \Gamma_i \mathbf{e}_i$ is defined as a vector from which a displacement field $\mathbf{u} = u_i \mathbf{e}_i$, satisfying the Navier equations, is obtained by differentiation according to a linear second-order differential operator, that is

$$\mathbf{u} = (\Delta - \alpha \text{ grad div})\, \mathbf{\Gamma}. \tag{3.1}$$

In this expression Δ is the Laplace operator, grad and div the well-known vector operators, and $\alpha = (\lambda+\mu)/(\lambda+2\mu)$. The operator in (3.1) is constructed by combining certain operators, which, each on their own, are invariant under rotations. It follows that the operator in (3.1) is also invariant under rotations.

It was previously shown (St.58) that each component Γ_i is a biharmonic function, that is

$$\Delta\Delta\Gamma_i = 0. \tag{3.2}$$

Further, it is trivially obvious that two displacement fields will be the same

if the components of their Galerkin vectors are the same. Because of the rotational invariance of the operator in (3.1), this theorem still holds if the components of the Galerkin vectors become identical only after a rotation of the coordinate system.

The converse of this theorem, which states that the same displacement fields have the same Galerkin vectors, is, however, not true, as was shown by Westergaard (1952).

We shall use the preceding theorem to show that the displacement fields represented by the nuclei D and B in Fig. 2 are identical, by showing that their Galerkin vectors are the same.

We have seen in the preceding paper (St.58) that the displacement field generated in an infinite elastic medium by a force $\mathbf{F} = 8\pi\mu\mathbf{e}_k$ at O is obtained from the Galerkin vector

$$\mathbf{\Gamma} = r\mathbf{e}_k, \tag{3.3}$$

where r is the distance to O.

The displacement fields of double forces are obtained by differentiation of the single-force displacement field. It is then clear that the Galerkin vector for the static nucleus B in Fig. 2 (or Fig. 1) is given by

$$\mathbf{\Gamma} = -r_{,2}\,\mathbf{e}_1 - r_{,1}\,\mathbf{e}_2. \tag{3.4}$$

Rotation of the axes over an angle of 45° around the x_3-axis gives us the transformation formulae

$$x_1^* = \frac{1}{\sqrt{2}}(x_1+x_2), \qquad \mathbf{e}_1 = \frac{1}{\sqrt{2}}(\mathbf{e}_1^*-\mathbf{e}_2^*), \tag{3.5}$$

$$x_2^* = \frac{1}{\sqrt{2}}(x_2-x_1), \qquad \mathbf{e}_2 = \frac{1}{\sqrt{2}}(\mathbf{e}_1^*+\mathbf{e}_2^*).$$

Transforming the vector in (3.4) with (3.5) gives us on the new set of axes

$$\mathbf{\Gamma} = -r_{,1}\mathbf{e}_1^*+r_{,2}\mathbf{e}_2^*, \tag{3.6}$$

where the subscripts stand for differentiations with respect to x_1^* and x_2^*. This Galerkin vector is recognized as a combination of two mutually perpendicular double forces without moments, which is represented by nucleus D in Fig. 2. (It is easily checked that also the sign of the double forces is correct; the double force along $\mathbf{e}_2^*$ compressive in the x_2 direction, etc.). The Galerkin vectors (3.4) and (3.6) which are the Galerkin vectors for the nuclei B and D respectively are therefore the same and it follows from the theorem stated before that the displacement fields also are the same.

In the preceding paper (St.58) we have also indicated that the Somigliana tensor $u_i^k(P, Q)$ can be obtained from the Galerkin tensor

$$\Gamma_i^k(P, Q) = \delta_i^k r = \delta_{ik} r, \tag{3.7}$$

where r is the distance $\overline{PQ}$. It was shown further that the displacement field $\tau_{ij}^k(P, Q)$ with i and j fixed can be obtained from the Galerkin tensor

$$\Gamma^k_{ij}(P, Q) = \lambda\delta_{ij}\, r_{,i} + \mu(\delta_{ik}\, r_{,j} + \delta_{jk}\, r_{,i}), \tag{3.8}$$

where i and j have to be kept fixed.

It may be convenient to extend this process a step further and to consider also the Galerkin vector $\Gamma_k(Q)$ of the displacement field generated by a dislocation over Σ. If the differentiations under the integration sign may all be performed, and in general this will be the case, we can write

$$\Gamma_k(Q) = \frac{1}{8\pi\mu}\int\int_\Sigma \Delta u_i\, \Gamma^k_{ij}(P, Q)\, \nu_j\, d\Sigma. \tag{3.9}$$

This relation shows a formal analogy with the expression (2.9). Differentiation of (3.9) according to (3.1) will give in general the displacement field (2.9). While the Galerkin vector has little interest for its own sake, the relation (3.9) may be useful as the integrations in (3.9) will be usually simpler than the integrations in (2.9).

4. THE GRIFFITH CRACK

In this section we consider a two-dimensional problem, which has received a certain amount of attention in the literature. Its direct geophysical significance is only small. (It is mentioned in Anderson (1942) in relation to the fracture of rocks.)

Some thirty years ago Griffith (1921–24) put forward a theory of fracture for materials like glass based on the assumption that the surface of the material contains a large number of cracks. To compute the stresses and strains associated with such a crack, Griffith used an analysis of Inglis (1913) in which is considered the two-dimensional problem of the equilibrium of an elastic medium containing a thin elliptic crack which is being opened by a uniform pressure. The solution of the problem is in this case obtained by using the confocal coordinates of Lamé, in which the crack is the limiting ellipse. The same case, with some generalizations, has been recomputed twice by I. N. Sneddon, the first time (Sneddon 1946) by using a stress function due to Westergaard, the second time (Sneddon and Elliott 1946) by using a Fourier transform method. Green and Zerna (1954) solve the problem with special complex variable methods.

Here we shall show that the Griffith crack can also be considered as a type of Somigliana dislocation. It is our main concern to show that this crack problem, and therefore also other crack problems (Sack 1946; Starr 1928) can be put in terms of dislocation theory and we shall restrict ourselves, therefore, to a reconstruction of the formulae for the displacement and stress field. For further details and discussions on the physical significance the reader may be referred to the literature which has been mentioned.

The problem under consideration is two-dimensional and one may therefore begin with the computation of the two-dimensional Somigliana tensor. It turns out to be slightly easier to consider the two-dimensional crack as the limiting case of a three-dimensional crack which stretches in one direction to infinity. In this way we define the Griffith crack as a dislocation for which Σ

is the strip $|x_1| \leqslant c \quad x_2 = 0 \quad |x_3| \leqslant \infty$ while the discontinuity in displacement is given by

$$\Delta u_1 = \Delta u_3 = 0 \qquad \Delta u_2 = \frac{p_0}{\mu\alpha}\sqrt{(c^2-x_1^2)}. \tag{4.1}$$

It will be found that p_0 in (4.1) is the pressure in the crack.

The normal to Σ is clearly in the x_2-direction and the general expression (2.9) from which the displacement field generated by the crack is determined reduces to

$$u_k(Q) = \frac{1}{8\pi\mu}\int_{-c}^{+c} dx_1 \int_{-\infty}^{+\infty} dx_3 \, \Delta u_2 \, \tau_{22}^k(P, Q), \tag{4.2}$$

where P denotes a point $(x_1, 0, x_3)$ on Σ and Q a point $(y_1, y_2, 0)$. The choice $y_3 = 0$ leaves the generality of the problem unimpaired.

The stress $\tau_{22}^k(P, Q)$, which can also be considered as the displacement vector generated by a nucleus of type A (Fig. 1) has to be obtained from the Somigliana tensor (St.58—2.1). We find

$$\tau_{22}^k(P, Q) = 2\lambda(1-\alpha)\left(\frac{1}{r}\right)_{,k} + 4\mu\delta_{2k}\left(\frac{1}{r}\right)_{,2} - 2\mu\alpha r_{,22k} \tag{4.3}$$

where $r = \sqrt{\{(y_1-x_1)^2+y_2^2+x_3^2\}}$ while we further remember that

$$r_{,i} = \frac{\partial r}{\partial x_i} = -\frac{\partial r}{\partial y_i} = -r^{,i}. \tag{4.4}$$

It is clear from (4.2) and (4.3) that the calculation of the displacement field requires the evaluation of six integrals. Two of these integrals vanish, however, as their integrands contain derivatives to x_3. It follows that $u_3(Q) = 0$ and the problem is then clearly a case of plain strain. The four remaining integrals are

$$\begin{aligned}
I_1 &= \int_{-\infty}^{+\infty} dx_3 \int_{-c}^{+c} dx_1 \sqrt{(c^2-x_1^2)}\left(\frac{1}{r}\right)_{,1}, \\
I_2 &= \int_{-\infty}^{+\infty} dx_3 \int_{-c}^{+c} dx_1 \sqrt{(c^2-x_1^2)}\left(\frac{1}{r}\right)_{,2}, \\
I_3 &= \int_{-\infty}^{+\infty} dx_3 \int_{-c}^{+c} dx_1 \sqrt{(c^2-x_1^2)} r_{,221}, \\
I_4 &= \int_{-\infty}^{+\infty} dx_3 \int_{-c}^{+c} dx_1 \sqrt{(c^2-x_1^2)} r_{,111}.
\end{aligned} \tag{4.5}$$

With this notation the two remaining displacement components can be written

$$\begin{aligned}
u_1(Q) &= \frac{p_0}{4\pi\alpha\mu^2}\{\lambda(1-\alpha)I_1 - \mu\alpha I_3\}, \\
u_2(Q) &= \frac{p_0}{4\pi\alpha\mu^2}\{\mu(2\alpha+1)I_2 - \mu\alpha I_4\}.
\end{aligned} \tag{4.6}$$

The integrals in (4.5) can be reduced to some different forms if we use the well-known expression

$$\lim_{L\to\infty}\int_{-L}^{+L}\frac{dx_3}{\sqrt{(x_1^2+x_2^2+x_3^2)}}=-2\ln\sqrt{(x_1^2+x_2^2)}. \tag{4.7}$$

One obtains then easily

$$\begin{aligned}
I_1 &= -2\int_{-c}^{+c}dx_1\sqrt{(c^2-x_1^2)}\,\frac{x_1-y_1}{\rho^2},\\
I_2 &= \quad 2\int_{-c}^{+c}dx_1\sqrt{(c^2-x_1^2)}\,\frac{y_2}{\rho^2},\\
I_3 &= -2\int_{-c}^{+c}dx_1\sqrt{(c^2-x_1^2)}\,\frac{x_1-y_1}{\rho^2}+2\int_{-c}^{+c}\frac{y_2^2}{\rho^2}d(\sqrt{(c^2-x_1^2)}),\\
I_4 &= \quad 4\int_{-c}^{+c}dx_1\sqrt{(c^2-x^2)}\,\frac{y_2}{\rho^2}+2\int_{-c}^{+c}\frac{y_2(x_1-y_1)}{\rho^2}d(\sqrt{(c^2-x_1^2)}).
\end{aligned} \tag{4.8}$$

Substitution of (4.8) into (4.6) and some further elementary reductions enable us to put (4.6) in the form

$$\begin{aligned}
u_1(Q) &= \frac{p_0}{2\pi\mu\alpha}\{-(1-\alpha)\pi y_1+[y_2^2+(1-\alpha)(c^2-y_1^2)]\,I_5\\
&\qquad +(1-\alpha)y_1(r^2-c^2)\,I_6\},\\
u_2(Q) &= \frac{p_0}{2\pi\mu\alpha}\{-(1-\alpha)\pi y_2-(2-\alpha)y_1y_2\,I_5+[(1-\alpha)r^2+c^2]y_2\,I_6\},
\end{aligned} \tag{4.9}$$

where

$$\begin{aligned}
I_5 &= \int_{-c}^{+c}\frac{x_1dx_1}{(x_1^2-2y_1x_1+r^2)\sqrt{(c^2-x_1^2)}},\\
I_6 &= \int_{-c}^{+c}\frac{dx_1}{(x_1^2-2y_1x_1+r^2)\sqrt{(c^2-x_1^2)}},
\end{aligned} \tag{4.10}$$

and r^2 denotes now $r^2=y_1^2+y_2^2$. To evaluate the two remaining integrals we introduce the complex variables

$$z=y_1+iy_2=re^{i\theta},\qquad \bar{z}=y_1-iy_2=re^{-i\theta}. \tag{4.11}$$

It is then easily found that

$$\begin{aligned}
I_5 &= \frac{i\pi}{2y_2}\left\{\frac{z}{\sqrt{(z^2-c^2)}}-\frac{\bar{z}}{\sqrt{(\bar{z}^2-c^2)}}\right\}=-\frac{\pi}{y_2}\mathscr{I}\left\{\frac{z}{\sqrt{(z^2-c^2)}}\right\},\\
I_6 &= \frac{i\pi}{2y_2}\left\{\frac{1}{\sqrt{(z^2-c^2)}}-\frac{1}{\sqrt{(\bar{z}^2-c^2)}}\right\}=-\frac{\pi}{y_2}\mathscr{I}\left\{\frac{1}{\sqrt{(z^2-c^2)}}\right\}.
\end{aligned} \tag{4.12}$$

Using the results of (4.12) we can finally put the displacement components in the form:

$$\begin{aligned}
u_1(Q) &= \frac{p_0}{2\mu\alpha}\left\{-(1-\alpha)y_1+\frac{1-\alpha}{2}y_1B^+-\frac{iy_2}{2}B^--\frac{(1-\alpha)c^2}{2}A^+\right\},\\
u_2(Q) &= \frac{p_0}{2\mu\alpha}\left\{-(1-\alpha)y_2+\frac{1-\alpha}{2}y_2B^+-\frac{iy_1}{2}B^-+\frac{ic^2}{2}A^-\right\},
\end{aligned} \tag{4.13}$$

where

$$A^+ = \frac{1}{\sqrt{(z^2-c^2)}} + \frac{1}{\sqrt{(\bar{z}^2-c^2)}}, \qquad B^+ = \frac{z}{\sqrt{(z^2-c^2)}} + \frac{\bar{z}}{\sqrt{(\bar{z}^2-c^2)}},$$
$$A^- = \frac{1}{\sqrt{(z^2-c^2)}} - \frac{1}{\sqrt{(\bar{z}^2-c^2)}}, \qquad B^- = \frac{z}{\sqrt{(z^2-c^2)}} - \frac{\bar{z}}{\sqrt{(\bar{z}^2-c^2)}}. \tag{4.14}$$

Once the displacement field is known the strains and stresses can be found by straightforward differentiations. It is easily computed that

$$\begin{aligned} \tau_{11}(Q)+\tau_{22}(Q) &= p_0(B^+-2), \\ \tau_{11}(Q)-\tau_{22}(Q) &= -ip_0\, y_2\, c^2\, C^-, \\ \tau_{12}(Q) &= \tfrac{1}{2}\, p_0\, c^2\, y_2\, C^+ \end{aligned} \tag{4.15}$$

where C^+ and C^- stand for

$$C^+ = \frac{1}{\sqrt{(z^2-c^2)^3}} + \frac{1}{\sqrt{(\bar{z}^2-c^2)^3}}, \qquad C^- = \frac{1}{\sqrt{(z^2-c^2)^3}} - \frac{1}{\sqrt{(\bar{z}^2-c^2)^3}}. \tag{4.16}$$

To compare these relations with the formulae of Sneddon we put

$$z-c = r_1\, e^{i\theta_1}, \qquad z+c = r_2\, e^{i\theta_2}. \tag{4.17}$$

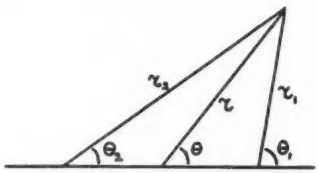

FIG. 3.

With these notations and (4.11) the relations (4.16) can be put in the form

$$\begin{aligned} \tau_{11}(Q)+\tau_{22}(Q) &= 2p_0\left\{\frac{r}{\sqrt{r_1 r_2}}\cos(\theta-\tfrac{1}{2}\theta_1-\tfrac{1}{2}\theta_2)-1\right\}, \\ \tau_{11}(Q)-\tau_{22}(Q) &= -2p_0\frac{r}{c}\left(\frac{c^2}{r_1 r_2}\right)^{3/2}\sin\theta\,\sin\frac{3}{2}(\theta_1+\theta_2), \\ \tau_{12}(Q) &= p_0\frac{r}{c}\left(\frac{c^2}{r_1 r_2}\right)^{3/2}\sin\theta\,\cos\frac{3}{2}(\theta_1+\theta_2). \end{aligned} \tag{4.18}$$

It is easily seen that the relations (4.18) are the same formulae which appear on p.428 of Sneddon (1951). Sneddon has taken the crack along the x_2-axis, and the angles θ_1, θ, and θ_2 are measured from the normal to the crack in his case. It is immediately seen that for points on the crack we have

$$\tau_{11}(Q)-\tau_{22}(Q) = 0, \qquad \tau_{11}(Q)+\tau_{22}(Q) = -2p_0, \tag{4.19}$$

which shows that p_0 is the pressure in the crack.

5. DOUBLE FORCES WITH MOMENTS

In the preceding section we discussed a particular distribution of nuclei of type A. Here we shall be concerned with the nuclei B and C. It has been remarked at the end of Section 1 that there is some uncertainty among seismologists whether the mechanism in an earthquake is best approximated by the equivalent nuclei B and D in Fig. 2, or whether type C is the most proper representation (cf. Honda 1957); while most of the Japanese investigators favor mechanisms represented by B- or D-nuclei, there seem to be several indications from Russian work which favor C-nuclei (Hodgson 1957; Scheidegger 1957).

If the nuclei B and C are compared, a significant dynamical difference is noticed; while the nucleus B is in equilibrium, the nucleus C is not. If we compute the displacement and stress field associated with a static B nucleus and, moreover, calculate the resulting force and moment on a part of the elastic medium containing the nucleus, it is found that the resulting force and moment both vanish. If the same is done for a static C nucleus it is found that equilibrium of the medium is maintained only by a moment on the surface of the medium containing the C nucleus.

In the case of dynamic nuclei the situation is more complicated and we cannot give such a simple argument. Firstly the two couples of the B nucleus may vary with time in different ways. In this case it may be preferable to speak of two different and mutually perpendicular C nuclei, but it is clear that this phase difference will leave, in general, a resulting moment which disturbs the equilibrium. Secondly, if we consider an elastic body which is different from a sphere with the nucleus at the center the P- and S-waves reach different points on the surface at different times. If we integrate the forces over the surface at a particular instant it is clear that there will be no equilibrium in general; parts of the surface may still be undisturbed while other parts have already been reached and strained by the P- and S-waves.

To associate this result with the mechanics of earthquakes we recall that the information, from which conclusions concerning earthquakes are drawn, is mainly the sign and time of arrival of the first P-, S-, and other phases which supposedly left the focus at the initial moment of the collapse. This information may be supplemented with visual observations and with results from triangulations before and after the earthquake.

From the idealized situation in the theory of dislocations we have found that the equilibrium state of a slip fault is described by a distribution of static B-nuclei. It must be considered improbable that the equilibrium state can be represented by a distribution of static C-nuclei as an additional moment will be required which has to be supplied at the surface of the medium (in our case at the earth's surface) to maintain equilibrium. The statement has been qualified as improbable since one can imagine special configurations in which some C-nuclei will not disturb the equilibrium, while it must also be remembered that the earth is not at rest but performs complicated motions which may accelerate or decelerate slightly as a result of some unbalanced moments inside the earth.

If we omit, however, these special configurations and neglect also the motion of the earth we conclude that the slip fault in the focus of the earthquake can only be described by a distribution of B-nuclei once equilibrium has been established. The information obtained from triangulations is therefore expected to favor the model with the B-nucleus.

The first arrivals of P- and S-waves give information which concerns a non-equilibrium state, for the occurrence of the earthquake is essentially the collapse of equilibrium. So far as this information is concerned there is no à priori reason to prefer either the B- or C-nucleus. If, however, the information of first arrivals would indicate the C-nuclei as the proper mechanism, it is still true that in the final equilibrium position there must be B-nuclei, which means that between the initial collapse and the final equilibrium state a second couple has to be supplied at the focus. The most reasonable way to generate this second couple is a rotation of the fault plane, giving compressions in certain quadrants and dilatations in other quadrants, all together resulting in the required couple.

We arrive, therefore, at the following suggestion: if the information from seismic waves favors a mechanism with C-nuclei it must be assumed that in addition to slipping of the fault faces, a rotation of the fault plane takes place before equilibrium is re-established. If the information from seismic waves favors a mechanism with B-nuclei it must be assumed that slipping of the fault faces over each other will suffice to reach a new equilibrium state. It follows also that it must be possible to obtain a mechanism which favors two mutually perpendicular C-nuclei of unequal strength, which reach equality as a result of rotation of the fault plane at the time that equilibrium is re-established.

To illustrate some of the differences between the B- and C-nuclei we shall consider some aspects connected with the two nuclei. We begin with a detailed analysis of the displacement and stress field associated with the B- and C-nuclei. Starting from the Somigliana tensor $u_i^k(P, O)$ (St.58—2.1) we obtain easily for the displacement field of a double force with moment

$$
\begin{aligned}
u_i^{1,2}(P, O) &= -2\delta_{1i}\left(\frac{1}{r}\right)_{,2} + \alpha r_{,12i}, \\
u_i^{2,1}(P, O) &= -2\delta_{2i}\left(\frac{1}{r}\right)_{,1} + \alpha r_{,12i}.
\end{aligned}
\tag{5.1}
$$

Expanding these expressions gives us for the C-nucleus

$$
\begin{aligned}
u_1^{1,2}(P, O) &= (2-\alpha)\frac{x_2}{r^3} + 3\alpha\frac{x_1^2 x_2}{r^5}, \\
u_2^{1,2}(P, O) &= -\alpha\frac{x_1}{r^3} + 3\alpha\frac{x_1 x_2^2}{r^5}, \\
u_3^{1,2}(P, O) &= 3\alpha\frac{x_1 x_2 x_3}{r^5},
\end{aligned}
\tag{5.2}
$$

and for the B-nucleus

$$u_1^{1,2}+u_1^{2,1} = 2(1-\alpha)\frac{x_2}{r^3}+6\alpha\frac{x_1^2x_2}{r^5},$$

$$u_2^{1,2}+u_2^{2,1} = 2(1-\alpha)\frac{x_1}{r^3}+6\alpha\frac{x_1x_2^2}{r^5}, \tag{5.3}$$

$$u_3^{1,2}+u_3^{2,1} = 6\alpha\frac{x_1x_2x_3}{r^5}.$$

Substituting cylindrical polars by putting

$$x_1 = \rho\cos\theta, \quad x_2 = \rho\sin\theta, \quad x_3 = x_3, \tag{5.4}$$

we obtain easily for the C-nucleus

$$u_\rho = \left\{(1-\alpha)\frac{\rho}{r^3}+\frac{3}{2}\alpha\frac{\rho^3}{r^5}\right\}\sin2\theta,$$

$$u_\theta = -\frac{\rho}{r^3}+(1-\alpha)\frac{\rho}{r^3}\cos2\theta, \tag{5.5}$$

$$u_3 = \frac{3}{2}\alpha\frac{\rho^2x_3}{r^5}\sin2\theta.$$

For the B-nucleus we obtain in the same way

$$u_\rho = \left\{2(1-\alpha)\frac{\rho}{r^3}+3\alpha\frac{\rho^3}{r^5}\right\}\sin2\theta,$$

$$u_\theta = 2(1-\alpha)\frac{\rho}{r^3}\cos2\theta, \tag{5.6}$$

$$u_3 = 3\alpha\frac{\rho^2x_3}{r^5}\sin2\theta.$$

It is observed that u_ρ reaches for both nuclei extreme values for $\theta = \pi/4$, $3\pi/4$, etc. In case of the B-nucleus, u_θ vanishes for these angles. In case of the C-nucleus, u_θ is composed of two terms, the first one independent of θ, the second similar to u_θ for the B-nucleus. The first term in u_θ is negative and is therefore a displacement in the clockwise direction, corresponding with the sense of the generating couple. For the B-nucleus this constant term has vanished since the second couple contributes a similar term in anticlockwise direction. For $\theta = 0$ we find for the C- and B-nucleus respectively

$$u_\theta = -\alpha\frac{\rho}{r^3}, \qquad u_\theta = 2(1-\alpha)\frac{\rho}{r^3}. \tag{5.7}$$

We see that the displacements on the x_1-axis are in opposite directions, in particular with $\lambda = \mu$ we have $\alpha = 2/3$ and the displacement components are in opposite directions and of equal magnitude.

We compute also the forces and moments with respect to the origin, acting upon a sphere which has O as center. We therefore compute first the stress tensor and then the components T_i of the force, keeping in mind that

$$\nu_j = x_j/r. \tag{5.8}$$

For the C-nucleus we find

$$\tau_{11} = -6\mu(1-\alpha)\frac{x_1x_2}{r^5} - 30\alpha\mu\frac{x_1^3x_2}{r^7},$$

$$\tau_{22} = 6\mu(1+\alpha)\frac{x_1x_2}{r^5} - 30\alpha\mu\frac{x_1x_2^3}{r^7},$$

$$\tau_{33} = 6\mu(1-\alpha)\frac{x_1x_2}{r^5} - 30\alpha\mu\frac{x_1x_2x_3^2}{r^7},$$

$$\tau_{23} = 6\mu\alpha\frac{x_1x_3}{r^5} - 30\alpha\mu\frac{x_1x_2^2x_3}{r^7}.$$

(5.9)
$$\tau_{31} = -6\alpha\mu(1-\alpha)\frac{x_2x_3}{r^5} - 30\alpha\mu\frac{x_1^2x_2x_3}{r^7},$$

$$\tau_{12} = 2\mu(1-\alpha)\frac{1}{r^3} - 6\mu\frac{x_2^2}{r^5} + 6\alpha\mu\frac{x_1^2+x_2^2}{r^5} - 30\alpha\mu\frac{x_1^2x_2^2}{r^7},$$

$$\overset{\nu}{T}_1 = -4\mu(1-\alpha)\frac{x_2}{r^4} - 24\alpha\mu\frac{x_1^2x_2}{r^6},$$

$$\overset{\nu}{T}_2 = 2\mu(1+2\alpha)\frac{x_1}{r^4} - 24\alpha\mu\frac{x_1x_2^2}{r^6},$$

$$\overset{\nu}{T}_3 = -24\alpha\mu\frac{x_1x_2x_3}{r^6}.$$

Because of the odd powers of x_j in $\overset{\nu}{T}_i$ the resulting forces on the surface of the sphere vanish, that is

$$\int \overset{\nu}{T}_i\, dS = 0. \tag{5.10}$$

For the same reason two components of the moment vanish. There remains only the component of the moment vector along the x_3-axis, that is

$$\int_S (x_1\overset{\nu}{T}_2 - x_2\overset{\nu}{T}_1)\, dS = \int_S \left\{2\mu(1+2\alpha)\frac{x_1^2}{r^4} + 4\mu(1-\alpha)\frac{x_2^2}{r^4}\right\} dS. \tag{5.11}$$

Substitution of the spherical polars

$$x_1 = r\sin\theta\cos\phi, \quad x_2 = r\sin\theta\sin\phi, \quad dS = r^2\sin\theta\, d\theta\, d\phi \tag{5.12}$$

reduces (5.11) to the form

$$\int_0^{2\pi} d\phi \int_0^{\pi} d\theta \sin\theta\{2\mu(1+2\alpha)\sin^2\theta\cos^2\phi + 4\mu(1-\alpha)\sin^2\theta\sin^2\phi\}, \tag{5.13}$$

which gives the answer $8\pi\mu$. It is this moment on the surface which maintains the equilibrium of the sphere with the single couple in the center.

Repeating the calculations for the B-nucleus we obtain

$$\tau_{11} = 12\mu\alpha\frac{x_1x_2}{r^5} - 60\alpha\mu\frac{x_1^3x_2}{r^7},$$

$$\tau_{22} = 12\mu\alpha\frac{x_1x_2}{r^5} - 60\alpha\mu\frac{x_1x_2^3}{r^7},$$

$$\tau_{33} = 12\mu(1-\alpha)\frac{x_1x_2}{r^5} - 60\alpha\mu\frac{x_1x_2x_3^2}{r^7},$$

$$\tau_{23} = 6\mu(2\alpha-1)\frac{x_1x_3}{r^5} - 60\alpha\mu\frac{x_1x_2^2x_3}{r^7}.$$

(5.14)
$$\tau_{31} = 6\mu(2\alpha-1)\frac{x_2x_3}{r^5} - 60\alpha\mu\frac{x_1^2x_2x_3}{r^7},$$

$$\tau_{12} = 4\mu(1-\alpha)\frac{1}{r^3} + 6\mu(2\alpha-1)\frac{x_1^2+x_2^2}{r^5} - 60\alpha\mu\frac{x_1^2x_2^2}{r^7},$$

$$\overset{r}{T}_1 = 2\mu(4\alpha-1)\frac{x_2}{r^4} - 48\alpha\mu\frac{x_1^2x_2}{r^6},$$

$$\overset{r}{T}_2 = 2\mu(4\alpha-1)\frac{x_1}{r^4} - 48\alpha\mu\frac{x_1x_2^2}{r^6},$$

$$\overset{r}{T}_3 = -48\alpha\mu\frac{x_1x_2x_3}{r^6}.$$

The last three terms represent again the force components acting upon a sphere with the nucleus in its center. It is easily checked in this case that both the resulting force and the resulting moment vanish.

We finally introduce in the expressions for the B-nucleus spherical polars by means of the relations

(5.15)
$$x_1 = r\cos\theta, \quad x_2 = r\sin\theta\cos\phi, \quad x_3 = r\sin\theta\sin\phi,$$

and compute the components $\overset{r}{T}_r$, $\overset{r}{T}_\theta$, $\overset{r}{T}_\phi$ of the force acting upon a sphere with the nucleus at the center. The expressions $\overset{r}{T}_r$, etc., are obtained from

$$\overset{r}{T}_r = \overset{r}{T}_1\cos\theta + (\overset{r}{T}_2\cos\phi + \overset{r}{T}_3\sin\phi)\sin\theta,$$

(5.16)
$$\overset{r}{T}_\theta = -\overset{r}{T}_1\sin\theta + (\overset{r}{T}_2\cos\phi + \overset{r}{T}_3\sin\phi)\cos\theta,$$

$$\overset{r}{T}_\phi = \overset{r}{T}_3\cos\phi - \overset{r}{T}_2\sin\phi.$$

We obtain then from (5.14) and (5.16)

$$\overset{r}{T}_r = -\mu(20\alpha+1)\frac{\sin2\theta\cos\phi}{r^3},$$

(5.17)
$$\overset{r}{T}_\theta = 2\mu(4\alpha-1)\frac{\cos2\theta\cos\phi}{r^3},$$

$$\overset{r}{T} = -2\mu(4\alpha-1)\frac{\cos\theta\sin\phi}{r^3}$$

It has been suggested (Honda and Masatsuka 1952) that the mechanism of a deep focus earthquake is properly described by an impulsive radial force distribution in a small spherical cavity of radius a, which is determined by

$$(5.18) \qquad (F_r)_{r=a} = F \sin 2\theta \cos\phi \quad (F_\theta)_{r=a} = (F_\phi)_{r=a} = 0,$$

while the mechanism of a shallow earthquake is properly described by a B-nucleus. In a more recent paper, Honda (1957) shows that the wave patterns of the two mechanisms are essentially the same. Inspection of the formulae (5.17), although obtained for only a static case, indicates the same result. For the case $\lambda = \mu$, we have $\alpha = 2/3$ and one finds

$$(5.19) \qquad \mu(20\alpha+1) = 43/3\mu, \quad 2\mu(4\alpha-1) = 10/3\mu,$$

which shows that the radial force exerted on a sphere with the B-nucleus at its center is more than four times as large as the tangential forces; thus the effect of the tangential forces may be easily overlooked in practice and result in formulae of the type (5.18).

We shall now consider a two-dimensional case and begin with the computation of the two-dimensional Somigliana tensor. There are several methods by which this result can be obtained (Love 1944, pp. 208–214). We distribute forces in the x_2-direction along the x_3-axis from $-\infty \leqslant x_3 \leqslant +\infty$ in such a way that the force per unit length is $8\pi\mu\mathbf{e}_2$. Remembering that

$$(5.20) \qquad \lim_{L\to\infty} \int_{-L}^{+L} \frac{dx_3}{\sqrt{x_1^2+x_2^2+x_3^2}} = -2 \ln\sqrt{(x_1^2+x_2^2)},$$

one easily obtains

$$(5.21) \qquad \begin{aligned} u_1^2 &= \int_{-\infty}^{+\infty} dy_3(-\alpha r_{,21}) = 2\alpha(x_2 \ln \rho)_{,1}, \\ u_2^2 &= \int_{-\infty}^{+\infty} dy_3\left(\frac{2}{r}-\alpha r_{,22}\right) = -4 \ln \rho+2\alpha(x_2 \ln \rho)_{,2}, \\ u_3^2 &= \int_{-\infty}^{+\infty} dy_3(-\alpha r_{,23}) = 0, \end{aligned}$$

where $\qquad r = \sqrt{\{x_1^2+x_2^2+(x_3-y_3)^2\}} \qquad \rho = \sqrt{(x_1^2+x_2^2)}.$

In a similar way we find u_1^1 and u_2^1 and the two-dimensional Somigliana tensor. To keep the formulae in this case as simple as possible we normalize them to a force of $4\pi\mu$ instead of $8\pi\mu$ per unit length. The two-dimensional Somigliana tensor then becomes

$$(5.22) \qquad u_i^k(P, O) = -2\,\delta_{ik} \ln \rho+\alpha(x_k \ln \rho)_{,i}.$$

Computing the displacement field of a C- and B-nucleus gives us:

$$(5.23) \qquad \begin{aligned} u_1^{1,2} &= (2-\alpha)\frac{x_2}{\rho^2}+2\alpha\frac{x_1^2 x_2}{\rho^4}, \\ u_2^{1,2} &= -\alpha\frac{x_1}{\rho^2}+2\alpha\frac{x_1 x_2^2}{\rho^4}. \end{aligned}$$

$$
\begin{aligned}
u_1^{1,2}+u_1^{2,1} &= 2(1-\alpha)\frac{x_2}{\rho^2}+4\alpha\frac{x_1^2x_2}{\rho^4},\\
u_2^{1,2}+u_2^{2,1} &= 2(1-\alpha)\frac{x_1}{\rho^2}+4\alpha\frac{x_1x_2^2}{\rho^4}.
\end{aligned}
\tag{5.24}
$$

Substituting polar coordinates $x_1=\rho\cos\theta \quad x_2=\rho\sin\theta$ gives us from (5.23)

$$
\begin{aligned}
u_\rho &= \frac{1}{\rho}\sin 2\theta,\\
u_\theta &= -\frac{1}{\rho}+(1-\alpha)\frac{\cos 2\theta}{\rho}.
\end{aligned}
\tag{5.25}
$$

From (5.24) we obtain

$$
\begin{aligned}
u_\rho &= \frac{2}{\rho}\sin 2\theta\\
u_\theta &= 2(1-\alpha)\frac{\cos 2\theta}{\rho}.
\end{aligned}
\tag{5.26}
$$

It is clear that the displacement fields display the same features we have already found for the three-dimensional *C*- and *B*-nuclei.

We distribute now the two types of two-dimensional nuclei in a uniform fashion along the x_1-axis over the interval $-1 \leqslant y_1 \leqslant +1 \quad y_2 = 0$ and study the displacement field so obtained. The displacement field generated by the *C*-nuclei is determined from

$$
u_k(P) = \frac{U_1}{4\pi}\int_{-1}^{+1} dy_1\, u_k^{1,2}(P, Q). \tag{5.27}
$$

The displacement field generated by the *B*-nuclei is determined from

$$
u_k(P) = \frac{U_1}{4\pi}\int_{-1}^{+1} dy_1\{u_k^{1,2}(P, Q)+u_k^{2,1}(P, Q)\}, \tag{5.28}
$$

which is a special form of the general relation (2.9). The situation considered here may in fact be considered as the expression for the displacement field of a two-dimensional Volterra dislocation with $\Delta u_1 = U_1$, $\Delta u_2 = \Delta u_3 = 0$, while Σ is the strip $|y_1|\leqslant 1 \quad y_2=0 \quad |y_3|\leqslant\infty$. The second term in (5.28) can be integrated immediately. If we denote with Q^+ and Q^- the points $(1, 0)$ and $(-1, 0)$ (5.28) can be written

$$
u_k(P) = \frac{U_1}{4\pi}\left\{u_k^2(P, Q^+)-u_k^2(P, Q^-)+\int_{-1}^{+1} dy_1\, u_k^{1,2}(P, Q)\right\}. \tag{5.29}
$$

Physically this result is clear; the couples $u_k^{2,1}(P, Q)$ all cancel each other inside the interval $-1 \leqslant y_1 \leqslant +1$ in such a way that only two forces at the end-points remain. It is then also clear that in this case the nuclei $u_k^{1,2}(P, Q)$ are responsible for the discontinuity in the displacement field across the x_1-axis in the interval $|y_1| \leqslant 1$, while the second couples are necessary only to maintain the equilibrium. Evaluation of (5.27) using (5.23) gives us the displacement field

$$
\begin{aligned}
u_1(P) &= \frac{U_1}{2\pi}\left\{\tan^{-1}\frac{x_1+1}{x_2}-\tan^{-1}\frac{x_1-1}{x_2}+\frac{\alpha}{2}x_2\left(\frac{x_1-1}{R_1^2}-\frac{x_1+1}{R_2^2}\right)\right\},\\
u_2(P) &= \frac{U_1}{2\pi}\left\{\frac{\alpha}{2}\ln\frac{R_1}{R_2}+\frac{\alpha}{2}x_2^2\left(\frac{1}{R_1^2}-\frac{1}{R_2^2}\right)\right\}.
\end{aligned}
\tag{5.30}
$$

Adding the displacement field

$$u_k^2(P, Q^+)-u_k^2(P, Q^-)$$

to (5.30) results in the displacement field (5.29). That is

$$
\begin{aligned}
u_1(P) &= \frac{U_1}{2\pi}\left\{\tan^{-1}\frac{x_1+1}{x_2}-\tan^{-1}\frac{x_1-1}{x_2}+\alpha x_2\left(\frac{x_1-1}{R_1^2}-\frac{x_1+1}{R_2^2}\right)\right\}\\
u_2(P) &= \frac{U_1}{2\pi}\left\{(1-\alpha)\ln\frac{R_2}{R_1}+\alpha x_2^2\left(\frac{1}{R_1^2}-\frac{1}{R_2^2}\right)\right\}.
\end{aligned}
\tag{5.31}
$$

In these expressions

$$R_1=\sqrt{\{(x_1-1)^2+x_2^2\}}, \qquad R_2=\sqrt{\{(x_1+1)^2+x_2^2\}}.$$

It is easily checked that $u_1(P)$ suffers a discontinuity of magnitude U_1 when crossing the x_1-axis in the interval $|x_1| \leqslant 1$. This result holds for both displacement fields (5.30) and (5.31).

If the stress field is computed it is found that the displacement field (5.30) is maintained only by a moment acting along the circumference of any segment of elastic material which contains the section $|x_1| \leqslant 1$ of the x_1-axis. In the case of (5.31) there is no resulting force or moment acting upon a segment which contains the section $|x_1| \leqslant 1$ of the x_1-axis. It is clear that the moment which keeps the displacement field (5.30) in equilibrium has the magnitude $2\mu U_1$.

If we consider the displacement component $u_2(P)$ on the x_1-axis we find from (5.30) and (5.31) respectively

$$u_2(P)=\frac{U_1\alpha}{4\pi}\ln\frac{R_1}{R_2}, \qquad u_2(P)=-\frac{U_1(1-\alpha)}{2\pi}\ln\frac{R_1}{R_2}. \tag{5.32}$$

It is again clear from these expressions that the displacement components on the x_1-axis are in opposite directions. In particular for $\alpha = 2/3$ their magnitudes are equal. While the displacement of the C-distribution corresponds with the clockwise sense of rotation of the C-nuclei, the displacement component of the B-distribution is in the opposite direction. Although the results here obtained are derived for the statical case only it is not impossible that they may throw some light on certain dynamical experiments performed by Press (1957) which were reported at the recent I.U.G.G. Congress in Toronto. The experiments were performed with a thin disk, in which there was a slit along part of a diameter (Fig. 4). If the faces of the slit were moved in the way as indicated by the horizontal arrows the first movement of a point P on the rim was in the direction indicated by the vertical arrow. Assuming that it is again permissible to extrapolate the results from the static case to the dynamic problem it is seen that the slit in the experiments should be considered

as a distribution of B-nuclei and not C-nuclei. This is borne out by the fact that the rim was free in the experiments while the slit was held in a fixed position, no rotation of the disk as a whole being allowed. There are, in addition to analogies, some differences also between the case of Press and the

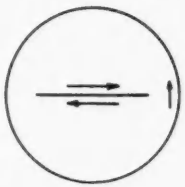

FIG. 4.

situation we considered here. The thin disk is in general considered as a case of plane stress while our case is essentially a case of plane strain. It is, however, well known that the one solution can be converted into the other by a suitable change of elastic constants. Secondly, our calculations are essentially performed for an infinite elastic medium while the disk is definitely finite. To counter this argument it may be pointed out that the experiments of Press were concerned with only the first arrival of the waves from the slit at the rim. Up to that time the waves were still unaware of the existence of a boundary and therefore behaved in the way in which they would in an infinite medium. Finally, we once again recall that the result will be definite only after a recalculation of the same case with the dynamic formulae.

6. THE STRAIN ENERGY OF THE DISLOCATION

We have seen that in a body which is unstressed, stresses are generated if a dislocation is produced. To obtain an expression for the strain energy we recall that the elastic potential or strain energy per unit volume is given by:

$$w = \tfrac{1}{2}\tau_{ij}\, e_{ij}. \tag{6.1}$$

For the total strain energy of a body with volume V we have then immediately

$$W = \int_V w dV. \tag{6.2}$$

The integral (6.2) can be transformed into the form

$$W = \tfrac{1}{2}\int_V \tau_{ij} u_{i,j} dV = \tfrac{1}{2}\int_V (\tau_{ij} u_i)_{,j} dV, \tag{6.3}$$

where we used the expression $\tau_{ij}\,\omega_{ij} = 0$, with $\omega_{ij} = \tfrac{1}{2}(u_{j,i} - u_{i,j})$, and the equilibrium equation. The last integral can be replaced by two surface integrals if the divergence theorem is used. We obtain

$$W = \tfrac{1}{2}\int\int_S u_i \vec{T}_i dS + \tfrac{1}{2}\int\int_\Sigma \Delta u_i \vec{T}_i d\Sigma. \tag{6.4}$$

The first integral vanishes if no forces are applied on S when the dislocation is made, and we obtain for the strain energy

$$W = \tfrac{1}{2}\int\int_{\Sigma} \Delta u_i \overset{\nu}{T}_i \, d\Sigma. \tag{6.5}$$

The integral (6.5) is in most cases an improper integral as a result of singularities of $\overset{\nu}{T}_i$ on Σ and especially along the edge of Σ. The straightforward evaluation of the strain energy using (6.5) presents therefore a number of analytical difficulties which will require further study. For the time being, however, it is assumed that the analytical tools which are used, for example in aerodynamics (leading edge singularities, vorticity singularities, etc.), will be sufficient to cope with this situation.

We suppose now that the body is already strained before the dislocation is made and let e^*_{ij}, τ^*_{ij}, w^* define the initial equilibrium stress distribution in the body. If e_{ij}, τ_{ij}, and w denote as before the strains, stresses, etc., due to the dislocation we have for the elastic potential w' in the final state the expression

$$\begin{aligned} w' &= \tfrac{1}{2}(\overset{*}{\tau}_{ij}+\tau_{ij})(\overset{*}{e}_{ij}+e_{ij}), \\ &= w^*+w+\tfrac{1}{2}(\overset{*}{\tau}_{ij}e_{ij}+\tau_{ij}\overset{*}{e}_{ij}). \end{aligned} \tag{6.6}$$

The expression between parentheses in (6.6) may be written in the forms

$$\tfrac{1}{2}(\overset{*}{\tau}_{ij}e_{ij}+\tau_{ij}\overset{*}{e}_{ij}) = \overset{*}{\tau}_{ij}e_{ij} = \tau_{ij}\overset{*}{e}_{ij}. \tag{6.7}$$

The total strain energy in the body in the final state is then given by

$$W' = W^*+W+\int_V \overset{*}{\tau}_{ij}u_{i,j}\,dV = W^*+W+\int_V \tau_{ij}\overset{*}{u}_{i,j}\,dV, \tag{6.8}$$

where we have denoted with W', W, and W^* the volume integrals of w', w, and w^* respectively, while we also used the expressions

$$\overset{*}{\tau}_{ij}\omega_{ij} = \tau_{ij}\overset{*}{\omega}_{ij} = 0. \tag{6.9}$$

The volume integrals in (6.8) can be transformed into surface integrals. Considering that τ_{ij} and τ^*_{ij} each on their own satisfy the equilibrium equations we obtain in turn

$$\begin{aligned} W' &= W^*+W+\int\int_S u_i \overset{\nu*}{T}_i \, dS+\int\int_{\Sigma} \Delta u_i \overset{\nu*}{T}_i \, d\Sigma. \\ &= W^*+W+\int\int_S \overset{*}{u}_i \overset{\nu}{T}_i \, dS+\int\int_{\Sigma} \Delta \overset{*}{u}_i \overset{\nu}{T}_i \, d\Sigma. \end{aligned} \tag{6.10}$$

We suppose that to make the dislocation, forces were applied over Σ while the forces on S were left unchanged. In that case $\overset{\nu}{T}_i = 0$ on S. Furthermore,

$\Delta u_i^* = 0$ on Σ as the initial displacement field is continuous throughout the body. From (6.10) we then deduce the two relations

$$W' = W^* + W,$$
$$\iint_S u_i \overset{\nu}{T}{}_i^* \, dS + \iint_\Sigma \Delta u_i \overset{\nu}{T}{}_i^* \, d\Sigma = 0. \tag{6.11}$$

This is the Theorem of Colonnetti (1915).

The last relation states that the work performed by the initial forces over Σ while making the dislocation is equal and opposite to the work performed by the initial forces on S when the dislocation is made.

The first equation in (6.11) shows that the strain energy in a body with a dislocation is equal to the sum of two strain energies: (i) the strain energy of the initial stress distribution, (ii) the strain energy accumulated in the body when we produce a dislocation in the unstressed body, leaving the surface S free from forces.

The Theorem of Colonnetti shows that the strain energy associated with the dislocation is independent of the initial state of stress or strain which may exist in the body. This result is in agreement with the statement that the displacement field in an elastic body that is due to a dislocation over Σ is also independent of the initial state of stress or strain in the body, which was mentioned in Section 2.

If one considers problems of fracture in geophysics, the Theorem of Colonnetti seems puzzling, as it is felt intuitively that a fracture should relax the stress distribution while it is found that the strain energy is increased when a dislocation is made. To put this difficulty in the proper light we recall that so far we have considered mainly cases where an elastic body was strained exclusively by a dislocation. If boundary conditions were considered we prescribed that the surface was essentially free when the dislocation was produced, no additional forces being applied on S. With these boundary conditions the Theorem of Colonnetti inevitably follows.

It is, however, possible to select other boundary conditions. One can assume that the outer surface S is held fixed while the dislocation is made. It is clear that in that case also forces on S have to be applied while the dislocation is made, and the displacement and stress field generated in the body will be different from the displacement and stress field obtained under the former assumptions, even if Σ and Δu_i will be the same. It is easily found that with the conditions of a fixed boundary the relation (2.8) has to be replaced by the expression

$$u_k(Q) = \frac{1}{8\pi\mu} \iint_S u_i^k \overset{\nu}{T}{}_i \, dS + \frac{1}{8\pi\mu} \iint_\Sigma \Delta u_i \overset{\nu}{T}{}_i^k \, d\Sigma. \tag{6.12}$$

where $\overset{\nu}{T}{}_i$ in the first integral is now the force to be applied on S to keep the surface fixed. This same relation is also found if the body is already in a state of initial stress, but the surface S is held fixed in that initial position when

the dislocation is made. If the boundary condition $u_i = 0$ on S is applied in the formulae (6.10) we obtain

$$\begin{aligned} W' &= W^* + W + \int\int_\Sigma \Delta u_i \overset{\nu}{T}{}_i^* \, d\Sigma, \\ &= W^* + W + \int\int_S u_i^* \overset{\nu}{T}_i \, dS. \end{aligned} \tag{6.13}$$

In these formulae W can be written in the form (6.5) as the first integral in (6.4) vanishes also if $u_i = 0$ on S. The integral in (6.13) can have several different values and W' is not necessarily greater than W^*. The value of W' will be determined if we know Δu_i or $\overset{\nu}{T}_i$ on Σ. In connection with fracture G. I. Taylor (cf. Starr 1928) has suggested that over the fractured surface Σ complete relaxation of stresses will take place. We have then in the final position for points on Σ the condition

$$\overset{\nu}{T}{}_i^* + \overset{\nu}{T}_i = 0. \tag{6.14}$$

With this condition it follows from (6.10) that $W' = W^* - W$,

$$\int\int_\Sigma \Delta u_i \overset{\nu}{T}{}_i^* \, d\Sigma = \int\int_S u_i^* \overset{\nu}{T}_i \, dS, \tag{6.15}$$

where W is given by the expression (6.5).

It is noticed that with these conditions the formula (6.12) loses a considerable amount of its usefulness for the calculation of the displacement field as Δu_i is not known over Σ but has to be determined first. Under these circumstances a different formulation of the problem will be necessary.

With these new boundary conditions many new problems arise. A body can be held fixed over part of its surface while other parts are free, or again parts of the surface can be subjected to given loads while the dislocation is made. Also on Σ the discontinuity Δu_i can be prescribed or certain conditions of partial or complete stress relaxation can be imposed. Depending on these conditions the strain energy will increase or, starting from a given initial state, the strain energy may decrease, as for example in (6.15).

It is clear that for geophysical problems only such boundary conditions will be physically realistic which will cause a reduction in strain energy when the dislocation is produced. On the other hand we have to recognize that the surface of the earth is essentially free and if a dislocation is made under those circumstances, Colonnetti's Theorem shows that the strain energy can only increase.

In this dilemma one may perhaps see an additional argument for the generally accepted idea that earthquakes are not world-wide phenomena but that their cause lies in local conditions; if one considers the whole earth it is difficult to see any restriction on the displacement of its surface; on the other hand if a particular region is considered it is easy to imagine that certain parts may obstruct or prevent the displacement of others and give rise in this

way to boundary conditions of the type in which parts of the surface are no longer free, creating in that way the possibility of escaping Colonnetti's Theorem.

It is clear that the problem of applying dislocation theory to geophysical features becomes very complex if the strain energy is required to decrease when the fracture is made. In the cases which have been considered so far the situation was usually simplified. Housner (1955) applied dislocation theory to earthquakes and introduced certain physical and statistical assumptions which enabled him to obtain amongst other things an estimate for the relation (6.5) and to relate his results to certain formulae obtained by Gutenberg and Richter. Rochester (1956) obtained approximate expressions for the displacements and stresses in a semi-infinite elastic medium which was stressed by a Volterra dislocation over a rectangular surface. The strain energy is determined from (6.5). It is then assumed that this is also the strain energy which will be released if an earthquake produces the given Volterra dislocation. This seems the most reasonable and most simple assumption. As no initial stress was given, the condition (6.14) could not be used. The only remark which can be brought against this method is that it may be better to impose the boundary conditions that the displacements have to vanish far away than to assume that there are no forces applied at infinity. It is, however, also clear that this will complicate the situation. If the strain energy is computed for the examples discussed in this paper and for other cases where strain nuclei are distributed in an elastic medium we shall obtain expressions similar to Rochester's procedure, as it is assumed that these strain nuclei are the only cause of stress in the body. The paper of Starr (1928) is more satisfactory from the point of strain energy but his analysis is not yet entirely correct; while the discontinuity Δu_i across the crack should be computed on the assumptions of a shear at infinity and complete stress relaxation over the crack, the crack is prescribed as an ellipse in his special confocal coordinate system. The analysis of Starr has been taken up again recently by Knopoff (1957). For completeness sake it may be mentioned that there is also some Russian work on dislocations in geophysics (Vvedenskaya 1956), but the author had so far no opportunity to see this paper.

It should be pointed out finally that the approximations on which our theorems are based in the case of initial stress are suitable only if the initial stresses are sufficiently small. The stresses in the earth are usually so large that these approximations are not justified. The next step is then to consider the dislocations as problems in initial stress (Love 1944, pp. 109–111; Jeffreys 1929, pp. 161–163).

7. THE DISPLACEMENT FIELD $w_{12}^{k}(P,Q)$ AT THE SURFACE OF THE SEMI-INFINITE MEDIUM

The considerations in the preceding sections were concerned mainly with an infinite elastic medium. If we wish to consider dislocations in the earth we have to supplement these considerations with certain suitable boundary conditions. We have seen in Section 6 that a proper choice of boundary

conditions in addition to a suitable initial stress distribution is necessary to obtain a physically satisfactory picture of the strain energy.

Following other authors (cf. for example Lamb 1904; Pekeris and Lifson 1957) we approximate the earth by a semi-infinite medium with a stress-free surface. The medium is unstressed to begin with and is then stressed by making a dislocation while no additional forces are supplied at infinity. We have seen in Section 6 that under those circumstances no satisfactory picture of the strain energy is obtained, but this disadvantage is considered to be compensated for by the simplicity of this model.

In the preceding paper (St. 58) a Green's function method was developed to deal with this problem. To obtain the displacement field, generated by a dislocation, in that case, we have the relation

$$u_k(Q) = \frac{1}{8\pi\mu}\int\int_{\Sigma} \Delta u_i w_{ij}^k(P, Q)\nu_j \, d\Sigma, \tag{7.1}$$

which differs only from equation (2.9) in its kernel; the functions $\tau_{ij}^k(P, Q)$ have been replaced by $w_{ij}^k(P, Q)$. A method was indicated for the construction of the $w_{ij}^k(P, Q)$ functions and the set $w_{12}^k(P, Q)$ was explicitly constructed.†

In this section we wish to consider in some more detail the displacement field $w_{12}^k(P, Q)$ at the surface of the semi-infinite medium, which is given by (St. 58—7.20).

The B-nucleus lies in a plane parallel with the free surface ($x_3 = 0$) and at a depth c. The displacement components were written in the general notation with two fixed subscripts and one free superscript but we shall denote them here simply as u_i ($i = 1, 2, 3$) while we also replace y_i by x_i. Omitting the elastic constant the displacement components at $x_3 = 0$ can then be written in the form

$$\begin{aligned} u_1 &= \frac{x_2\rho}{r^4}\left\{A + \frac{x_1^2}{r^2}B\right\}, \\ u_2 &= \frac{x_1\rho}{r^4}\left\{A + \frac{x_2^2}{r^2}B\right\}, \\ u_3 &= \frac{x_1x_2}{r^4}C, \end{aligned} \tag{7.2}$$

where

$$\begin{aligned} A &= 2 - 4\frac{c}{\rho} + 2\frac{c^2}{\rho^2}, \\ B &= 6 + 16\frac{c}{\rho} - 48\frac{c^2}{\rho^2} + 38\frac{c^4}{\rho^4} - 12\frac{c^6}{\rho^6}, \end{aligned} \tag{7.3}$$

*In (St. 58) we wrote out all the expressions for the case of a Volterra dislocation, but one easily verifies that the procedure applies also to the more general Somigliana dislocations.

†It may be good to indicate that in Section 7 of (St. 58) some confusion may arise from the use of $\tau_{12}^k(P, Q)$ throughout. In particular, in the heading of the section and in the final formulae (7.18) and (7.20), $\tau_{12}^k(P, Q)$ should be replaced by $w_{12}^k(P, Q)$ to maintain agreement with the notation of the preceding sections in that paper.

$$C = 4-18\frac{c}{\rho}+26\frac{c^3}{\rho^3}-12\frac{c^5}{\rho^5},$$

$$r^2 = x_1^2+x_2^2,$$

$$\rho^2 = c^2+r^2.$$

It has to be remembered that u_3 is positive in the direction into the medium.

To investigate the above expressions further we substitute polar coordinates $x_1 = r\cos\theta$, $x_2 = r\sin\theta$, and obtain the radial- and tangential-displacement components u_r and u_θ in the plane $x_3 = 0$. We find

$$u_r = \frac{\rho}{r^3}\{A+\tfrac{1}{2}B\}\sin 2\theta,$$

$$u_\theta = \frac{\rho}{r^3}A\cos 2\theta, \tag{7.4}$$

$$u_3 = \frac{1}{2r^2}C\sin 2\theta.$$

For a given depth of focus c and radius ρ, only the trigonometric functions vary in (7.4) and one easily notices the distribution in quadrants; u_r and u_3 change sign on the coordinate axes while u_θ reaches extreme values, u_θ changes sign at 45°, 135°, etc., and u_r and u_3 then reach extreme values.

To study further the displacement as functions of the distance to the focus we express ρ and r in terms of c and the angle ψ (Fig. 5). If we substitute

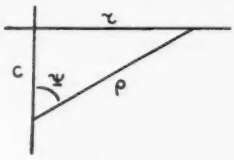

FIG. 5.

$p = \cos\psi = c/\rho$ it is easily checked that $A+\frac{1}{2}B$, A, and C have $p = 1$ as a double root. After simplification, the expressions (7.4) can then be put in the form

$$u_r = \frac{p^2\sqrt{(1-p^2)}(5+14p+p^2-12p^3-6p^4)}{(1+p)^2}\frac{\sin 2\theta}{c^2},$$

$$u_\theta = \frac{2p^2\sqrt{(1-p^2)}}{(1+p)^2}\frac{\cos 2\theta}{c^2}, \tag{7.5}$$

$$u_3 = \frac{p^2(1-p)(2-5p-12p^2-6p^3)}{1+p}\frac{\sin 2\theta}{c^2}.$$

We notice that the displacements at the surface decrease with increasing depth. This decrease is fairly rapid as the square of the depth appears in the formulae. To obtain an idea of the dependence on p we plotted in Fig. 6 the relations (7.5) when c^2, $\cos 2\theta$, and $\sin 2\theta$ respectively were taken equal to one.

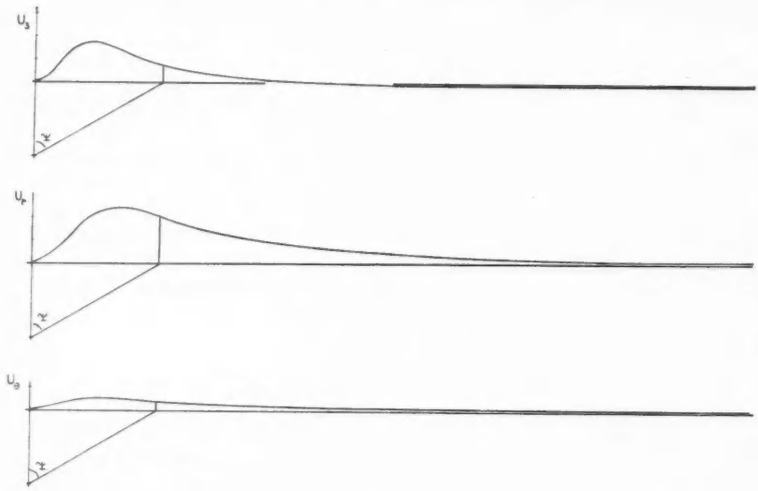

FIG. 6.

The curves for u_r and u_θ have few interesting features; the radial displacement reaches an extreme value near $p = 0,7$ and so does u_θ. The displacements u_r and u_θ keep the same sign for all angles ψ. The curve for u_3 reaches an extreme value at a value of p which is slightly larger than in the case of u_r and u_θ, but in addition u_3 changes sign. The expression $2-5p-12p^2-6p^3 = 0$ has a root which is approximately $p = 0,242$. The angle ψ is then slightly less than 76°. As tan 76° is about 4 we see that the vertical surface elevations change sign on a circle with a radius which is about 4 times the depth. To illustrate this behavior the distribution of u_3 in the plane $x_3 = 0$ is indicated in Fig. 7. The property of u_3 which has been found here raises the intriguing question

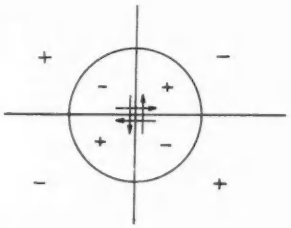

FIG. 7.

whether the same behavior will occur if the dynamic case is studied. It might throw some light on the difference between first arrivals at Berkeley from shallow and deep shocks in Southern California (Byerly 1955). Further investigations will no doubt be necessary here.

In several papers Tsuboi has reported the change in the surface of the land caused by an earthquake. In particular the horizontal displacements given for the Idu earthquake of 1930, which was associated with the Tana fault, show a pattern which is not unlike the pattern which we obtain for our resulting horizontal displacements (Tsuboi 1932 and 1939). Tsuboi also supplies information concerning dilatations, rotations, and several more features. To compare this with our model, we shall have to make further calculations.

8. FINAL REMARKS AND ACKNOWLEDGMENTS

In the preceding sections some simple cases in the theory of dislocations were discussed and an attempt was made to relate them to certain geophysical features. While the treatment is fairly systematic from the point of view of the theory, the geophysical aspects discussed show a fair amount of diversity. This aspect of the theory to order different features into one consistent scheme seems especially attractive in a field as geophysics where there is such a large scope for speculation.

The work is of a preliminary character and the conclusions reached are in several cases of a very tentative nature as only static cases were considered. Further work will no doubt be necessary, to confirm several of these points or to prove them wrong.

It is again a pleasure to thank Professor J. T. Wilson of the University of Toronto for his invitation to work during the summer of 1955 on geophysical problems. The author is grateful for financial assistance received during the summer of 1955 from the California Standard Oil Company and in the summer of 1957 from the National Research Council of Canada.

REFERENCES

ANDERSON, E. M. 1942. The dynamics of faulting (Oliver and Boyd, London, Edinburgh).
BURGERS, J. M. 1939. Proc. Koninkl. Ned. Akad. Wetenschap. **42**, 293, 378.
BYERLY, P. 1942. Seismology (Prentice-Hall, Inc., New York).
——— 1955. Geol. Soc. Am. Spec. Papers No. 62.
COLONNETTI, G. 1915. Atti. reale accad. Lincei, **24** (5) 404.
ESHELBY, J. D. 1951–52. Trans. Roy. Soc. (London), A, **244**, 87.
FRIEDEL, J. 1956. Les dislocations (Gauthier-Villars, Paris).
GRAMMEL, R. 1956. Deformation and flow of solids, IUTAM Colloquium, Madrid, 1955 (Springer-Verlag, Berlin, Göttingen, Heidelberg).
GREEN, A. E. and ZERNA, W. 1954. Theoretical elasticity (Oxford University Press, London).
GRIFFITH, A. A. 1921. Trans. Roy. Soc. (London), A, **221**, 180.
——— 1924. Proc. Intern. Congr. Appl. Mech. Delft, 55 (J. Waltman Jr., Delft).
HODGSON, J. H. 1957. Bull. Geol. Soc. Am. **68**, 661.
HONDA, H. 1957. Sci. Repts Tôhoku Univ. Fifth Ser. Geophysics, **9**, Suppl. (July).
HONDA, H. and MASATSUKA, A. 1952. Sci. Reports Tôhoku Univ. Fifth Ser. Geophysics, **4** (1), 41.
HOUSNER, G. W. 1955. Bull. Seismol. Soc. Am. **45**, 197.
INGLIS, C. E. 1913*a*. Trans. Inst. Naval. Arch. **55**, 219.
——— 1913*b*. Engineering, **95**, 415.
ISHIMOTO, M. 1932. Bull. Earthquake Research Inst., Tokyo Univ. **10**, 449.
JEFFREYS, H. 1929. The earth (Cambridge University Press, London).
KNOPOFF, L. 1957. Bull. Geol. Soc. Am. **68**, 1832.
LAMB, H. 1904. Trans. Roy. Soc. (London), A, **203**, 1.
LOVE, A. E. H. 1903–04. Proc. London Math. Soc. Ser. **2**, **1**, 291.
——— 1944. The mathematical theory of elasticity, (Dover Publications, New York).
NAKANO, H. 1923. Seismol. Bull. Centr. Met. Obs. Japan, **1**, 92–120.
PEKERIS, C. L. and LIFSON, H. 1957. J. Acoust. Soc. Am. **29** (11).

PRESS, F. 1957. Symposium on fault-plane work. IUGG Congress, Toronto. (To appear in publications of the Dominion Observatory, Vol. 20, No. 2. 1958.)
ROCHESTER, M. G. 1956. M. A. Thesis. University of Toronto, Toronto, Ontario.
SACK, R. A. 1946. Proc. Phys. Soc. **58**, 729.
SCHEIDEGGER, A. E. 1953. Bull. Geol. Soc. Am. **64**, 127.
——— 1957. Bull. Seismol. Soc. Am. **47**, 89.
——— 1958. Principles of geodynamics (Springer-Verlag, Berlin, Göttingen, Heidelberg).
SNEDDON, I. N. 1946. Proc. Roy. Soc. (London), A, **187**, 229.
SNEDDON, I. N. 1951. Fourier transforms. (McGraw-Hill Book Co., Inc., New York).
SNEDDON, I. N. and ELLIOTT, H. A. 1946. Quart. Appl. Math. **4**, 262.
SOKOLNIKOFF, I. S. and SPECHT, R. D. 1946. Mathematical theory of elasticity. (McGraw-Hill Book Co., Inc., New York).
SOMIGLIANA, C. 1908. Atti. IV Congr. intern. Mathematici, **3**, Roma.
——— 1914. Atti. reale accad. Lincei, **23** (5), 463.
——— 1915. Atti. reale accad. Lincei, **24** (5), 655.
STARR, A. T. 1928. Proc. Cambridge Phil. Soc. **24**, 489.
STEKETEE, J. A. 1958. Can. J. Phys. **36**, 192.
TSUBOI, C. 1932. Bull. Earthquake Research Inst., Tokyo Univ. **9**, 435.
——— 1939. Gerlands Beitr. Geophys. 4th Suppl. Cand. 106.
VOLTERRA, V. 1907. Ann. sci. école norm. supérieure, Paris, **24**, 401.
VVEDENSKAYA, A. V. 1956. Izvest. Akad. Nauk, SSSR. Ser. Geofiz. 277.
WESTERGAARD, H. M. 1952. Theory of elasticity and plasticity, (Harvard Univ. Press, Cambridge, Mass. and John Wiley & Sons, Inc., New York).
WILSON, J. T. 1954. *In* The earth as a planet *by* G. P. Kuiper (Univ. of Chicago Press, Chicago), Chap. 4.
——— 1957. *In* The planet earth, *by* D. R. Bates (Pergamon Press, London). (Also published by Basic Books, Inc., New York, with the title The earth and its atmosphere), Chap. 4.

THE THEORY OF FORBIDDEN β-DECAY[1]

G. E. LEE-WHITING

ABSTRACT

The angular distributions of electrons and of neutrinos and the polarization of the electrons emitted by an oriented source in β-decay of arbitrary forbiddenness are calculated in terms of various angular-momentum coupling constants and of certain generalizations of the well-known combinations of electron radial wave-functions, L_ν, M_ν, N_ν, ... The interaction Hamiltonian used encompasses all five invariants; neither parity conservation nor time-reversal invariance is assumed. A particularly simple procedure for calculating the longitudinal polarization of electrons emitted by an oriented source is pointed out. The polarization is equal to $\pm v/c$, to good approximation, if the two-component neutrino theory holds. Explicit results for various allowed and first-forbidden effects are quoted.

TABLE OF CONTENTS

1. INTRODUCTION

The work done in recent years on the properties of the various angular-momentum coupling coefficients—see, for example, Rose (1957) or Sharp (1957)—makes possible the formulation of a general procedure for calculating the consequences of the Fermi (1934) theory of β-decay in a transition of arbitrary forbiddenness. The revival of interest in β-decay experiments induced by the suggestion (Lee and Yang 1956) and the subsequent experimental discovery (Wu *et al.* 1957) of the nonconservation of parity increases the need for such a formulation. It is desirable to use the parity-nonconserving interaction Hamiltonian of Lee and Yang and to include the effects of the possible failure of time-reversal invariance. Some work along these lines has already been done by Alder *et al.* (1957) and by Dolginov (1958). Results applicable to first-forbidden transitions have been given by Curtis and Lewis (1957) and by Berestetsky *et al.* (1958) as well as by the former authors. Our purpose is

[1]Manuscript received June 10, 1958.
Contribution from Atomic Energy of Canada Ltd., Chalk River, Ontario.
Issued as A.E.C.L. No. 676.

to derive, in a manner both simple and general, results analogous in form to the well-known formulae for correction-factors (Greuling 1942 and Pursey 1951).

Because the succeeding sections of the paper abound in calculational detail, it is thought desirable to give at this stage a nonmathematical description of the path to be followed. At the same time the opportunity is taken to point out, for the benefit of the reader who is not particularly interested in the derivations, where formulae corresponding to different experiments may be found. An expansion in spherical waves of the wave-function of an emitted electron associated with a given nuclear transition and with the absorption of an antineutrino from a given state is calculated by time-dependent perturbation theory; the perturbation is the interaction Hamiltonian of Lee and Yang (1956). The form of perturbation theory used is identical except for notation to an adaptation to the relativistic case by Greuling and Meeks (1951) of some earlier work by Bethe (1930).

The asymptotic expansion of the electron wave-function contains matrix elements between the initial and final nuclear states of operators composed of Dirac operators and products of lepton wave-functions. The derivation of a comprehensive formula for these matrix elements appropriate to a β-interaction containing all five invariants is greatly facilitated by the use of a notation, devised by Banerjee and Saha (1954), for labelling the eight Dirac operators: I, β, $\mathfrak{d}$, $\beta\mathfrak{d}$, γ_5, $\beta\gamma_5$, $\boldsymbol{\alpha}$, $\beta\boldsymbol{\alpha}$. Each operator is put into one-to-one correspondence with one of the eight sets of values of three two-valued parameters, viz. ξ, η, and ζ. The value of ξ is 0 for the scalars and 1 for the vectors (in three-space); η takes the value 0 for the "nonrelativistic" operators (the first four in the list), and 1 for the others; ζ is 0 for those containing an explicit β, 1 for the rest. More fundamental properties of η and ζ are discussed later in Section 1. It is found necessary to introduce a particular representation of the Dirac operators by means of 4×4 matrices. With the aid of the parameters (ξ, η, ζ) one can obtain a simple formula for any element of any of the representative matrices. The use of this formula enables one to write the interaction Hamiltonian in manageable form. The lepton covariant in the matrix element for the transition can be reduced to a sum of products of functions of r and of electron energy with spherical harmonics. The dependence upon electron energy can be approximately factored out of the matrix element. Next, following Spiers and Blin-Stoyle (1952*a*), we express each product of a heavy-particle Dirac operator and a spherical harmonic as a sum of irreducible tensor operators (Rose 1957). Each term in the sum can be expressed (the Wigner-Eckart theorem) as the product of a vector-addition coefficient and a second factor, called the reduced matrix element, which is independent of magnetic quantum numbers. The reduced matrix elements, though independent both of electron energy and of magnetic quantum numbers, are dependent upon the structure of the nucleus; because of our ignorance they are usually treated as arbitrary parameters. There remains, however, under the integral sign a factor of the form $(r/\lambda\!\!\!^{-})^{l+l'}$, $\lambda\!\!\!^{-}$ being the Compton radian wave-length of the electron and l and l' being effective orbital angular-momentum quantum

numbers. Since the de Broglie wave-lengths of the electron and of the neutrino are rarely as small as 10λ, and since λ is very much larger than any nuclear radius, the most important terms are those with the smallest values of $l+l'$. The degree-of-forbiddenness approximation of β-decay theory is the rejection of all terms in the expansion of each type of matrix element except those having the minimum value of $l+l'$ consistent with conservation of angular momentum. Resulting from the steps which we have discussed is a general formula for the transition matrix element, and hence for the emitted electron wave-function, containing coupling constants, reduced nuclear matrix elements, energy-dependent lepton radial wave-functions, and assorted angular-momentum coupling coefficients; the angles specifying the direction of emission of the neutrino enter as the arguments of a spherical harmonic.

The angular distribution of electrons is obtained by calculating the outward radial component of the particle current using the asymptotic wave-function discussed in the preceding paragraph. The angles describing the direction of neutrino emission remain as parameters. Of course contributions from different orientations of the resultant nucleus and of the neutrino spin must be summed, and the appropriate average over orientations of the initial nucleus must be performed. The polarization of the electrons is found by calculating the statistical-mechanical average of the expectation value of the operator $\boldsymbol{\sigma}$ in the electron rest-frame. Taking advantage of the similarity in form of the expressions for the angular distribution and for the spherical components of the polarization vector we introduce functions $S_t{}^\mu$ such that $S_0{}^0$ gives the angular distribution and $S_1{}^\mu$ (with $\mu = \pm 1, 0$) gives the polarization. The sums over magnetic quantum numbers in the expression for $S_t{}^\mu$ are carried out with the aid of the properties of various angular momentum recoupling coefficients. In the resulting formula, (48), for $S_t{}^\mu$ the angular co-ordinates of the directions of emission of electrons and neutrinos appear as arguments of spherical harmonics of orders g and g' respectively. Information about the orientation of the source is contained in the factor $Z(k)$ (see (49)), which is essentially the "degree of orientation of order k" discussed by de Groot and Tolhoek (see Siegbahn 1955). Except for trivial factors the remainder of the quantities upon which $S_t{}^\mu$ depends have been collected into a set of coefficients $R(gg'kk't)$. In the general formula (58), for $R(gg'kk't)$ we have grouped the products of electron radial wave-functions into certain convenient combinations which we call $L_{\mu\nu}(\zeta\sigma\tau)$, etc.; these functions depend upon the electron energy and the nuclear charge as well as upon the nonmagnetic quantum numbers of two electron waves; they are, of course, generalizations of the L_ν, etc. defined by Greuling (1941). Simple formulae are derived for the generalized functions for the approximation in which the nuclear radius is negligibly small compared to the electron de Broglie wave-length.

The remainder of the paper is devoted to expressing the results corresponding to certain types of experiment in terms of the coefficients $R(gg'kk't)$, and to evaluating these coefficients for allowed and first-forbidden transitions. In Section 4 the formulae for the shapes of spectra of unoriented sources are examined, and the matrix elements of our spherical tensors are related to

those of the traditional Cartesian tensors. The formulae for longitudinal polarization of electrons emitted by such a source are shown in Section 5 to be very similar in form to the shape-factors of Section 4. We show how to calculate the polarization by means of a simple set of modifications of published shape-factors. The angular distribution of electrons emitted by an oriented source is given by the formula (83) of Section 6; expressions (87) and (88) can be used to calculate the polarization. The angular correlation of the directions of emission of electrons and neutrinos is to be found in (94) of Section 7; electron polarizations can be calculated from (95) and (96). Explicit formulae for many of the pertinent coefficients $R(gg'kk't)$ for allowed and first-forbidden transitions are to be found in Sections 8 and 9.

Beta-decay is more complicated than many other somewhat similar problems of nuclear physics, because two particles are emitted simultaneously, and because both these particles must be treated relativistically. The emission of a pair of particles introduces no great difficulty in principle, though it does increase the complexity of the results considerably. One of the more noticeable effects of the two sources of difficulty is the large number of different types of nuclear matrix elements which must be handled.

In treating the motion of an electron in a general, central, electrostatic field it seems to be necessary, or at least more convenient, to introduce a particular representation of the Dirac operators. We shall use a notation in which the Dirac equation for the four-component wave-function, ψ, of an electron of energy E is

$$[-\boldsymbol{\alpha}\cdot\mathbf{p}-\beta+V(r)]\psi = E\psi. \tag{1}$$

$V(r)$ is the potential energy of the electron in the electrostatic field of the nucleus. In (1) we have used the customary units in which the unit of mass is the electron mass, m, the unit of length is $\hbar m^{-1}c^{-1}$, the unit of momentum is mc, and the unit of energy is mc^2. The traditional representation used in β-decay theory is that given by

$$\beta = \begin{pmatrix} I' & 0 \\ 0 & -I' \end{pmatrix}, \qquad \boldsymbol{\alpha} = \begin{pmatrix} 0 & \boldsymbol{\sigma}' \\ \boldsymbol{\sigma}' & 0 \end{pmatrix}; \tag{2}$$

the 2×2 matrices I' and $\boldsymbol{\sigma}'$ are the unit-matrix and the Pauli matrices—our $\boldsymbol{\sigma}'$ is identical with the $\boldsymbol{\sigma}$ of Schiff (1955, p. 232). If γ_5 is defined by the equation $\gamma_5 = -i\alpha_x\alpha_y\alpha_z$, then it can be shown that the operator for the spin of a Dirac particle is $\frac{1}{2}\boldsymbol{\sigma}$, with $\boldsymbol{\sigma} = \gamma_5\boldsymbol{\alpha} \equiv \boldsymbol{\alpha}\gamma_5$. In the representation (2) we have

$$\gamma_5 = \begin{pmatrix} 0 & I' \\ I' & 0 \end{pmatrix}, \qquad \boldsymbol{\sigma} = \begin{pmatrix} \boldsymbol{\sigma}' & 0 \\ 0 & \boldsymbol{\sigma}' \end{pmatrix}. \tag{3}$$

The form of the Hamiltonian density for the interaction responsible for β-decay, $\mathcal{H}_\beta$, which we use is that given by Lee and Yang (1956, Appendix). Because we will need to discuss selection rules for transitions between nuclear states of definite parities, it is convenient to express $\mathcal{H}_\beta$ in terms of operators with simple behaviors under spatial reflections. In other words we wish to express the products of the matrices γ_μ used by Lee and Yang in terms of I,

β, $\boldsymbol{\alpha}$, $\boldsymbol{\alpha}$, and γ_5. Let us suppose that the γ-matrices are so defined that the time-dependent wave-equation for a free particle is

$$[\boldsymbol{\gamma}\cdot\nabla - i\gamma_4(\partial/\partial t)+I]\psi = 0.$$

If ∇ is replaced by $i\mathbf{p}$ and $\partial/\partial t$ by $-iE$, this wave-equation can be transformed into the free-particle form of (1) if

$$\gamma_4 = -\beta, \quad \gamma_k = -i\beta\alpha_k \quad \text{for } k = 1, 2, 3. \tag{4}$$

Elimination of the γ-matrices from the Hamiltonian density of Lee and Yang by means of the relations (4) leads to the formula (5) for $\mathscr{H}_\beta$.

$$\begin{aligned}\mathscr{H}_\beta = {} & (\Psi^*\beta\Phi)\cdot[\psi^*\beta(C_S+C_S'\gamma_5)\phi] \\ & +(\Psi^*\Phi)\cdot[\psi^*(C_V+C_V'\gamma_5)\phi]-(\Psi^*\boldsymbol{\alpha}\Phi)\cdot[\psi^*\boldsymbol{\alpha}(C_V+C_V'\gamma_5)\phi] \\ & +(\Psi^*\beta\boldsymbol{\alpha}\Phi)\cdot[\psi^*\beta\boldsymbol{\alpha}(C_T+C_T'\gamma_5)\phi]+(\Psi^*\beta\boldsymbol{\alpha}\Phi)\cdot[\psi^*\beta\boldsymbol{\alpha}(C_T+C_T'\gamma_5)\phi] \\ & +(\Psi^*\boldsymbol{\alpha}\Phi)\cdot[\psi^*\boldsymbol{\alpha}(C_A+C_A'\gamma_5)\phi]-(\Psi^*\gamma_5\Phi)\cdot[\psi^*\gamma_5(C_A+C_A'\gamma_5)\phi] \\ & +(\Psi^*\beta\gamma_5\Phi)\cdot[\psi^*\beta\gamma_5(C_P+C_P'\gamma_5)\phi].\end{aligned} \tag{5}$$

The symbols Ψ, Φ, ψ, and ϕ stand for the Dirac wave-functions for the proton, neutron, electron, and neutrino respectively; Ψ^* is the Hermitian adjoint of Ψ. When the primed coupling constants are equated to zero, expression (5) reduces to the customary β-decay interaction—see the chapter by Konopinski in *Beta- and Gamma-Ray Spectroscopy* (Siegbahn (1955)). The operator $\gamma_5 = \gamma_1\gamma_2\gamma_3\gamma_4$ defined by Lee and Yang is identical with the operator $\gamma_5 = -i\alpha_x\alpha_y\alpha_z$ which we have already defined; hence the coupling constants of the two forms of $\mathscr{H}_\beta$ are precisely equivalent.

A notation which enables us to write (5) in a convenient, shorter form has been devised by Banerjee and Saha (1954). The eight Dirac operators appearing in (5) are put into correspondence with the eight different combinations of the values of three two-valued parameters ξ, η, and ζ. The definitions of these parameters depend upon the properties of covariants of the form $(\psi^*K\psi)$, K being one of the eight Dirac operators, ψ being a solution of an equation of the form (1). The variable ξ is 0 or 1 as the covariant is a scalar or a vector; η is 0 or 1 as this covariant is invariant or changes sign under a spatial reflection; ζ is 0 or 1 as the covariant is invariant or changes sign under a total reflection. The operators for which $\eta = 0$ are those sometimes described as "nonrelativistic", viz. I, β, $\boldsymbol{\alpha}$, and $\beta\boldsymbol{\alpha}$. Those operators in which β appears explicitly have $\zeta = 0$. The parameters η and ζ also specify the commutation properties of the operator K with β and γ_5 respectively, i.e.

$$\beta K = (-1)^\eta K\beta \tag{6}$$

and

$$\gamma_5 K = (-1)^{\xi+1}K\gamma_5. \tag{7}$$

It is worth noting that the operator formed by multiplying the operator with parameters (ξ, η, ζ) on the right with γ_5 has parameters $(\xi, \eta+1, \zeta)$, $\eta = 2$ being here defined as equivalent to $\eta = 0$.

In order to write (5) in the desired simplified form we need the spherical components A^μ of a three-vector $\mathbf{A}$; according to the usual definition

$$(8) \qquad A^1 = -2^{-\frac{1}{2}}(A_x+iA_y), \qquad A^0 = A_z, \qquad A^{-1} = 2^{-\frac{1}{2}}(A_x-iA_y).$$

The spherical components of $\mathbf{r}$, for example, are $(4\pi/3)^{\frac{1}{2}}rY_1{}^\mu$. With this notation the scalar product of two vectors $\mathbf{A}$ and $\mathbf{B}$ becomes

$$\mathbf{A}\cdot\mathbf{B} = \sum_\mu (-1)^\mu A^{-\mu}B^\mu.$$

It is also convenient to extend the definition of spherical components to a scalar, A, with $A^{\pm 1} = 0$, $A^0 = A$. We are now able to write the interaction Hamiltonian density in the form

$$(9) \qquad \mathscr{H}_\beta = \sum_{n=1}^{8} (-1)^{\eta\xi} \sum_{\mu=-1}^{1} (-1)^\mu (\Psi^* K_n{}^{-\mu}\Phi)[\psi^* K_n{}^\mu (C_n + C_n'\gamma_5)\phi].$$

The coupling constants C_n and C_n' are equal to the C_X and C_X' for the interaction to which K_n belongs. The parameters ξ, η, and ζ are assumed to be functions of n. In what follows no significance is attached to the exact correspondence between the K_n and the eight integers spanned by n.

Observable quantities connected with single β-decay depend upon the coupling constants only through certain quadratic combinations. To facilitate our discussion in later sections let us introduce abbreviations for these combinations now.

$$(10a) \qquad D_{XY} = \quad D_{YX} = \mathrm{Re}(C_X C_Y^* + C_X' C_Y'^*),$$

$$(10b) \qquad \Delta_{XY} = -\Delta_{YX} = \mathrm{Im}(C_X C_Y^* + C_X' C_Y'^*),$$

$$(10c) \qquad G_{XY} = \quad G_{YX} = \mathrm{Re}(C_X' C_Y^* + C_X C_Y'^*),$$

$$(10d) \qquad \Gamma_{XY} = -\Gamma_{YX} = \mathrm{Im}(C_X' C_Y^* + C_X C_Y'^*).$$

If Pauli's (1957) more general interaction is to be used, then our formulae are to be changed by replacing D_{XY} and Δ_{XY} by the real and imaginary parts of Pauli's invariant K_{XY}, and by replacing G_{XY} and Γ_{XY} by the real and imaginary parts respectively of the invariant L_{XY} (Lüders 1958).

The practicability of working out the consequences of a general $\mathscr{H}_\beta$ of the form (9) for arbitrarily forbidden transitions stems from the discovery of a simple analytical formula for the elements of the matrices $K_n{}^\mu$. Following Spiers and Blin-Stoyle (1952*a*) we write each of the eight matrices appearing in (5) as the Kronecker product, as defined by Banerjee and Saha, of two 2×2 matrices. By inspection one learns that each of the scalars is of the form $b \times I'$ and that each of the vectors is of the form $b \times \sigma'$, b being a 2×2 matrix whose elements are functions of η and ζ. The four components of a Dirac wave-function are to be labelled by two two-valued indices, β and σ. The two upper elements have $\beta = 1$, the lower two $\beta = -1$; the upper element of each pair has $\sigma = \frac{1}{2}$, the lower $\sigma = -\frac{1}{2}$. Similarly we write $A_{\beta\sigma\beta'\sigma'}$ for an element of a 4×4 matrix A. In the factorization into Kronecker products

which we have been discussing, the elements of b are designated by the indices β and β', those of the matrices I' and $\mathfrak{d}'$ by the indices σ and σ'. In fact

$$b_{\beta\beta'} = \beta^{\xi+1}\delta_{\beta,(1-2\eta)\beta'}.$$

Next note that the matrix whose $\sigma\sigma'$-element is

$$(-1)^{\frac{1}{2}-\sigma'}\, 2^{\frac{1}{2}}(\tfrac{1}{2}\,\tfrac{1}{2}\,\sigma\, -\sigma'|\xi\,\mu)$$

reduces to I' when $\xi = 0$ and to σ'^{μ} when $\xi = 1$. We use the notation $(j_1j_2m_1m_2|jm)$ for the vector-addition coefficient $(j_1j_2m_1m_2|j_1j_2jm)$ of Condon and Shortley (1953). Thus we have

$$(K_n^{\mu})_{\beta\sigma\beta'\sigma'} = \beta^{\xi+1}\delta_{\beta,(1-2\eta)\beta'}(-1)^{\frac{1}{2}-\sigma'}2^{\frac{1}{2}}(\tfrac{1}{2}\tfrac{1}{2}\,\sigma\, -\sigma'|\xi\,\mu). \tag{11}$$

Note that we have been able to write the dependence on σ,σ' in a form convenient for carrying out sums over magnetic quantum numbers.

The representation defined by (2) and the sign conventions of (1) are believed to be those most commonly used in β-decay. The author wishes to express his thanks to Drs. Konopinski, Greuling, and Pursey for confirmatory correspondence on this point. Though Spiers and Blin-Stoyle do not specify a representation explicitly, one can deduce from their Table 2 that the representation used is equivalent to ours with the signs of $\boldsymbol{\alpha}$ and γ_5 changed; there appears to be a misprint of sign in this table in the case of the elements of $\beta\boldsymbol{\alpha}$. Likewise one can deduce from their expression (29) that Banerjee and Saha used the same representation as Spiers and Blin-Stoyle. Since it is easily shown, using theorems given by Pauli (1936), that quantities of the form $(\psi^*K\phi)$ are invariant under change of representation, the expressions for the various observable quantities worked out with the different representations must be precisely the same, even though the nuclear matrix elements appear to depend upon the K_n.

So far, we have discussed negative-electron decay only. The Hamiltonian density for positron decay is of course the complex conjugate of (5), and may be put into a form analogous to (5) by a transformation of the coupling constants. Let $C_X{}^+$ and $C_X{}'^+$ be coupling constants in the positron-emitting part of interaction after it has been brought into the form (5). It is easily shown that the new coupling constants must satisfy $C_X{}'^+/C_X{}^+ = -C_X{}'^*/C_X{}^*$. The definition of the transformation may be completed by putting $C_X{}^+ = C_X{}^*$ when X stands for V or T and $C_X{}^+ = -C_X{}^*$ when X stands for S, A, or P. It is also necessary to take the appropriate sign for $V(r)$ in equation (1), which defines ψ. In the remainder of this paper we shall deal with negatron decay only; results for positron decay can be obtained by making a suitable transformation of the coupling constants and by changing the sign of Z.

2. ELECTRON WAVE-FUNCTION

In this section we calculate the probability amplitude for electron position at a large distance from the transforming nucleus. As is customary the absorption of an antineutrino is considered instead of the emission of a neutrino; plane-wave eigenfunctions are used for the antineutrino. The nucleus is

supposed to make a transition between states with definite magnetic quantum numbers. Thus the calculated electron amplitude is a function of the nuclear quantum numbers as well as of the momentum and spin of the antineutrino.

It is convenient to follow the simple treatment of Greuling and Meeks (1951), who use ordinary time-dependent perturbation theory, in order to find the amplitude of the emitted electron wave. The field-theoretic Hamiltonian density of Section 1 is replaced by the Hamiltonian H_β; in place of expression (9) we now consider

$$(12)\quad H_\beta = \sum_n \sum_\mu (-1)^{\eta\zeta+\mu} K_n^{-\mu}(\mathrm{H}) K_n^{\mu}(\mathrm{L})(C_n + C_n'\gamma_5)\tau_\mathrm{H}\tau_\mathrm{L}\delta(\mathbf{x}_\mathrm{H}-\mathbf{x}_\mathrm{L}).$$

The indices H and L refer to heavy and to light particles; τ_H and τ_L are operators transforming neutrons and antineutrinos into protons and electrons respectively; $\mathbf{x}_\mathrm{H}$ and $\mathbf{x}_\mathrm{L}$ are position vectors for the heavy and light particles. In writing (12) a summation over all neutrons in the nucleus has been omitted for the sake of simplicity.

The initial wave-function of the system is the product of a nuclear wave-function, Φ, and the antineutrino wave-function. Wave-functions of a free particle in our representation are well known; see Schiff (1955, page 327). By inspection of these expressions one can show without difficulty that the components of the wave-function of a particle of zero mass, of energy $-q$, and of momentum $-\mathbf{q}$ can be written as

$$(13)\quad \phi_{\beta\sigma}^{\mathbf{q},s} = (2\pi)^{\frac{1}{2}}(e\,\tfrac{1}{2}\,s-\sigma\,\sigma|\tfrac{1}{2}\,s)\,Y_e^{s-\sigma}(\theta',\,\phi')e^{-i\mathbf{q}\cdot\mathbf{r}},$$

with

$$e = \tfrac{1}{2}-\tfrac{1}{2}\beta.$$

Two orthogonal solutions are specified by the two values, $\pm\frac{1}{2}$, of the parameter s; the normalization $\phi^*\phi = 1$ has been used. For a particle of nonzero mass, s is an eigenvalue of σ_z in the nonrelativistic limit; since we shall always sum over all values of s, we need not enquire further about its physical significance. The angles θ' and ϕ' are the spherical polar co-ordinates of $\mathbf{q}$, the neutrino momentum vector, with respect to the z-axis; Y_e^μ is a normalized spherical harmonic equivalent to that defined by Condon and Shortley.

The wave-function of the final state of the system is the product of a nuclear wave-function and an electron wave-function, ψ. We expand ψ in a complete set of wave-functions, ψ^{jma}. The quantum numbers j and m refer to angular momentum and its z-component; the two types of solution obtained from the two values, ± 1, of a are analogous to the two solutions with different orbital angular momentum for a given value of j in a nonrelativistic theory. If the relativistic parity operator is defined as $-\beta\times$ (a spatial inversion), then its eigenvalues are $(-1)^{j-\frac{1}{2}a}$.

$$(14)\quad \psi_{\beta\sigma}^{jma} = r^{l}F_l^{\beta,a}(p,r)(l\,\tfrac{1}{2}\,m-\sigma\,\sigma|j\,m)\,Y_l^{m-\sigma}(\theta,\,\phi),$$

with

$$l = j+\tfrac{1}{2}a\beta.$$

The wave-function (14) is identical with that given by Rose (1955), who uses the same representation, if the following relations between the radial parts are satisfied:

$$r^l F_l^{1,a} = -if_\kappa, \qquad r^l F_l^{-1,a} = g_\kappa, \qquad \kappa = -a(j+\tfrac{1}{2}). \tag{15}$$

Differential equations satisfied by f_κ and g_κ are given by Rose. The quantity p is the magnitude of the linear momentum at a large distance from the nucleus, and is related to the total energy, E, by $p = (E^2-1)^{\frac{1}{2}}$. The normalization of the radial wave-functions is fixed by insisting that they have the asymptotic expansions

$$f_\kappa = -r^{-1}(1-E^{-1})^{\frac{1}{2}} \sin(pr+\delta), \tag{16a}$$

$$g_\kappa = r^{-1}(1+E^{-1})^{\frac{1}{2}} \cos(pr+\delta). \tag{16b}$$

The normalization (16) is usually used in β-decay (Konopinski and Uhlenbeck 1940; Rose *et al.* 1953); it gives rise to the relation

$$\int \psi^{jma*}(E, \mathbf{r})\psi^{j'm'a'}(E', \mathbf{r})d\mathbf{r} = \pi p E^{-1}\delta(E-E')\delta_{jj'}\delta_{mm'}\delta_{aa'}. \tag{17}$$

The phase-shift δ depends upon κ (i.e. upon j and a); if $V(r)$ falls off as r^{-1}, δ also has a logarithmic dependence upon r (Rose 1937). If the potential energy, $V(r)$, is nonsingular at $r = 0$, then the factor $F_l^{\beta,a}$ of the radial wave-function approaches a finite, nonzero value as r approaches zero. For the values of E usually encountered in β-decay, $F_l^{\beta,a}$ is practically constant throughout the nucleus. Our relations (15) differ in sign from the corresponding equations of Spiers and Blin-Stoyle and of Banerjee and Saha, because these authors use a different representation of $\boldsymbol{\alpha}$.

The application of the time-dependent perturbation theory is straightforward except for the apparent presence of ingoing as well as outgoing waves in the asymptotic expansion of the electron amplitude. Using a method originated by Bethe (1930), Greuling and Meeks showed that the ingoing waves remove themselves by destructive interference; note, however, that because of an apparent misprint of sign their expression (9) appears to lead to a cancellation of outgoing rather than of ingoing waves. Dropping the time-dependent factors, the operator τ_H, and a unimodular factor, we may write the asymptotic expansion of the outgoing wave as

$$\psi_{\beta\sigma} \sim [E(E-\beta)]^{\frac{1}{2}}(pr)^{-1}e^{ipr}\sum_{jma} e^{i\delta(j,a)}(f|H_\beta|i)(\lambda\tfrac{1}{2}m-\sigma\sigma|jm)\,Y^{m-\sigma}(\theta, \phi), \tag{18}$$

with

$$\lambda = j+\tfrac{1}{2}a\beta,$$

$$(f|H_\beta|i) \equiv \sum_n \sum_\mu (-1)^{n_5+\mu}\int (\Psi^* K_n^{-\mu}\Phi)[\psi^{jma*}K_n^{\mu}(C_n+C_n'\gamma_5)\phi^{\mathbf{q},s}]d\mathbf{r}. \tag{19}$$

$\delta(j, a)$ is the phase-shift, as in (16), associated with ψ^{jma}. Relation (18) gives a formula for calculating a component, $\psi_{\beta\sigma}$, of the outgoing electron wave.

The various results to be obtained in the rest of the paper all flow from the use of the formula (18). But before we can proceed much further, we must, of course, evaluate the matrix element defined in (19).

Expression (19) consists of a sum of matrix elements, between two nuclear states, of operators of the form Q,

$$Q = (-1)^{\mu} K_n^{-\mu} (\psi^{jma*} K_n^{\mu} \phi^{\mathbf{q},s}).$$

In order to relate the quantum numbers of the electron–neutrino emission to the nuclear angular momentum quantum numbers, we next express Q as a sum of spherical tensor operators. The lepton covariant in Q is a function of $\mathbf{r}$; it must therefore be expressed as a sum of spherical harmonics. The plane wave in the neutrino wave-function is expanded in terms of spherical waves in the usual way (Blatt and Weisskopf 1952, Appendix A). It is convenient to define a function $G_l(qr) = (qr)^{-l} j_l(qr)$, $j_l(z)$ being the spherical Bessel function; $G_l(qr)$ is very nearly constant throughout the nucleus. Using the analytic formulae for wave-functions and for the K_n one may write

$$Q = 8\pi^{3/2} K_n^{-\mu} \sum_{\beta\beta'} \beta^{l+1} \delta_{\beta,(1-2\eta)\beta'} \sum_{l'} (-i)^{l'} q^{l'} r^{l+l'} F_l^{\beta,a*}(p,r) G_{l'}(qr)$$

$$\times \sum_{\sigma\sigma'\mu'} (-1)^{m-\frac{1}{2}+\mu'} (l\ \tfrac{1}{2}\ m-\sigma\ \sigma | j\ m)(e\ \tfrac{1}{2}\ s-\sigma'\ \sigma' | \tfrac{1}{2}\ s)(\tfrac{1}{2}\ \tfrac{1}{2}\ \sigma\ -\sigma' | \xi\ \mu)$$

$$\times Y_l^{-m+\sigma}(\theta,\phi)\, Y_{l'}{}^{\mu'}(\theta,\phi)\, Y_e^{s-\sigma'}(\theta',\phi')\, Y_{l'}{}^{-\mu'}(\theta',\phi').$$

It is well known (e.g., see Blatt and Weisskopf, Appendix A) that products of the form $Y_l{}^m(\theta,\phi)\ Y_{l'}{}^{m'}(\theta,\phi)$ can be expressed as linear combinations of $Y_L^{m+m'}(\theta,\phi)$ with L ranging from $|l'-l|$ to $l+l'$. We next express the product $r^L Y_L^{M+\mu} K_n^{-\mu}$ as a linear combination of the tensor operators $T_n{}^M(J,L)$, defined by (20).

$$(20)\quad T_n{}^M(J,L) = (4\pi)^{\frac{1}{2}}\, i^L\, U^{-1}(J,L,\xi) \sum_{\mu} (L\ \xi\ M+\mu\ -\mu | J\ M) r^L Y_L^{M+\mu} K_n^{-\mu},$$

$$U(J,L,\xi) = [J(L+\xi)^{-1}]^{\frac{1}{2}}\, (L!)^{-1} [(2L+1)!\, 2^{-L}]^{\frac{1}{2}} \quad \text{for } J > 0.$$

$$(21)\quad U(000) = U(011) = 1.$$

Recall that ξ is a function of n. The presence of the factor i^L in the definition (20) leads to a convenient behavior of reduced matrix elements under time-reversal, as will be seen later; $U^{-1}(J,L,\xi)$ is included to bring about an equality between certain products of our reduced matrix elements and the corresponding sums of products of components of Cartesian tensors found in the work of Greuling and of Pursey. It should now be clear that the left side of (19) can be written as a linear combination of terms of the form

$$(22)\quad \int \Psi^*\, F_l^{\beta,a*}\, G_{l'} r^{l+l'-L}\, T_n{}^M(J,L)\, \Phi d\mathbf{r}.$$

In order to separate the energy-dependent factors from the nuclear matrix elements we apply the mean-value theorem to (22); i.e. we take $F_l^{\beta,a*} G_{l'}$ outside the integration and evaluate it at ρ_l, an appropriate mean-value of r roughly equal to the nuclear radius. Because $F_l^{\beta,a*} G_{l'}$ does not vary much

within the nucleus (in other words, because the electron and neutrino de Broglie wave-lengths are much larger than the nuclear radius), it is not necessary to use the true value of ρ. With electron wave-functions pertaining to a point-charge it has been customary to put ρ equal to the nuclear radius; with the wave-functions for a distributed charge it would probably be better to use half the nuclear radius. Although one would expect, in general, to find a different value of ρ for each different matrix element, we shall follow the usual approximation of using the same value for all.

Next we apply the Wigner-Eckart theorem (Rose 1957) to the modified form of (22). The quantity $r^{l+l'-L}\ T_n^M(J, L)$ is, of course, a tensor operator of order J. Let J_i, M_i and J_f, M_f be the quantum numbers of the nuclear spin and of its z-component in the initial and final nuclear states. Then the Wigner-Eckart theorem says that, if we write

$$(23) \qquad (f|r^k T_n^{-M}(J, L)|i) = \langle K_n; JL; k\rangle (-1)^{J+M}(J_f J M_f M|J_i M_i),$$

the reduced matrix element $\langle K_n; JL; k\rangle$ is independent of the magnetic quantum numbers; the notation for the reduced matrix elements employed is meaningful only for tensor operators which differ from those defined in (20) by at most a power of r. This definition of reduced matrix element differs from those of Rose (1957) and of Sharp (1957) by trivial factors.

After the right side of (19) has been expressed in terms of reduced matrix elements, all summations over the magnetic quantum numbers μ', σ, and σ' can be carried out with the aid of recoupling theorems. The properties of the Racah coefficient $W(abcd, ef)$ are now well known (Biedenharn *et al.* 1952), and will be used freely in the next sections; relevant properties of the X-coefficient are summarized in the Appendix. By the operations we have described the matrix element of (19) can be brought into the form

$$\begin{aligned}(f|H_\beta|i) = {} & \tfrac{1}{2}(-1)^{s-\frac{1}{2}}\sum_n (-1)^{\eta\xi+\xi}\sum_{\beta\beta'} \beta^{\xi+1}\beta'[C_n\delta_{\beta,(1-2\eta)\beta'}+C_n'\delta_{\beta,(2\eta-1)\beta'}] \\ & \times \sum_{JLl'} (J_f J M_f M|J_i M_i)\,\langle K_n; JL; l+l'-L\rangle\, U(J, L, \xi) \\ & \times \sum_{j'h} (\tfrac{1}{2}h\ s\ m-M-s|j'\ m-M)(j\ j'\ m\ M-m|J\ M)\, Y_h^{M-m+s}(\theta', \phi') \\ & \times i^{L-l'}q^{l'}F_l^{\beta,a*}[1+(-1)^{e+l'+h}]A_0\begin{pmatrix} l & \frac{1}{2} & j \\ l' & \frac{1}{2} & j' \\ L & \xi & J\end{pmatrix},\end{aligned} \tag{24}$$

$$l = j+\tfrac{1}{2}a\beta, \qquad M = M_i - M_f, \qquad e = \tfrac{1}{2}-\tfrac{1}{2}\beta'.$$

$$A_0\begin{pmatrix} l & \frac{1}{2} & j \\ l' & \frac{1}{2} & j' \\ L & \xi & J\end{pmatrix}$$

is a modified X-coefficient and is defined in the Appendix; it is zero unless $l+l'+L$ is even. Because $K_n''\gamma_5$ is obtained from K_n'' by changing the value of η, the coefficient of C_n' in (24) is the same as the coefficient of C_n except for

a change in the value of η. In deriving (24) use was made of the identity (25) containing a Racah coefficient with special values for some of the parameters; a proof is given in the Appendix.

$$(25) \qquad [2(2e+1)(2l'+1)]^{\frac{1}{2}}(el'00|h0)W(e\tfrac{1}{2}l'j', \tfrac{1}{2}h) = \tfrac{1}{2}[1+(-1)^{e+l'+h}].$$

Conservation laws can be used to eliminate reduced matrix elements specified by certain combinations of J, L, ξ, and η from the expansion (24). Note that J is the quantum number of the total angular momentum carried off by the electron–neutrino pair; L and ξ represent the corresponding orbital and spin angular momenta. As may be seen from the first vector-addition coefficient in (24), conservation of angular momentum requires that

$$(26) \qquad \Delta J \equiv |J_i - J_f| \leqslant J \leqslant J_i + J_f;$$

we shall call ΔJ the change in nuclear spin. Let the nuclear parity change $\Delta\pi$ be defined to be $+1$ when the initial and final nuclear states have the same parity and -1 when they have opposite parity. Then the nuclear matrix element is zero unless

$$(27) \qquad \Delta\pi = (-1)^{L+\eta}.$$

The reduced matrix elements in the expansion (24) of $(f|H_\beta|i)$ contain a factor $r^{l+l'}$; l and l' play a role here analogous to that of the orbital angular momenta in a nonrelativistic theory. Because the value of r (in units of $\hbar m^{-1}c^{-1}$) is of the order of magnitude of 0.02, the dominant terms in (24) are those with the smallest value of $l+l'$. The approximation usually made in β-decay theory is that of discarding all terms in the expansion of $(f|H_\beta|i)$ except those with the minimum value of the degree-of-forbiddenness parameter, $f \equiv l+l'+\eta$, permitted by the nuclear quantum numbers. The term η is included in the definition of f because matrix elements containing a K_n^μ for which $\eta = 1$ are expected to be smaller than those for $\eta = 0$ by a factor roughly equal to some mean value of v/c for the nuclear states in question. With this definition, matrix elements satisfying the nuclear selection-rules (26) and (27) are of approximately the same magnitude if they have the same value of f. Note that there are no allowed, i.e. $f = 0$, matrix elements with $\eta = 1$. The minimum value of $l+l'$ is L. In discussing the dependence of L upon nuclear parameters it is convenient to divide the nuclear transitions into two classes dependent upon the relation between ΔJ and $\Delta\pi$.

I. If $\Delta\pi = (-1)^{\Delta J}$, then the minimum value of f is ΔJ, and three types of matrix element must be considered.

(i) $\eta = 0$,	$\xi = 0$ or 1,	$L = J$,	$J = \Delta J$;
(ii) $\eta = 1$,	$\xi = 1$,	$L = J-1$,	$J = \Delta J$;
(iii) $\eta = 0$,	$\xi = 1$,	$L = J-1$,	$J = \Delta J+1$.

When $\Delta J = 0$, case (ii) and the $\xi = 1$ alternative of case (i) are to be omitted; case (iii) does not satisfy (26) if either J_i or J_f is 0.

II. If $\Delta\pi = (-1)^{\Delta J+1}$, then the minimum value of f is $\Delta J-1$, for $\Delta J \neq 0$,

and only terms with $\eta = 0$ and $\xi = 1$ contribute. These matrix elements are the same as those considered in case (iii) of I. If $J_i = J_f = 0$, then the only types of matrix element which can occur are:

(i) $\eta = 0, \quad \xi = 1, \quad L = 1, \quad J = 0;$

(ii) $\eta = 1, \quad \xi = 0, \quad L = 0, \quad J = 0.$

Both these types are first-forbidden, i.e. have $f = 1$. If $J_i = J_f \neq 0$, matrix elements of types (i) to (iii) of I also occur, with ΔJ put equal to 1.

If the β-interaction is completely lacking in either A or T, then the shapes of spectra of Class II are completely calculable—i.e. they do not depend upon unknown ratios of coupling constants or matrix elements. Such transitions are often said to be unique. We shall extend the definition slightly and term the transitions of II the U class; similarly transitions of I will be called the non-U class. The degree of forbiddenness of a given transition is defined to be the minimum value of f corresponding to a matrix element in the relevant expansion of the form (24).

In treating the effect of the P-interaction in first-forbidden ($\Delta J = 0$) transitions we have not followed those authors who have assumed that $\int \Psi^* \beta\gamma_5 \Phi d\mathbf{r} \equiv \langle \beta\gamma_5; 00 \rangle$ is so small that the contributions from P are negligible for any reasonable value of C_P. A brief discussion of this question with references to the literature is given by Konopinski (Siegbahn 1955).

Although it is only in the most careful measurements of spectral shapes that the presence of matrix elements other than those of minimum forbiddenness could be detected, we shall include all terms in our general formulae of the next section. With the formalism employed this inclusion requires no extra effort. Only dominant terms will be given, however, in the particular formulae discussed in the remaining sections. The degree of forbiddenness of the most important higher terms is always two greater than that of the dominant terms. Formulae for the second-degree corrections to allowed spectra have been given by Zweifel (1954).

Let us assume with Longmire and Messiah (1951) that the action of the Wigner time-reversal operator, $\mathcal{K}$, on nuclear wave-functions is described by (28),

$$\mathcal{K}\Psi_J{}^M = e^{i\phi}\Psi_J{}^{-M}, \tag{28}$$

the phase ϕ being dependent on the nuclear state. $\mathcal{K}$ is the product of a unitary matrix, U, and an operator which takes complex conjugates. In our representation we may put $U = i\sigma_Y$, or

$$U_{\beta\sigma\beta'\sigma'} = \delta_{\beta\beta'}(-1)^{\sigma-\frac{1}{2}}\delta_{\sigma,-\sigma'},$$

whence it follows that

$$U[T_n{}^{M*}(JL)]^T U^* = (-1)^{J+M} T_n{}^{-M}(JL). \tag{29}$$

(The elements of the matrix $[A^*]^T$ are the complex conjugates of the elements of A.) Using (29) one can show without difficulty that

$$\langle K_1; J_1 L_1; k_1 \rangle^* \langle K_2; J_2 L_2; k_2 \rangle = \langle K_1; J_1 L_1; k_1 \rangle \langle K_2; J_2 L_2; k_2 \rangle^*. \tag{30}$$

3. GENERAL ANGULAR CORRELATIONS

The angular distribution of electrons emitted when the absorption of an antineutrino of given momentum and spin causes a particular nuclear transition may be obtained by calculating the particle-current for the wave-function (18). For ψ's satisfying the wave-equation (1) the current is $-(\psi^*\boldsymbol{\alpha}\psi)$; the angular distribution function for the electrons is found by multiplying the radial component of this current by r^2. To obtain results comparable with experiment we must sum over all possible values of M_f (because of the orthogonality of final nuclear wave-functions, cross terms between ψ's corresponding to different values of M_f do not occur) and average over all possible values of M_i. We shall write $P(M_i)$ for the probability that the nucleus is initially in a state with magnetic quantum number M_i, the normalization condition

$$\sum_{M_i} P(M_i) = 1$$

being understood; the form of the dependence of P upon M_i is determined by the mode of producing the oriented nuclei. Summations over s and over the states in an appropriate part of the neutrino momentum space are also to be performed. Let the probability that an electron is emitted into an element of solid angle $d\Omega$ at (θ, ϕ) with its energy in an interval dE at E while a neutrino is emitted into $d\Omega'$ at (θ', ϕ') be $W(\theta, \theta', \phi-\phi')d\Omega d\Omega' dE$. Then

$$W(\theta, \theta', \phi-\phi') = -\sum_{M_i M_f s} P(M_i)(2\pi)^{-3}q^2r^2(\psi^*\alpha_r\psi). \tag{31}$$

Note that the ψ in (31) depends implicitly upon M_i, M_f, and s, all quantum numbers related to orientation of angular momentum vectors. The symbol α_r in (31) represents the component of the vector $\boldsymbol{\alpha}$ in the outward radial direction. It is customary in the theory of β-decay to quote results in the form of a correction factor, $S_0(\theta, \theta', \phi-\phi')$ as defined in (32), which relates the statistical distribution to the true distribution.

$$W(\theta, \theta', \phi-\phi') = (2\pi^3)^{-1}Epq^2F_0(E, Z)S_0(\theta, \theta', \phi-\phi'). \tag{32}$$

$F_0(E, Z)$ is the Fermi function as defined by Greuling (1942); extensive tables of a closely related function have been published by the National Bureau of Standards (Fano 1952).

Simplification of the right side of (31) is facilitated by the use of a more convenient form of the current. Equation (1) may be rewritten in the form

$$\psi = (V-E)\beta\psi - \beta\boldsymbol{\alpha}\cdot\mathbf{p}\psi. \tag{33}$$

By taking the arithmetic mean of the two formulae found by substituting expression (33) for each of the ψ's in $-(\psi^*\boldsymbol{\alpha}\psi)$ in turn, one can show that

$$-(\psi^*\boldsymbol{\alpha}\psi) = \tfrac{1}{2}\{[(\mathbf{p}\psi)^*\cdot\boldsymbol{\alpha}]\beta\boldsymbol{\alpha}\psi + \psi^*\boldsymbol{\alpha}\beta(\boldsymbol{\alpha}\cdot\mathbf{p})\psi\}. \tag{34}$$

Now to the first order in r^{-1} the ψ of (18) satisfies

$$\mathbf{p}\psi = p\mathbf{n}\psi; \tag{35}$$

here $\mathbf{p}$ is the linear momentum operator, $\mathbf{n}$ is a unit outward radial vector, and p is a number equal to $(E^2-1)^{\frac{1}{2}}$. Substitution of (35) in (34) with the use of the anticommutation relations for $(\beta, \boldsymbol{\alpha})$ leads to

$$-(\psi^*\alpha_r\psi) = -p(\psi^*\beta\psi). \tag{36}$$

Similar to the derivation of (34) is the proof that

$$\psi^*\psi = (V-E)(\psi^*\beta\psi) - \tfrac{1}{2}[(\psi^*\beta\boldsymbol{\alpha}\cdot\mathbf{p}\psi) + (\mathbf{p}\psi)^*\cdot\boldsymbol{\alpha}\beta\psi]. \tag{37}$$

Since $V(r)$ approaches zero as r goes to infinity, we can, with the aid of (35) and of the anticommutation relations, transform (37) into

$$\psi^*\psi = -E(\psi^*\beta\psi), \text{ valid for large values of } r. \tag{38}$$

The application of (38) to (36) gives rise to the asymptotic formula (39) for the outward radial current.

$$-(\psi^*\alpha_r\psi) = pE^{-1}(\psi^*\psi). \tag{39}$$

Since in the units being used pE^{-1} is equal to the magnitude of the velocity of the emitted electrons, expression (39) simply says that the asymptotic current is the product of velocity and particle density. It is of interest to note that the relation (35), and hence the equations (36) and (38), are exactly true for the momentum eigenfunctions of a free particle (Bethe 1948). Combination of (31), (32), and (39) leads to the formula (40) for the correction-factor.

$$S_0(\theta, \theta', \phi-\phi') = [4E^2F_0(E, Z)]^{-1} \sum_{M_i M_f s} P(M_i) r^2 (\psi^*\psi). \tag{40}$$

The question of a suitable definition of a vector polarization, $\boldsymbol{\zeta}$, for a Dirac electron has been discussed by Tolhoek (1956), who has pointed out that the direction of $\boldsymbol{\zeta}$ is that of $\psi^*(I-\beta)\boldsymbol{\sigma}\psi$. If, as is desired, the magnitude of $\boldsymbol{\zeta}$ is to be equal to the degree of polarization, then $\boldsymbol{\zeta}$ should be defined to be the appropriate statistical-mechanical average of the expectation value of the operator $(1+E^{-1})^{-1}(I-\beta)\boldsymbol{\sigma}$. Thus

$$\boldsymbol{\zeta} \sum_{M_i M_f s} P(M_i)(\psi^*\psi) = \sum_{M_i M_f s} P(M_i)(1+E^{-1})^{-1}[\psi^*(I-\beta)\boldsymbol{\sigma}\psi]. \tag{41}$$

Because the efficiencies of the various methods for measuring polarizations described by Tolhoek are given in terms of $\boldsymbol{\zeta}$, this vector provides a convenient way of expressing polarization results.

In deriving formulae for $\boldsymbol{\zeta}$, it is more convenient, of course, to work with the spherical components, ζ^μ. Let us define a set of four quantities S_t^μ; $\mu = 0$ when $t = 0$ and $\mu = \pm 1$ or 0 when $t = 1$.

$$S_t^\mu = [4E^2F_0(E, Z)]^{-1} \sum_{M_i M_f s} P(M_i) r^2 (\psi^* \mathcal{O}_t^\mu \psi). \tag{42}$$

For $t = 0$ we put $\mathcal{O}_0 = I$, and S_0^0 of (42) is the correction-factor S_0 of (40). For $t = 1$ we put $\mathcal{O}_1^\mu = (1+E^{-1})^{-1}(I-\beta)\sigma^\mu$; the spherical components of the vector polarization are then given by (43).

$$\zeta^\mu = S_1^\mu / S_0. \tag{43}$$

Thus all the required information about the distributions can be obtained from a knowledge of the quantities S_t^{μ}.

Next we turn our attention to the evaluation of $(\psi^* \mathcal{O}_t^{\mu} \psi)$, using the ψ of (18). By a slight adjustment of formula (11) for the matrix elements of K_n^{μ}, one can show that

$$(\mathcal{O}_t^{\mu})_{\beta\sigma\beta'\sigma'} = (1+\delta_{t1}E^{-1})^{-1}\delta_{\beta\beta'}(1-\delta_{t1}\beta)(-1)^{\sigma'-\frac{1}{2}}2^{\frac{1}{2}}(\tfrac{1}{2}\ \tfrac{1}{2}\ \sigma\ -\sigma'|t\ \mu).$$

In carrying out the required contraction, sums of the form (44) are encountered.

$$(44)\quad B \equiv \sum_{\beta}(1-\beta E^{-1})(1-\delta_{t1}\beta)\sum_{\sigma\sigma'}(-1)^{\sigma'-\frac{1}{2}}(\tfrac{1}{2}\ \tfrac{1}{2}\ \sigma\ -\sigma'|t\ \mu)$$
$$\times(\lambda_1\ \tfrac{1}{2}\ m_1-\sigma\ \sigma|j_1\ m_1)(\lambda_2\ \tfrac{1}{2}\ m_2-\sigma'\ \sigma'|j_2\ m_2)\,Y_{\lambda_1}^{m_1-\sigma *}(\theta,\phi)\,Y_{\lambda_2}^{m_2-\sigma'}(\theta,\phi).$$
$$\lambda_i = j_i+\tfrac{1}{2}a_i\beta.$$

By expanding the product of the two spherical harmonics and by recoupling the two vector-addition coefficients, expression (44) can be transformed into (45).

$$(45)\quad B = \sum_{k',g}[(4\pi)^{-1}(2j_1+1)(2j_2+1)(2t+1)(2k'+1)(2g+1)^{-1}]^{\frac{1}{2}}$$
$$\times(j_1 j_2\ -m_1\ m_2|k'\ m_2-m_1)(k'\ t\ m_2-m_1\ \mu|g\ m_2-m_1+\mu)\,Y_g^{m_2-m_1+\mu}(\theta,\phi)$$
$$\sum_{\beta}(-1)^{j_2+m_1-\lambda_2}(1-\beta E^{-1})(1-\delta_{t1}\beta)[(2\lambda_1+1)(2\lambda_2+1)]^{\frac{1}{2}}$$
$$(\lambda_1\lambda_2 00|g0)X\begin{pmatrix} j_1 & \frac{1}{2} & \lambda_1 \\ j_2 & \frac{1}{2} & \lambda_2 \\ k' & t & g \end{pmatrix}.$$

Because λ_1 and λ_2 are functions of β, it would appear at first sight that the summation over β in (45) could not be carried out explicitly. However, we show in the Appendix that

$$(46)\quad [(2\lambda_1+1)(2\lambda_2+1)]^{\frac{1}{2}}(\lambda_1\lambda_2 00|g0)X\begin{pmatrix} j_1 & \frac{1}{2} & \lambda_1 \\ j_2 & \frac{1}{2} & \lambda_2 \\ k' & t & g \end{pmatrix}$$
$$=(-1)^t 2^{-3/2}[1+(-1)^{\lambda_1+\lambda_2+g}][(2t+1)(2k'+1)]^{-\frac{1}{2}}(j_1 j_2\ \tfrac{1}{2}\ -\tfrac{1}{2}|k'\ 0)$$
$$\times[(-1)^{j_2-\frac{1}{2}+\lambda_2}(tk'00|g0)-\delta_{t1}\Delta_{j_2-\frac{1}{2},j_1-\frac{1}{2}}(k',g)]$$

with

$$(47)\quad \Delta_{\mu\nu}(k',g) = 2^{\frac{1}{2}}[k'(k'+1)]^{-\frac{1}{2}}(1k'1-1|g0)[(\mu+1)+(-1)^{\mu+\nu+k'+1}(\nu+1)].$$

Now, recalling that $\lambda_i = j_i+\frac{1}{2}a_i\beta$, one sees that

$$(-1)^{j_2-\frac{1}{2}+\lambda_2} = -\beta a_2$$

and that

$$(-1)^{\lambda_1+\lambda_2} = (-1)^{j_1-j_2}a_1 a_2.$$

Substituting (46) in (45) and using

$$\sum_{\beta} \beta^n = 1+(-1)^n,$$

we can now carry out the summation over β in the last line of (45) without difficulty. The presence of the factor

$$[1+(-1)^{g+j_1-j_2}a_1a_2]$$

shows that the order of the spherical harmonic describing the electron emission is even or odd as the parities of the electron states

$$\psi^{j_1m_1a_1} \quad \text{and} \quad \psi^{j_2m_2a_2}$$

are the same or opposite; this fact is used extensively in the manipulations which follow.

Once the spinor contraction has been performed one can bring S_t^{μ} of (42) into the form (48) using the definitions of the two recoupling coefficients, the orthonormality relations for the vector-addition coefficients, and the identity (A.15) of the Appendix.

$$(48) \quad S_t^{\mu} = \sum_{kk'gg'} (4\pi)^{-1}(-1)^{g'}[(2t+1)(2g'+1)]^{-\frac{1}{2}}Z(k)R(gg'kk't)$$
$$\times \sum_{m} (kg'0m|k'm)(k'\, g\, m\, \mu-m|t\, \mu)\, Y_{g'}{}^{m}(\theta',\, \phi')\, Y_g{}^{\mu-m}(\theta,\, \phi).$$

The angles (θ', ϕ') and (θ, ϕ) are, it may be recalled, the spherical polar coordinates with respect to the axis of nuclear orientation of the directions of emission of the neutrino and electron respectively. Information about the degree of nuclear orientation is contained in the functions $Z(k)$ defined by (49).

$$(49) \qquad Z(k) = \sum_{M_i} (-1)^{J_i-M_i}(2J_i+1)^{\frac{1}{2}}(J_i\, J_i\, M_i\, -M_i|k\, 0)P(M_i).$$

It follows from the properties of the vector-addition coefficients that $Z(k)$ is zero if k is greater than $2J_i$. Note that

$$(50) \qquad Z(0) = 1 \quad \text{and} \quad Z(1) = 3^{\frac{1}{2}}[J_i(J_i+1)]^{-\frac{1}{2}}\, \langle J_{iz}\rangle,$$

$\langle J_{iz}\rangle$ being the mean value of the component of nuclear spin in the direction of the axis of orientation in the initial state. If the decaying nuclei are aligned but not polarized, i.e. if $P(-M_i) = P(M_i)$, then $Z(k)$ is zero for odd values of k. When the initial nuclei are unoriented, i.e. when $P(M_i) = (2J_i+1)^{-1}$, then (49) reduces to

$$(51) \qquad Z(k) = \delta_{k0}.$$

A discussion of earlier uses of coefficients similar to $Z(k)$ is given by de Groot and Tolhoek in *Beta- and Gamma-Ray Spectroscopy* (Siegbahn 1955).

The outstanding coefficient in (48), $R(gg'kk't)$, contains combinations of coupling constants, reduced nuclear matrix elements, electron phase-shifts, electron and neutrino radial wave-functions evaluated at $r = \rho$, and various functions of "angular momentum" quantum numbers.

$$(52)\quad R(gg'kk't) = (-1)^{g+J_f-J_i}(8F_0p^2)^{-1}[(2J_i+1)(2k+1)(2k'+1)^{-1}]^{\frac{1}{2}}$$

$$\sum_{n_1n_2}(-1)^{\eta_1\xi_1+\eta_2\xi_2+\xi_1+\xi_2}\sum_{J_1J_2L_1L_2l_1'l_2'}i^{L_2-l_2'-L_1+l_1'}q^{l_1'+l_2'}$$

$$U(J_1L_1\xi_1)U(J_2L_2\xi_2)W(J_1J_2J_iJ_i, kJ_f)\sum_{j_1j_2j_1'j_2'}(-1)^{J_1+j_1-j_1'}$$

$$[(2j_1+1)(2j_2+1)(2j_1'+1)(2j_2'+1)]^{\frac{1}{2}}(j_1j_2\tfrac{1}{2}-\tfrac{1}{2}|k'0)(j_1'j_2'\tfrac{1}{2}-\tfrac{1}{2}|g'0)$$

$$A\begin{pmatrix} j_1 & j_1' & J_1 \\ j_2 & j_2' & J_2 \\ k' & g' & k \end{pmatrix}\sum_{a_1a_2}e^{i[\delta(j_2,a_2)-\delta(j_1,a_1)]}[1+(-1)^{g+j_1-j_2}a_1a_2]$$

$$[(tk'00|g0)-a_2\delta_{t1}\Delta_{j_2-\frac{1}{2},j_1-\frac{1}{2}}(k',g)]\sum_{\beta_1\beta_2}\beta_1^{\xi_1+1}\beta_2^{\xi_2+1}F_{l_1}^{\beta_1,a_1}F_{l_2}^{\beta_2,a_2*}$$

$$A_0\begin{pmatrix} l_1 & \frac{1}{2} & j_1 \\ l_1' & \frac{1}{2} & j_1' \\ L_1 & \xi_1 & J_1 \end{pmatrix}\quad A_0\begin{pmatrix} l_2 & \frac{1}{2} & j_2 \\ l_2' & \frac{1}{2} & j_2' \\ L_2 & \xi_2 & J_2 \end{pmatrix}$$

$$\langle K_{n_1};J_1L_1;l_1+l_1'-L_1\rangle^*\langle K_{n_2};$$
$$J_2L_2;l_2+l_2'-L_2\rangle\sum_{\beta_1'\beta_2'}\beta_1'\beta_2'[1+\beta_1'\beta_2'(-1)^{l_1'+l_2'+g'}]$$

$$[C_{n_1}{}^*\delta_{\beta_1,(1-2\eta_1)\beta_1'}+C_{n_1}{}'^*\delta_{\beta_1,(2\eta_1-1)\beta_1'}][C_{n_2}\delta_{\beta_2,(1-2\eta_2)\beta_2'}+C_{n_2}{}'\delta_{\beta_2,(2\eta_2-1)\beta_2'}]$$

By inspection of the last lines of (52) one can see that the two parity conserving terms (Lee and Yang 1956) $C_{n_1}{}^*C_{n_2}$ and $C_{n_1}{}'^*C_{n_2}{}'$ have the same coefficient. Similarly the coefficients of the two parity nonconserving terms $C_{n_1}{}^*C_{n_2}{}'$ and $C_{n_1}{}'^*C_{n_2}$ are the same. In the coefficient of the product of two coupling constants of which ν are primed the nonvanishing of the Kronecker deltas demand that

$$\beta_1'\beta_2' = (-1)^{\eta_1+\eta_2+\nu}\beta_1\beta_2.$$

Now from the nuclear parity selection-rule (27) we can show that

$$(-1)^{\eta_1+\eta_2} = (-1)^{L_1+L_2},$$

and from the properties of the A_0-coefficient we recall that

$$(-1)^{L_i+l_i'} = (-1)^{l_i}, \qquad i = 1, 2.$$

Thus

$$\begin{aligned}\beta_1'\beta_2'(-1)^{l_1'+l_2'+g'} &= (-1)^{\nu+g'+l_1+l_2}\beta_1\beta_2\\ &= (-1)^{\nu+g'+j_1-j_2+\frac{1}{2}a_1\beta_1-\frac{1}{2}a_2\beta_2}\beta_1\beta_2\\ &= (-1)^{\nu+g'+j_1-j_2}a_1a_2 = (-1)^{\nu+g'+g}.\end{aligned}$$

Hence we have shown, as expected, that for the parity-conserving terms, $\nu = 0$ or 2, the sum of the orders of the spherical harmonics describing the electrons and the neutrinos must be even; for the parity nonconserving terms, $\nu = 1$, this sum must be odd.

To simplify the rewriting of (52) and to conform to custom, we replace the summations over j_1 and j_2 by summations over the non-negative integral parameters $\mu = j_2 - \frac{1}{2}$ and $\nu = j_1 - \frac{1}{2}$. We have shown in the preceding paragraph how the summations over β_1' and β_2' in (52) may be performed. The summations over a_1, a_2, β_1, and β_2 result in the appearance of generalizations of the functions L_ν, M_ν, and N_ν defined by Greuling (1942). The way in which this step is carried out depends upon the relative sign of a_1 and a_2; it is therefore convenient to eliminate the sum over a_1 in favor of one over a new parameter σ, also taking the values ± 1, defined by $a_1 = \sigma a_2$. In order to arrange that the combinations of electron wave-functions that we are about to define be real numbers we make the expansion

$$e^{i[\delta(j_2,a_2)-\delta(j_1,a_1)]} = \sum_{\tau=0}^{1} i^\tau[\delta_{\tau 0}\cos\Omega_{\mu\nu}(a_2,\sigma)+\delta_{\tau 1}\sin\Omega_{\mu\nu}(a_2,\sigma)]$$

wherein

$$\Omega_{\mu\nu}(a,\sigma) = \delta(\mu+\tfrac{1}{2},a)-\delta(\nu+\tfrac{1}{2},\sigma a). \tag{53}$$

With each of the four choices $\beta_1 = \pm a_1$, $\beta_2 = \pm a_2$ the summation over a_2 in (52) gives one of the three types of function defined in (54)

$$L_{\mu\nu}(\zeta\sigma\tau) = i^{\frac{1}{2}-\frac{1}{2}\sigma}(2p^2F_0)^{-1}\sum_a a^\zeta F_\mu^{-a,a*}F_\nu^{-\sigma a,\sigma a}\begin{matrix}\cos\\ \sin\end{matrix}\Omega_{\mu\nu}(a,\sigma), \tag{54a}$$

$$M_{\mu\nu}(\zeta\sigma\tau) = i^{\frac{1}{2}-\frac{1}{2}\sigma}(2p^2F_0)^{-1}\sum_a (-a)^\zeta F_{\mu+1}^{a,a*}F_{\nu+1}^{\sigma a,\sigma a}\begin{matrix}\cos\\ \sin\end{matrix}\Omega_{\mu\nu}(a,\sigma), \tag{54b}$$

$$N_{\mu\nu}(\zeta\sigma\tau) = i^{-\frac{1}{2}-\frac{1}{2}\sigma}(2p^2F_0)^{-1}\sum_a a^\zeta F_{\mu+1}^{a,a*}F_\nu^{-\sigma a,\sigma a}\begin{matrix}\cos\\ \sin\end{matrix}\Omega_{\mu\nu}(a,\sigma). \tag{54c}$$

Note that each choice also corresponds to a definite relationship between l_1 and j_1 and between l_2 and j_2. For example, when $\beta_1 = -a_1$ and $\beta_2 = -a_2$ we have $l_1 = j_1 - \frac{1}{2}$ and $l_2 = j_2 - \frac{1}{2}$, and summation over a_2 yields $L_{\mu\nu}(\zeta\sigma\tau)$; there is also a term containing $L_{\mu\nu}(\zeta+1,\sigma\tau)$ when $t = 1$. The index τ in (54) takes values 0 and 1, the former corresponding to cos and the latter to sin in the $\begin{matrix}\cos\\ \sin\end{matrix}$ ambiguity. The parameter ζ in (54) is an abbreviation for $\zeta_1+\zeta_2$. Since ζ appears only as an exponent to the quantity $\pm a$, and since the dummy a takes the values ± 1 only, it is clear that all even values of ζ are equivalent to 0 and that all odd values are equivalent to 1. As has already been stated, σ has the two values ± 1, corresponding to $a_1 = \pm a_2$. Thus the two possible values for each of the three parameters ζ, σ, and τ inserted in the L-, M-, and N-functions of (54) give rise to 24 different functions of p and ρ (and of the nuclear charge distribution), each dependent upon the two integral indices μ and ν, in terms of which the general electron–neutrino polarization distribution can be expressed. For the L- and M-functions different choices of μ and ν do not always lead to independent functions. From the definitions (15) and from the reality of f_κ and g_κ, it follows that

$$F_l^{\beta,a*} = -\beta F_l^{\beta,a}. \tag{55}$$

Using (55) one can show without difficulty that

$$L_{\nu\mu}(\zeta\sigma\tau) = (-1)^{\tau}\sigma^{\zeta+1}L_{\mu\nu}(\zeta\sigma\tau), \tag{56a}$$

$$M_{\nu\mu}(\zeta\sigma\tau) = (-1)^{\tau}\sigma^{\zeta+1}M_{\mu\nu}(\zeta\sigma\tau). \tag{56b}$$

From (56) follow the useful results

$$L_{\nu\nu}(\zeta 11) \equiv 0 \equiv M_{\nu\nu}(\zeta 11), \qquad \text{for all } \zeta, \tag{57a}$$

and

$$L_{\nu\nu}(\zeta-1\tau) \equiv 0 \equiv M_{\nu\nu}(\zeta-1\tau), \qquad \text{if } \zeta+\tau \text{ is even.} \tag{57b}$$

Though $N_{\nu\nu}(\zeta 11) \equiv 0$, no relation analogous to (57*b*) holds for $N_{\nu\nu}(\zeta-1\tau)$. Equation (55) can also be used to show that each of the functions defined in (54) is real. The definitions (56) have been so devised that $L_{\nu\nu}(010)$, $M_{\nu\nu}(010)$, and $N_{\nu\nu}(010)$ are identical with the L_ν, M_ν, and N_ν of Greuling (1942). Similarly $L_{\nu\nu}(110)$, $M_{\nu\nu}(110)$, and $N_{\nu\nu}(110)$ are equal to the P_ν, Q_ν, and R_ν defined by Pursey (1951); these same three functions are called L_ν^-, M_ν^-, and N_ν^- by Banerjee and Saha (1954); they occur only if the β-interaction is drawn from both *STP* and *VA*.

Before rewriting $R(gg'kk't)$ in its final form we shall introduce one more simplification. Because n_1 and n_2 both run through the same eight values, the complex conjugate of the product of each pair of different matrix-elements occurring in (52) also occurs. Since, by (30), the complex conjugate of such a product is equal to the original product, we can see that each product of different matrix elements occurs twice. By re-naming summation dummies in such a way that the symbols bearing the subscripts 1 and 2 are interchanged, and by the use of the symmetry properties of the various angular-momentum coefficients, one can show that the two coefficients of a twice-occurring matrix-element product differ by the sign $(-1)^{k+g'+t+\tau}$ and by the complex conjugation of the coupling constants. The incorporation into (52) of this simplification and of the changes described in the preceding paragraphs gives rise to (58).

$$\begin{aligned}
R(gg'kk't) = {} & \tfrac{1}{4}[(2k+1)(2k'+1)^{-1}]^{\frac{1}{2}} \sum_{n_1 \leqslant n_2} (1+\delta_{12})^{-1} \\
& \sum_{J_1 L_1 J_2 L_2} (-1)^{S+J_1-J_f+g} (2J_1+1)^{\frac{1}{2}}\, W(J_1 J_2 J_i J_i, kJ_f) U(J_1 L_1 \xi_1) U(J_2 L_2 \xi_2) \\
& \sum_{\tau} i^{\tau} \{[(C_{n_1}{}^* C_{n_2} + C_{n_1}{}'^* C_{n_2}') + (-1)^{\omega}(C_{n_1} C_{n_2}{}^* + C_{n_1}' C_{n_2}'^*)][1+(-1)^{g+g'}] \\
& -[(C_{n_1}{}'^* C_{n_2} + C_{n_1}{}^* C_{n_2}') + (-1)^{\omega}(C_{n_1}' C_{n_2}{}^* + C_{n_1} C_{n_2}'^*)][1-(-1)^{g+g'}]\} \\
& \sum_{\sigma} \sigma^{\xi_1} i^{\frac{1}{2}\sigma-\frac{1}{2}} \sum_{\mu\nu} \sum_{j_1' j_2' l_1' l_2'} [(2j_1+1)(2j_2+1)(2j_1'+1)(2j_2'+1)]^{\frac{1}{2}} \\
& \qquad (j_1 j_2 \tfrac{1}{2} | k'0)(j_1' j_2' \tfrac{1}{2} - \tfrac{1}{2} | g'0)\, A \begin{pmatrix} j_1 & j_1' & J_1 \\ j_2 & j_2' & J_2 \\ k' & g' & k \end{pmatrix} \\
& \qquad (-1)^{J_1+j_1-j_1'} i^{L_2-l_2'-L_1+l_1'} q^{l_1'+l_2'} [1+(-1)^{g+j_1-j_2}\sigma]
\end{aligned} \tag{58}$$

$$\{\langle K_{n_2};\, J_2L_2;\, \mu+l_2'-L_2\rangle\langle K_{n_1};\, J_1L_1;\, \nu+l_1'-L_1\rangle^*$$

$$A_0\begin{pmatrix}\mu & \frac{1}{2} & j_2\\ l_2' & \frac{1}{2} & j_2'\\ L_2 & \xi_2 & J_2\end{pmatrix}\quad A_0\begin{pmatrix}\nu & \frac{1}{2} & j_1\\ l_1' & \frac{1}{2} & j_1'\\ L_1 & \xi_1 & J_1\end{pmatrix}$$

$$\times\,[(tk'00|g0)L_{\mu\nu}(\zeta\sigma\tau)-\delta_{t_1}\Delta_{\mu\nu}L_{\mu\nu}(\zeta+1\;\sigma\;\tau)]$$

$$+\langle K_{n_2};\, J_2L_2;\, \mu+1+l_2'-L_2\rangle\langle K_{n_1};\, J_1L_1;\, \nu+1+l_1'-L_1\rangle^*$$

$$A_0\begin{pmatrix}\mu+1 & \frac{1}{2} & j_2\\ l_2' & \frac{1}{2} & j_2'\\ L_2 & \xi_2 & J_2\end{pmatrix}\quad A_0\begin{pmatrix}\nu+1 & \frac{1}{2} & j_1\\ l_1' & \frac{1}{2} & j_1'\\ L_1 & \xi_1 & J_1\end{pmatrix}$$

$$\times[(tk'00|g0)M_{\mu\nu}(\zeta\sigma\tau)-\delta_{t_1}\Delta_{\mu\nu}M_{\mu\nu}(\zeta+1\;\sigma\;\tau)]$$

$$+i(-1)^{\zeta_2}\langle K_{n_2};\, J_2L_2;\, \mu+1+l_2'-L_2\rangle\langle K_{n_1};\, J_1L_1;\, \nu+l_1'-L_1\rangle^*$$

$$A_0\begin{pmatrix}\mu+1 & \frac{1}{2} & j_2\\ l_2' & \frac{1}{2} & j_2'\\ L_2 & \xi_2 & J_2\end{pmatrix}\quad A_0\begin{pmatrix}\nu & \frac{1}{2} & j_1\\ l_1' & \frac{1}{2} & j_1'\\ L_1 & \xi_1 & J_1\end{pmatrix}$$

$$\times[(tk'00|g0)N_{\mu\nu}(\zeta\sigma\tau)-\delta_{t1}\Delta_{\mu\nu}N_{\mu\nu}(\zeta+1\sigma\tau)]$$

$$-i(-1)^{\zeta_1+\tau}\sigma^{\zeta+1}\langle K_{n_2};\, J_2L_2;\, \mu+l_2'-L_2\rangle\langle K_{n_1};\, J_1L_1;\, \nu+1+l_1'-L_1\rangle^*$$

$$A_0\begin{pmatrix}\mu & \frac{1}{2} & j_2\\ l_2' & \frac{1}{2} & j_2'\\ L_2 & \xi_2 & J_2\end{pmatrix}\quad A_0\begin{pmatrix}\nu+1 & \frac{1}{2} & j_1\\ l_1' & \frac{1}{2} & j_1'\\ L_1 & \xi_1 & J_1\end{pmatrix}$$

$$\times\,[(tk'00|g0)N_{\nu\mu}(\zeta\sigma\tau)-\sigma\delta_{t1}\Delta_{\mu\nu}N_{\nu\mu}(\zeta+1\sigma\tau)]\}$$

$$S=\eta_1\zeta_1+\eta_2\zeta_2+\zeta_1+\zeta_2+\eta_1+\eta_2+\xi_1+\xi_2\quad \omega=g'+k+t+\tau\quad \Delta_{\mu\nu}\equiv\Delta_{\mu\nu}(k',g)$$

$$\zeta=\zeta_1+\zeta_2\qquad j_2=\mu+\tfrac{1}{2}\qquad j_1=\nu+\tfrac{1}{2}\qquad \delta_{12}=\delta_{n_1n_2}\delta_{J_1J_2}\delta_{L_1L_2}\delta_{\mu\nu}\delta_{l_1'l_2'}$$

There are several tests that one may apply to (58). First, the expression must be invariant under interchange of all the quantities with subscript 1 with the corresponding quantities with subscript 2, since the ordering of the operators K_n can have no physical significance. That such an invariance holds may be demonstrated with the use of (30) and (56) and of well-known properties of the various angular momentum coefficients. From the required reality of $S_0{}^0$ and of each Cartesian component of $\boldsymbol{\zeta}$ it follows that $S_t{}^{\mu*}=(-1)^{\mu}S_t{}^{-\mu}$, which condition in turn requires that

$$R^*(gg'kk't)=(-1)^{k+g+g'+t}R(gg'kk't). \tag{59}$$

It is not difficult to show that the formula (58) satisfies (59). Other tests of the correctness of the complicated manipulations leading to (58) are the agreements with formulae previously derived for various special cases as discussed in succeeding sections.

In order to make use of the formula (58) one must have some estimate of the magnitudes of the combinations of electron wave-functions defined in (54). A convenient rough approximation, with which we shall be contented for the present, is to use a point nuclear charge and to retain only the first

term in the expansions of the radial wave-functions in powers of $(p\rho)$; this procedure will be termed the zeroth-order approximation. Note that no expansion in powers of (αZ) is implied. Retention of more than the first term in the $(p\rho)$-expansion is probably not justified in a calculation in which the finite distribution of nuclear charge is ignored. Series expansions for f_κ and g_κ are given by Rose *et al.* (1953); the phase-shift is given by Rose (1937). The presentation of the zeroth-order approximations obtained with the aid of these expansions is facilitated by the use of the following definitions:

$$(60a)\quad L_{\mu\nu}(\zeta\sigma 0) = \tfrac{1}{4}\rho^{-\mu-\nu}T_\mu T_\nu[\bar{L}_{\mu\nu}(\zeta\sigma 0)\cos(\epsilon_\mu-\epsilon_\nu)+\bar{L}_{\mu\nu}(\zeta\sigma 1)\sin(\epsilon_\mu-\epsilon_\nu)],$$

$$(60b)\quad L_{\mu\nu}(\zeta\sigma 1) = \tfrac{1}{4}\rho^{-\mu-\nu}T_\mu T_\nu[\bar{L}_{\mu\nu}(\zeta\sigma 1)\cos(\epsilon_\mu-\epsilon_\nu)-\bar{L}_{\mu\nu}(\zeta\sigma 0)\sin(\epsilon_\mu-\epsilon_\nu)]$$

$$\gamma_\nu = [(\nu+1)^2-\alpha^2Z^2]^{\frac{1}{2}} \qquad y = \alpha ZEp^{-1}$$

$$T_\nu = (2p\rho)^{\gamma_\nu-\gamma_0}\frac{\Gamma(2\gamma_0+1)}{\Gamma(2\gamma_\nu+1)}\left|\frac{\Gamma(\gamma_\nu+iy)}{\Gamma(\gamma_0+iy)}\right|$$

$$\epsilon_\nu = \tfrac{1}{2}\pi\gamma_\nu + \arg\Gamma(\gamma_\nu+iy).$$

Z and α are the atomic number and the fine-structure constant. The M- and N-functions are to be expressed in forms analogous to (60) except for factors ρ^{-2} and ρ^{-1} to be included on the right side for the former and latter respectively. In the zeroth order the results are:

$$(61a)\quad \begin{aligned}
\bar{L}_{\mu\nu}(010) &= [(\mu+1+\gamma_\mu)(\nu+1+\gamma_\nu)+\alpha^2Z^2]\\
\bar{L}_{\mu\nu}(110) &= E^{-1}[(\mu+1+\gamma_\mu)(\nu+1+\gamma_\nu)-\alpha^2Z^2]\\
\bar{L}_{\mu\nu}(011) &= -pE^{-1}\bar{L}_{\mu\nu}(0-10)\\
\bar{L}_{\mu\nu}(111) &= 0\\
\bar{L}_{\mu\nu}(0-10) &= -\alpha Z[(\mu+\gamma_\mu)-(\nu+\gamma_\nu)]\\
\bar{L}_{\mu\nu}(1-10) &= -\alpha ZE^{-1}[\mu+\gamma_\mu+\nu+\gamma_\nu+2]\\
\bar{L}_{\mu\nu}(0-11) &= pE^{-1}\bar{L}_{\mu\nu}(010)\\
\bar{L}_{\mu\nu}(1-11) &= 0.
\end{aligned}$$

$$(61b)\quad \begin{aligned}
\bar{M}_{\mu\nu}(010) &= [(\mu+1-\gamma_\mu)(\nu+1-\gamma_\nu)+\alpha^2Z^2]\\
\bar{M}_{\mu\nu}(110) &= E^{-1}[(\mu+1-\gamma_\mu)(\nu+1-\gamma_\nu)-\alpha^2Z^2]\\
\bar{M}_{\mu\nu}(011) &= -pE^{-1}\bar{M}_{\mu\nu}(0-10)\\
\bar{M}_{\mu\nu}(111) &= 0\\
\bar{M}_{\mu\nu}(0-10) &= \alpha Z[(\mu-\gamma_\mu)-(\nu-\gamma_\nu)]\\
\bar{M}_{\mu\nu}(1-10) &= \alpha ZE^{-1}[\mu-\gamma_\mu+\nu-\gamma_\nu+2]\\
\bar{M}_{\mu\nu}(0-11) &= pE^{-1}\bar{M}_{\mu\nu}(010)\\
\bar{M}_{\mu\nu}(1-11) &= 0.
\end{aligned}$$

$$(61c)\quad \begin{aligned}
\bar{N}_{\mu\nu}(010) &= -\alpha Z[\mu-\gamma_\mu+\nu+\gamma_\nu+2]\\
\bar{N}_{\mu\nu}(110) &= \alpha ZE^{-1}[\mu-\gamma_\mu-\nu-\gamma_\nu]\\
\bar{N}_{\mu\nu}(011) &= -pE^{-1}\bar{N}_{\mu\nu}(0-10)\\
\bar{N}_{\mu\nu}(111) &= 0\\
\bar{N}_{\mu\nu}(0-10) &= -[(\mu+1-\gamma_\mu)(\nu+1+\gamma_\nu)-\alpha^2Z^2]\\
\bar{N}_{\mu\nu}(1-10) &= E^{-1}[(\mu+1-\gamma_\mu)(\nu+1+\gamma_\nu)+\alpha^2Z^2]\\
\bar{N}_{\mu\nu}(0-11) &= pE^{-1}\bar{N}_{\mu\nu}(010)\\
\bar{N}_{\mu\nu}(1-11) &= 0.
\end{aligned}$$

The combinations of electron wave-functions of the forms (54) most commonly needed are those for which $\mu = \nu$. To simplify the notation a little for use in the complicated formulae of succeeding sections let us write $L_\nu(\zeta\sigma\tau)$ for $L_{\nu\nu}(\zeta\sigma\tau)$, etc.; also $L_{\nu\nu}(010)$ will be abbreviated to L_ν, etc. In the zeroth-order approximation one finds

$$
\begin{aligned}
(62) \qquad & L_\nu(110) = \gamma_\nu(\nu+1)^{-1}E^{-1}L_\nu \\
& L_\nu(0-11) = pE^{-1}L_\nu \\
& L_\nu(1-10) = -\alpha Z\gamma_\nu{}^{-1}L_\nu(110) \\
& L_\nu(011) = L_\nu(111) = L_\nu(0-10) = L_\nu(1-11) = 0.
\end{aligned}
$$

With one exception relations analogous to (62) hold also for the M- and N-functions; the exception is a negative sign in the formula relating $M_\nu(110)$ to M_ν. The formulae for L_ν, $M_\nu \ldots R_\nu$ obtained from (60) and (61) are in agreement with the first terms of the expansions given by Greuling and by Pursey.

The W-coefficients occurring in (58) can usually be calculated from the algebraic formulae listed by Biedenharn *et al.* (1952). It may sometimes be more convenient to use tables, references to which are given by Rose (1957). The X-coefficient, almost identical with the A-coefficient, is now also well tabulated (Kennedy *et al.* (1954); Smith and Stevenson (1957)). However, the values of the particular coefficients needed here are usually easily obtained without the aid of the tables. If the source is unoriented or if the neutrino is unobserved then either k or g' is zero and

$$
A\begin{pmatrix} j_1 & j_1' & J_1 \\ j_2 & j_2' & J_2 \\ k' & g' & k \end{pmatrix}
$$

reduces to a Racah coefficient multiplied by a trivial factor. Formulae for other reducible cases are given in the Appendix, where also are given simple formulae for evaluating the A_0's. $U(JL\xi)$ and $\Delta_{\mu\nu}$ are easily computed from their definitions, relations (21) and (47) respectively. The only coefficients in (58) not yet discussed are the vector-addition coefficients of the forms $(ll'00|L0)$ and $(jj'\,\tfrac{1}{2}\,-\tfrac{1}{2}|J\,0)$. References to papers containing algebraic formulae for certain special cases of vector-addition coefficients and to tables of values are given by Rose (1957). Rose also quotes the well-known formula for $(ll'00|L0)$, a table of which has been prepared by Sharp *et al.* (1953). De-Shalit (1953) has published a table of values of $(jj'\,\tfrac{1}{2}\,-\tfrac{1}{2}|J\,0)$, in which we have found two errors. The corrected values are

$$
\left(\frac{9}{2}\frac{9}{2}\frac{1}{2}\,-\frac{1}{2}\middle|3\,0\right) = -(12/715)^{\frac{1}{2}} \quad \text{and} \quad \left(\frac{9}{2}\frac{9}{2}\frac{1}{2}\,-\frac{1}{2}\middle|4\,0\right) = (81/715)^{\frac{1}{2}}.
$$

4. SPECTRA FROM UNORIENTED SOURCES

The correction-factor for the shapes of spectra emitted by unoriented sources with no neutrino detection is obtained by integrating the $S_0(\theta, \theta', \phi-\phi')$ of (48) over all electron and all neutrino directions, noting that $Z(k) = \delta_{k0}$;

thus $\iint S_0 d\Omega d\Omega' = R(00000)$. Considerable simplification occurs in $R(gg'kk't)$ of (58) when all the parameters take the value zero; σ is restricted to $+1$, and, because of (57*a*), only $\tau = 0$ occurs. In the discussions of this section, and in fact of all further sections, we shall drop the terms of degree of forbiddenness higher than the dominant. This is done by omitting the summations over L_1, L_2, l_1', and l_2' in (58). L is assumed to be fixed by the type of transition and by the values of ξ and η associated with K_n; the value of l' used is $L-l$. For some choices of L and K_n two values of J are to be used. To simplify the notation a little we shall write $\langle K_n; JL\rangle$ for $\langle K_n; JL; 0\rangle$. The dominant terms in the correction-factors for all five interactions are contained in the formula (63).

$$
\begin{aligned}
(63)\quad R(00000) = {} & \sum_{n_1 \leqslant n_2} (-1)^S 2(1+\delta_{n_1 n_2})^{-1} D_{n_2 n_1} \\
& \sum_J \delta_{J_1 J}\delta_{J_2 J} U(JL_2\xi_2)U(JL_1\xi_1)\,\langle K_{n_2}; J_2L_2\rangle\langle K_{n_1}; J_1L_1\rangle^* \\
& \sum_{\nu,j'} \Bigg\{ A_0\begin{pmatrix} \nu & \frac{1}{2} & j \\ L_2-\nu & \frac{1}{2} & j' \\ L_2 & \xi_2 & J \end{pmatrix} A_0\begin{pmatrix} \nu & \frac{1}{2} & j \\ L_1-\nu & \frac{1}{2} & j' \\ L_1 & \xi_1 & J \end{pmatrix} L_\nu(\zeta 10) q^{L_1+L_2-2\nu} \\
& + A_0\begin{pmatrix} \nu+1 & \frac{1}{2} & j \\ L_2-\nu-1 & \frac{1}{2} & j' \\ L_2 & \xi_2 & J \end{pmatrix} A_0\begin{pmatrix} \nu+1 & \frac{1}{2} & j \\ L_1-\nu-1 & \frac{1}{2} & j' \\ L_1 & \xi_1 & J \end{pmatrix} M_\nu(\zeta 10) q^{L_1+L_2-2\nu-2} \\
& + (-1)^{\zeta_2+1}\Bigg[A_0\begin{pmatrix} \nu+1 & \frac{1}{2} & j \\ L_2-\nu-1 & \frac{1}{2} & j' \\ L_2 & \xi_2 & J \end{pmatrix} A_0\begin{pmatrix} \nu & \frac{1}{2} & j \\ L_1-\nu & \frac{1}{2} & j' \\ L_1 & \xi_1 & J \end{pmatrix} \\
& + (-1)^t A_0\begin{pmatrix} \nu & \frac{1}{2} & j \\ L_2-\nu & \frac{1}{2} & j' \\ L_2 & \xi_2 & J \end{pmatrix} A_0\begin{pmatrix} \nu+1 & \frac{1}{2} & j \\ L_1-\nu-1 & \frac{1}{2} & j' \\ L_1 & \xi_1 & J \end{pmatrix}\Bigg] N_\nu(\zeta 10) q^{L_1+L_2-2\nu-1} \Bigg\}
\end{aligned}
$$

$$
S = \eta_1\zeta_1+\eta_2\zeta_2+\zeta_1+\zeta_2+\eta_1+\eta_2+\xi_1+\xi_2
$$

$$
\zeta = \zeta_1+\zeta_2 \qquad\qquad j = \nu+\tfrac{1}{2}.
$$

Formulae for the shapes of spectra in transitions of arbitrary forbiddenness have already been given, by Greuling (1942) for pure interactions and by Pursey (1951) for mixtures. In these works the nuclear matrix elements are defined in terms of certain Cartesian tensors which are not readily related, in general, to the spherical tensors used here. The formulae derived from (63), with the aid of values of A_0 as supplied in the Appendix, are all identical with the earlier work, if certain sums of contractions of the Cartesian tensors are assumed to be equal to products of pairs of reduced matrix elements. These equalities may be grouped into six types, one of which, (64), is quoted as an example.

$$
(64)\qquad Q_L(\mathbf{K}_1 \times \mathbf{r})\cdot Q_L^*(\mathbf{K}_2 \times \mathbf{r}) = \langle K_1; LL\rangle\,\langle K_2; LL\rangle^*.
$$

The symbol $Q_L(\mathbf{K} \times \mathbf{r})$, in the notation of Pursey, stands for the matrix element of a tensor of rank L constructed from $\mathbf{K} \times \mathbf{r}$ and $\mathbf{r}$, and is equivalent

to Greuling's notation $(L!)^{-1}\, Q_L(\mathbf{K} \times \mathbf{r}, \mathbf{r})$. The dot between the two factors on the left side of (64) implies contraction of the tensors plus a summation over M_f. Each of the other five conditions equates a left side similar to that in (64) to a product of reduced matrix elements, except for the possible presence of a factor of modulus unity. The six relations between the matrix elements of Greuling and Pursey and the reduced matrix elements of spherical tensors used in this paper can all be obtained from the following set of transformations:

$$Q_L(\mathbf{K}) \rightarrow \langle \mathbf{K}; L, L-1 \rangle, \tag{65a}$$

$$i\, Q_L(K\mathbf{r}) \rightarrow \langle K; L\, L \rangle, \tag{65b}$$

$$Q_L(\mathbf{K} \times \mathbf{r}) \rightarrow \langle \mathbf{K}; L\, L \rangle. \tag{65c}$$

Though a direct proof of the six equations implied by (65) has not been found, they can easily be shown to be true when $Q_L(\mathbf{a})$ is a scalar or a vector. Only one type of scalar occurs, namely $Q_0(K\mathbf{r}) = \int \Psi^* K \Phi d\mathbf{r}$. From the definitions of Section 2 it follows that

$$Q_0(K\mathbf{r}) = \langle K; 00 \rangle\, \delta_{J_i J_f};$$

thus

$$Q_0(K_1\mathbf{r}) \cdot Q_0^*(K_2\mathbf{r}) = \langle K_1; 00 \rangle \langle K_2; 00 \rangle^*,$$

the same result that is obtained by the use of (65b). In the formulae of Greuling and Pursey there are three different kinds of vectors, namely $Q_1(\mathbf{a})$ with $\mathbf{a}$ equal to $\mathbf{K}_n$, $K_n\mathbf{r}$, or $\mathbf{K}_n \times \mathbf{r}$. One can show that in each case a^μ can be written in the form $gT_n^\mu(1, L)$, g being a unimodular factor; L is 0 for $\mathbf{K}_n$, 1 for $K_n\mathbf{r}$ and $\mathbf{K}_n \times \mathbf{r}$. Hence

$$\begin{aligned} Q_1(\mathbf{a}) \cdot Q_1^*(\mathbf{b}) &= \sum_{M_f} \sum_{j=1}^{3} \left(\int \Psi^* a_j \Phi d\mathbf{r} \right) \left(\int \Psi^* b_j \Phi d\mathbf{r} \right)^*, \\ &= \sum_{M_f, \mu} \left(\int \Psi^* a^\mu \Phi d\mathbf{r} \right) \left(\int \Psi^* b^\mu \Phi d\mathbf{r} \right)^*, \\ &= g_a g_b^*\, \langle K_a; 1 L_a \rangle\, \langle K_b; 1 L_b \rangle^*. \end{aligned} \tag{66}$$

Now because $g = 1$ when $\mathbf{a}$ is $\mathbf{K}$ or $\mathbf{K} \times \mathbf{r}$ and $g = -i$ when $\mathbf{a}$ is $K\mathbf{r}$, the six relations contained in (66) are identical with those generated from (65). In deriving the value of g for $\mathbf{a} = \mathbf{K} \times \mathbf{r}$ we have used the fact that

$$A^\mu = -i 2^{\frac{1}{2}} \sum_\nu\, (1\, 1\, \nu\, \mu - \nu | 1\, \mu) B^\nu C^{\mu-\nu}, \qquad \text{if } \mathbf{A} = \mathbf{B} \times \mathbf{C}. \tag{67}$$

As is well known, the works of Greuling and Pursey omit some first-forbidden terms; these terms, containing matrix elements of tensors of rank zero, are among those discussed in Section 2 under transitions of the U class with $J_i = J_f$. The terms omitted by Greuling had already been given by Konopinski and Uhlenbeck (1941); some of the missing mixture terms have been supplied by Smith (1951). The cross-terms for P mixed with V, T, or A given by

Pursey, though evaluated correctly, are never of dominant order of forbiddenness if either T or A is present in the β-interaction; Greuling's term containing $Q_{n-1}([\boldsymbol{\alpha} \times \mathbf{r}], \mathbf{r})$ in his C_{nV} is in the same category. Our results for all first-forbidden transitions are exhibited explicitly in $R(00000)$ of Section 9. There is complete agreement with Konopinski and Uhlenbeck; to get agreement with Smith it is necessary to assume that he has replaced β by 1 throughout. In papers on allowed or first-forbidden decay the notation on the left of (68) has usually been used for the scalar and vector Q_L already discussed.

$$\int A = Q_0(A), \tag{68a}$$

$$\int \mathbf{B} = Q_1(\mathbf{B}). \tag{68b}$$

For the first-forbidden transitions with J_i equal to J_f there is another type of scalar of importance. In (69) the notation is defined and the matrix element related to the reduced matrix element used in this paper; $\mathbf{K}$ is any one of the four vector Dirac operators.

$$\int \mathbf{K}\cdot\mathbf{r} \equiv \int \Psi^* \mathbf{K}\cdot\mathbf{r}\,\Phi d\tau = i\langle \mathbf{K}; 01\rangle. \tag{69}$$

The second-rank tensor occurring in the first-forbidden correction-factors of Konopinski and Uhlenbeck is related to our notation by (70).

$$\tfrac{1}{4}\sum_{i,j} |B_{ij}|^2 = |Q_2(\mathfrak{d})|^2 = |\langle \mathfrak{d}; 21\rangle|^2. \tag{70}$$

The TA-mixture terms with $J = 0$ included in $R(00000)$ of Section 9 do not seem to have been published before; these terms have been included for the sake of completeness, though there is considerable evidence for the absence of TA mixing in the correction-factor.

The correction-factor (63) contains the results derived for special cases by Spiers and Blin-Stoyle (1952*a*). If an apparent misprint is corrected by including a factor 2^L within the square root in their definition (18) of $N(L)$, then the expressions i to iv of Banerjee and Saha (1954) seem to agree with (63).

Because most of the properties of (63) are already well known, discussion will be limited to minor features. By inspection one can see that the coefficient of a matrix-element product for which $L_1 = L_2$ and $\xi_1 = \xi_2$ contains no $N_\nu(\zeta 10)$ term if $\zeta = 1$, i.e. if the two matrix elements are drawn one from STP and the other from VA. Less obvious is the absence of the $N_\nu(\zeta 10)$ term for $\zeta = 0$ when $L_1 = L_2$ and $\xi_1 \neq \xi_2$. In the proof of this statement use is made of the identities

$$A_0\begin{pmatrix} \nu+1 & \frac{1}{2} & \nu+\frac{1}{2} \\ L-\nu-1 & \frac{1}{2} & L-\nu-\frac{1}{2} \\ L & 1 & L \end{pmatrix} = -[L^{-1}(L+1)]^{\frac{1}{2}} A_0\begin{pmatrix} \nu+1 & \frac{1}{2} & \nu+\frac{1}{2} \\ L-\nu-1 & \frac{1}{2} & L-\nu-\frac{1}{2} \\ L & 0 & L \end{pmatrix}, \tag{71a}$$

$$(71b)\quad A_0\begin{pmatrix} \nu & \frac{1}{2} & \nu+\frac{1}{2} \\ L-\nu & \frac{1}{2} & L-\nu-\frac{1}{2} \\ L & 1 & L \end{pmatrix} = [L^{-1}(L+1)]^{\frac{1}{2}} A_0\begin{pmatrix} \nu & \frac{1}{2} & \nu+\frac{1}{2} \\ L-\nu & \frac{1}{2} & L-\nu-\frac{1}{2} \\ L & 0 & L \end{pmatrix},$$

the justification of which depends upon formulae given in the Appendix. Note also that, because of the "stretched" orbital angular momenta, $l+l' = L$, at most two values of j' occur for each value of ν.

It is perhaps not inappropriate to give some defence of the introduction of yet another notation for nuclear matrix elements. The use of $\langle K; JL\rangle$ as defined by (23) and (20) yields correction-factors in precisely the customary form, and also gives a concise description, through the values of J and L and through the evident scalar or vector character of K, of the total, orbital, and spin angular momentum carried off by the emitted particles. From the symbol K one can tell immediately which β-interaction is involved. No cumbersome complex quantities occur in the correction-factor. An advantage of the use of spherical tensors is that the values of the nuclear matrix-element ratios found by fitting the theoretical to the experimental correction-factor are more easily compared with the shell model.

5. POLARIZATION OF ELECTRONS FROM AN UNORIENTED SOURCE

Let us consider the emission of electrons in the direction of a unit-vector $\mathbf{n}$ from an unoriented source, the neutrinos being unobserved. With the non-conservation of parity the longitudinal polarization of these electrons need not be zero. Let N^+ and N^- be the numbers of electrons observed with spins parallel and antiparallel to the direction of motion. Then the polarization, P, is defined by

$$(72)\qquad P \equiv (N^+-N^-)(N^++N^-)^{-1}.$$

The vector polarization $\boldsymbol{\zeta}$ has been defined in such a way that

$$(73)\qquad P = \boldsymbol{\zeta}\cdot\mathbf{n}.$$

Because only one direction has been defined in the experiment under discussion, $\boldsymbol{\zeta}$ must be parallel or antiparallel to $\mathbf{n}$; i.e. $|\boldsymbol{\zeta}| = |P|$.

Using the results of Section 3 we have

$$(74)\quad P\int S_0(\theta, \theta', \phi-\phi')d\Omega' = \sum_\mu (-1)^\mu n^\mu \int S_1^{-\mu}(\theta, \theta', \phi-\phi')d\Omega'.$$

It is easily demonstrated that

$$(75)\qquad n^\mu = (4\pi/3)^{\frac{1}{2}} Y_1^\mu(\theta, \phi).$$

Substituting (75) in (74) and using (48) we find that

$$(76)\qquad P = R(10001)/R(00000).$$

We shall call $R(10001)$ the modified correction-factor; the polarization is then the ratio of the modified to the normal correction-factor. A formula for $R(10001)$ similar to (63) for $R(00000)$ may be obtained from (58).

$$(77)\quad R(10001) = \sum_{n_1 \leqslant n_2} (-1)^{S+\zeta_1} 2(1+\delta_{n_2 n_1})^{-1} \sum_{\tau} (\delta_{\tau 1} G_{n_2 n_1} + \delta_{\tau 0} \Gamma_{n_2 n_1})$$

$$\sum_{J} \delta_{J_2 J} \delta_{J_1 J} U(J L_2 \xi_2) U(J L_1 \xi_1) \langle K_{n_2};\, J_2 L_2 \rangle \langle K_{n_1};\, J_1 L_1 \rangle^*$$

$$\sum_{\nu, j'} \Bigg\{ A_0 \begin{pmatrix} \nu & \frac{1}{2} & j \\ L_2 - \nu & \frac{1}{2} & j' \\ L_2 & \xi_2 & J \end{pmatrix} A_0 \begin{pmatrix} \nu & \frac{1}{2} & j \\ L_1 - \nu & \frac{1}{2} & j' \\ L_1 & \xi_1 & J \end{pmatrix} L_\nu(\zeta - 1\tau) q^{L_1 + L_2 - 2\nu}$$

$$+ A_0 \begin{pmatrix} \nu+1 & \frac{1}{2} & j \\ L_2 - \nu - 1 & \frac{1}{2} & j' \\ L_2 & \xi_2 & J \end{pmatrix} A_0 \begin{pmatrix} \nu+1 & \frac{1}{2} & j \\ L_1 - \nu - 1 & \frac{1}{2} & j' \\ L_1 & \xi_1 & J \end{pmatrix} M_\nu(\zeta - 1\tau) q^{L_1 + L_2 - 2\nu - 2}$$

$$+ (-1)^{\zeta_2 + 1} \Bigg[A_0 \begin{pmatrix} \nu+1 & \frac{1}{2} & j \\ L_2 - \nu - 1 & \frac{1}{2} & j' \\ L_2 & \xi_2 & J \end{pmatrix} A_0 \begin{pmatrix} \nu & \frac{1}{2} & j \\ L_1 - \nu & \frac{1}{2} & j' \\ L_1 & \xi_1 & J \end{pmatrix}$$

$$+ (-1)^{\tau+1} A_0 \begin{pmatrix} \nu & \frac{1}{2} & j \\ L_2 - \nu & \frac{1}{2} & j' \\ L_2 & \xi_2 & J \end{pmatrix} A_0 \begin{pmatrix} \nu+1 & \frac{1}{2} & j \\ L_1 - \nu - 1 & \frac{1}{2} & j' \\ L_1 & \xi_1 & J \end{pmatrix} \Bigg] N_\nu(\zeta - 1\tau) q^{L_1 + L_2 - 2\nu - 1} \Bigg\}.$$

Comparison of (77) and (63) shows that it is possible to formulate a simple set of rules for generating the modified correction-factor from the normal correction-factor. Because of (57*b*) $L_\nu(\zeta - 1\tau)$ and $M_\nu(\zeta - 1\tau)$ occur only if $\zeta + \tau$ is odd. The terms in the modified correction-factor containing $L_\nu(\zeta - 1\tau)$ may be obtained from the normal correction-factor by the following substitutions:

$$(78)\quad \begin{aligned} &\text{(i)}\quad \text{If } \zeta = 0,\ D_{n_2 n_1} \to (-1)^{\zeta_1} G_{n_2 n_1}, \quad \text{and} \quad L_\nu(010) \to L_\nu(0-11). \\ &\text{(ii)}\quad \text{If } \zeta = 1,\ D_{n_2 n_1} \to (-1)^{\zeta_1} \Gamma_{n_2 n_1}, \quad \text{and} \quad L_\nu(110) \to L_\nu(1-10). \end{aligned}$$

Rules precisely analogous to (78) hold for $M_\nu(\zeta - 1\tau)$. The same is true for the terms containing $N_\nu(\zeta - 1\tau)$ for which $\zeta + \tau$ is odd. However, because of the absence of a restriction of the form (57*b*) on the N-functions, there are additional terms in the correction-factor, namely those containing $N_\nu(1-11)$ and $N_\nu(0-10)$. As will be seen later these additional terms are not very important. They do not occur in allowed or U class transitions, except in the rather special $\Delta J = 0$, first-forbidden type. $N_\nu(1-11)$ is present only if the β-interaction is a mixture of contributions from STP and VA. The coefficient of $N_\nu(0-10)$ vanishes if the β-interaction is invariant under time-reversal. It is thus unlikely, with present ideas about the β-interaction, that either type of additional term actually exists. Also, the zeroth-order values of $N_\nu(0-10)$ and $N_\nu(1-11)$ are zero; the first nonvanishing terms in the $(p\rho)$-expansion for a point charge are:

$$(79a)\quad N_\nu(0-10) = -\alpha Z E^{-1} \gamma_\nu (2\gamma_\nu + 1)^{-1} \rho^{-2\nu} T_\nu^2,$$

$$(79b)\quad N_\nu(1-11) = pE^{-1}(\nu+1)\gamma_\nu (2\gamma_\nu + 1)^{-1} \rho^{-2\nu} T_\nu^2.$$

Because of their probable unimportance, no mention of the additional terms was made in the preliminary report on this work (Lee-Whiting 1958). Neverthe-

less, it is possible to give rules for obtaining the additional terms from the normal correction factor. Thus the coefficient of

$$G_{n_2n_1}\langle K_{n_2};\, J_2L_2\rangle\langle K_{n_1};\, J_1L_1\rangle^*N_\nu(1-11)$$

is equal to $(-1)^{\zeta_1+\eta_1+1}(1+\delta_{n_2n_1'})$ times the coefficient of

$$D_{n_2n_1'}\langle K_{n_2};\, J_2L_2\rangle\langle K_{n_1'}J_1L_1\rangle^*N_\nu(010);$$

the index n_1' refers to $K_{n_1'} = \beta K_{n_1}$. Similarly the coefficient of

$$\Gamma_{n_2n_1}\langle K_{n_2};\, J_2L_2\rangle\langle K_{n_1};\, J_1L_1\rangle^*N_\nu(0-10)$$

is equal to $(-1)^{\zeta_1+\eta_1+1}$ times the coefficient of

$$D_{n_2n_1'}\langle K_{n_2};\, J_2L_2\rangle\langle K_{n_1'};\, J_1L_1\rangle^*N_\nu(110).$$

Though each of the additional terms in the modified correction-factor can be generated from two terms of the correction-factor, only one is to be used.

To get a rough idea of the magnitude of the longitudinal polarization we turn again to the zeroth-order approximation discussed in Section 3. Then the troublesome additional terms of the last paragraph disappear. The remaining combinations of electron wave-functions can be estimated with the aid of (62). Note that $G_{n_2n_1}$ is always accompanied by the factor $p/E = v/c$, $\Gamma_{n_2n_1}$ by $-\alpha Z/E$. Thus the terms which would show a violation of time-reversal invariance, $\Gamma_{n_2n_1}$, are always accompanied by the factor $\alpha Z/E$, as shown by Jackson *et al.* (1957) for the allowed transitions. Hence to look for the failure of time-reversal invariance one should use a large value of Z and a small value of E; the $\Gamma_{n_2n_1}$ terms will not be present (in the zeroth-order approximation) unless the β-interaction contains contributions from both *STP* and *VA*.

If in addition to the zeroth-order approximation we assume no mixing of *STP* with *VA* and the validity of the two-component theory of the neutrino (Lee and Yang 1957), the expression for the polarization is particularly simple. No terms with $\zeta = 1$ appear, all $\Gamma_{n_2n_1}$ are zero, and $G_{n_2n_1} = \pm D_{n_2n_1}$, the choice of sign being independent of n_2 and n_1. Every remaining combination of electron wave-functions is equal to p/E times the corresponding combination in the normal correction-factor. Thus the polarization reduces to $\pm v/c$. This result is consistent with the now well-known fact (see Curtis and Lewis 1957) that the magnitude of the longitudinal polarization must approach unity as v approaches c, regardless of the order of forbiddenness.

One can show that the polarization is not always $\pm v/c$ by working to the second term in the expansion in powers of $(p\rho)$. Let us define the reduced polarization, P', as the ratio of $|P|$ to v/c. Then for an allowed transition in the field of a point charge we find that

$$P' \equiv [L_0(0-11)/L_0(010)](v/c)^{-1} \doteqdot 1+2\alpha Z\rho\gamma_0[E(\gamma_0+1)(2\gamma_0+1)]^{-1}; \tag{80}$$

it is here assumed that *ST* is not mixed with *VA*. Note that P' is greater than unity for negatrons, less than unity for positrons. Dr. L. G. Elliott has pointed out that this effect is explained qualitatively by the assumption

that the β-particle is created with a polarization equal to the value of v/c at its point of creation in the electrostatic field. The expansion of the type (80) in powers of $(p\rho)$ is probably of little use because of the relatively large effect of the finite distribution of nuclear charge. To provide evidence for this statement, P' for an allowed transition has been evaluated using the wave-functions of Sliv and Volchok (1956) for the case of the nuclear charge distributed uniformly throughout the volume of a sphere of radius $1.2 \times A^{1/3}$ fermis. The quantities tabulated are essentially our $F_l^{g.a}(p, 0)$; hence we have had to put ρ equal to zero. The behavior of the P' so computed is very similar to the P' of expression (80). In each case P' approaches unity monotonically as E increases or as Z decreases. With the finite charge distribution, however, the departure from unity can be considerably greater than with the point charge; for example, at $Z = 95$ and $E = 1.1$, P' is 1.021 for the distributed charge, 1.005 for the point charge.

Expressions for the longitudinal polarizations of electrons emitted in allowed and in certain first-forbidden transitions have already been published. Our formula (77) gives, in the zeroth-order approximation, results in complete agreement with those of Jackson *et al.* (1957) for allowed transitions. Curtis and Lewis (1957) have calculated the polarization for a ($\Delta J = 1$, yes)-transition with the assumption that the β-interaction is ST, but without assuming time-reversal invariance for nuclear forces. When this latter assumption is made, the formula (6) of Curtis and Lewis is found to be contained in the first-forbidden terms of (77). It should be noted that though the L_ν', M_ν', and N_ν' defined by these authors are exactly equal to our $L_\nu(0-11)$, $M_\nu(0-11)$, and $N_\nu(0-11)$, their R_ν' is equal to $-N_\nu(0-10)$. In their approximate expression for R_{k-1}', valid for $\alpha Z \ll 1$, a factor k^{-1} has been omitted. Formulae for all allowed and first-forbidden polarization terms occurring with an interaction ST have been derived by Alder *et al.* (1957) with the restriction $(\alpha Z)^2 \ll 1$. The $(p\rho)$-expansions of the wave-functions have been cut off in such a way that all terms in ρ^{-2}, ρ^{-1}, and ρ^0 have been retained. The use of our zeroth-order approximation with (77) only enables us to check that we agree with Alder *et al.* in the dominant power of ρ.

6. EMISSIONS FROM ORIENTED SOURCES

Four directions were considered in our discussion of Section 3, viz., those of electron momentum, $\mathbf{p}$, of electron polarization, $\boldsymbol{\zeta}$, of neutrino momentum, $\mathbf{q}$, and of nuclear orientation; the last will be indicated by the unit-vector $\mathbf{j}$. Following the precedent of Jackson *et al.* (1957) we shall limit our discussion of the more complicated experiments to those in which at most three of the four vectors $\mathbf{p}$, $\boldsymbol{\zeta}$, $\mathbf{q}$, and $\mathbf{j}$ appear. In this section we consider only those cases in which one of the three is $\mathbf{j}$.

The distribution of electrons and neutrinos from an oriented source is obtained by putting $t = 0$ in (48).

$$(81)\quad 4\pi S_0(\theta, \theta', \phi - \phi') = \sum_{kgg'} (-1)^{g'+k} Z(k)[(2k+1)(2g'+1)]^{-\frac{1}{2}} R(gg'kg0) \times \sum_m (g'\, g\, m\, -m|k\, 0)\, Y_{g'}{}^m(\theta', \phi')\, Y_g{}^{-m}(\theta, \phi).$$

Because the complicated expression (81) is unlikely to be required for transitions other than the allowed, for which a simplified form has already been given by Jackson *et al.* (1957), no further attention will be given to it. Considerable simplification of (81) results when either the electron or neutrino is unobserved. Taking the less important case first, we find that the distribution of neutrinos emitted by an oriented source is given by (82).

$$(82)\quad G(\theta') \equiv 4\pi \int S_0(\theta, \theta', \phi-\phi')d\Omega = \sum_k (2k+1)^{-\frac{1}{2}} Z(k) R(0kk00) P_k(\cos\theta').$$

The definition of the Legendre functions $P_k{}^m(x)$ used is that of Jahnke and Emde (1945). Though it is unlikely that it will ever be possible to measure $G(\theta')$, it is still of interest to point out that the combination $(G_{TT}+G_{AA})$ always occurs in the Gamow-Teller part of $R(0kk00)$, instead of the combination $(G_{TT}-G_{AA})$ which is measured in electron polarization or distribution experiments. For experiments in which the neutrino is unobserved we transform (81) into (83); $F(\theta)$ is, of course, the distribution of electrons from an oriented source.

$$(83)\quad F(\theta) \equiv 4\pi \int S_0(\theta, \theta', \phi-\phi')d\Omega',$$
$$= \sum_k (-1)^k Z(k) R(k0kk0) P_k(\cos\theta).$$

If $\boldsymbol{\zeta}$ is one of the three vectors to be considered, $\mathbf{p}$ must be another, and the third, in this section, is $\mathbf{j}$. We shall give formulae for computing the components of $\boldsymbol{\zeta}$ in the directions of the three members of a right-handed, orthogonal triad of unit-vectors, viz., $\mathbf{n}$, $\boldsymbol{\tau}$, $\mathbf{t}$. The direction of $\mathbf{n}$ is that of the electron momentum vector $\mathbf{p}$. The vector $\mathbf{t}$ lies in the plane of $\mathbf{n}$ and $\mathbf{j}$ and is perpendicular to $\mathbf{n}$; the sense of $\mathbf{t}$ is fixed by the condition that $\mathbf{t}$ be parallel to $\mathbf{j}$ when $\mathbf{n}$ is perpendicular to $\mathbf{j}$. The remaining unit-vector, $\boldsymbol{\tau}$, is perpendicular to the plane of $\mathbf{n}$ and $\mathbf{j}$; its sense is that of the increasing values of ϕ. An orthogonal projection of all the vectors of interest is shown in Fig. 1. Note that

$$(84)\quad \mathbf{t} = \mathbf{n} \times \boldsymbol{\tau}.$$

The three unit-vectors chosen correspond to the directions for which polarization measurements could be made most conveniently. It also happens that the expressions for the components of $\boldsymbol{\zeta}$ in these directions are considerably simpler than those for an arbitrary set of orthogonal directions.

Letting $\mathbf{k}$ represent any one of the three unit-vectors we can compute the component of $\boldsymbol{\zeta}$ in the direction of $\mathbf{k}$, ζ_k, from the relation (85).

$$(85)\quad \zeta_k = \mathbf{k}\cdot\boldsymbol{\zeta} = \left[\int S_0 d\Omega'\right]^{-1} \sum_\mu (-1)^\mu k^\mu \int S_1{}^{-\mu} d\Omega'.$$

The spherical components of the vector $\mathbf{n}$ have already been supplied—see (75). Those of $\boldsymbol{\tau}$ may be seen by inspection of Fig. 1 to be

$$(86)\quad \tau^{\pm 1} = -i2^{-\frac{1}{2}} e^{\pm i\phi}, \qquad \tau^0 = 0.$$

For $\mathbf{t}$ we use the formula (67), keeping the relation (84) in mind. The substi-

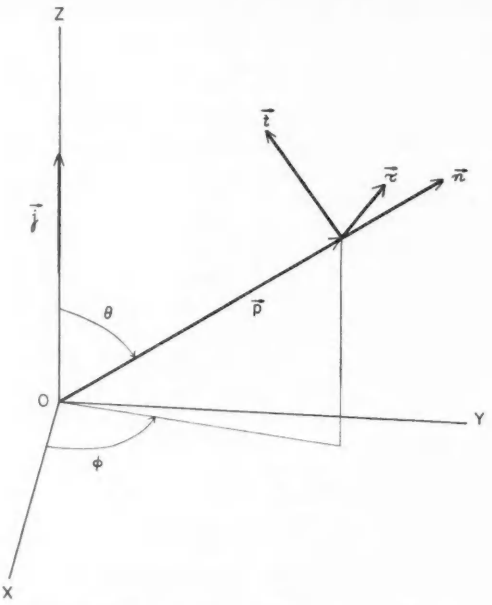

FIG. 1. The relative positions of the right-handed, orthogonal triad of unit-vectors ($\mathbf{n}$, $\boldsymbol{\tau}$, $\mathbf{t}$), the electron momentum vector $\mathbf{p}$, the direction of nuclear orientation $\mathbf{j}$, and the right-handed system of Cartesian axes (X, Y, Z) are illustrated.

tution into (85) of the expression (48) for $S_1^{-\mu}$ and of the appropriate formulae for spherical components leads to:

$$(87a)\quad F(\theta)\zeta_n = \sum_k (-1)^k Z(k) B_n(k) P_k(\cos\theta),$$

$$(87b)\quad F(\theta)\zeta_t = -\sum_k (-1)^k Z(k) B_t(k) [k(k+1)]^{-\frac{1}{2}} P_k^1(\cos\theta),$$

$$(87c)\quad F(\theta)\zeta_\tau = -i \sum_k (-1)^k Z(k) R(k0kk1) [k(k+1)]^{-\frac{1}{2}} P_k^1(\cos\theta).$$

$$(88a)\quad B_n(k) = \sum_g (1k00|g0) R(g0kk1),$$

$$(88b)\quad B_t(k) = [6(2k+1)]^{\frac{1}{2}} \sum_g (1k00|g0) W(11kk,1g) R(g0kk1).$$

It follows from (59) that $R(k0kk1)$ is a pure imaginary, and hence that ζ_τ is real. Fortunately the summations over g in (88) can be carried out explicitly. The essence of the g-sum in (88a) is

$$(89)\quad \sum_g \{X_{\mu\nu}(\zeta\sigma\tau)(1k00|g0)^2 - \Delta_{\mu\nu}' X_{\mu\nu}(\zeta+1\sigma\tau)(1k00|g0)(1k1-1|g0)\};$$

the symbol X stands for L, M, or N. We have used the abbreviation $\Delta_{\mu\nu}'$ for $\Delta_{\mu\nu}(k, g)[(1k1-1|g0)]^{-1}$; $\Delta_{\mu\nu}'$ is independent of g. The last term of the

last factor of (58) reduces to the form (89) because, for $g = k \pm 1$ with $k' = k$, we have

$$\sigma\Delta_{\mu\nu} = \sigma(-1)^{j_1+j_2+k'}\Delta_{\mu\nu} = (-1)^{g+1+k'}\Delta_{\nu\mu} = \Delta_{\nu\mu}. \tag{90}$$

The sums over g in (89) can be carried out with the aid of one of the unitarity relations for vector-addition coefficients, namely

$$\sum_j (j\,j'\,m\;M-m|J\;M)(j\,j'\,m'\;M-m'|J\;M) = \delta_{mm'}. \tag{91}$$

The first term in (89) yields simply $X_{\mu\nu}(\zeta\sigma\tau)$, the second gives zero. In performing the analogous sum over g in (88*b*) one encounters summations of the form (92).

$$[6(2k+1)]^{\frac{1}{2}} \sum_g W(11kk,\,1g)(1k00|g0) \times \{X_{\mu\nu}(\zeta\sigma\tau)(1k00|g0) - \Delta_{\mu\nu}'X_{\mu\nu}(\zeta+1\sigma\tau)(1\;k\;1-1|g\;0)\}. \tag{92}$$

With the aid of the elementary identity (93) one can show that the sum over g of the first term in (92) vanishes; the sum over the second term gives $-X_{\mu\nu}(\zeta\sigma\tau)\Delta_{\mu\nu}(k,\,k)$.

$$[6(2k+1)]^{\frac{1}{2}} \sum_g W(11kk,\,1g)(1k00|g0)(1\;k\;\nu\;-\nu|g\;0) = \delta_{|\nu|,1}(1\;k\;1\;-1|k\;0). \tag{93}$$

Thus both $B_n(k)$ and $B_t(k)$ can be calculated from formula (58) for $R(g0kk1)$, if the quantities of the form

$$[(1k00|g0)X_{\mu\nu}(\zeta\sigma\tau) - \Delta_{\mu\nu}(k,\,g)X_{\mu\nu}(\zeta+1\sigma\tau)]$$

are appropriately replaced. For $B_n(k)$ the replacement is simply $X_{\mu\nu}(\zeta\sigma\tau)$; for $B_t(k)$ it is $-\Delta_{\mu\nu}(k,\,k)X_{\mu\nu}(\zeta+1\sigma\tau)$. For g one may use either of the two values $k\pm1$, except, of course, when $k = 0$; $B_n(0) = R(10001)$.

It is possible to formulate rules, similar to those of Section 6, for obtaining the coefficients in the Legendre expansion of the components of polarization from the coefficients in the expansion of the electron distribution, i.e. from $R(k0kk0)$; however, the rules for the N-functions are so complicated that it is probably easier to work from (58) directly.

Note that the formula for ζ_n does not contain any of the quantities $\Delta_{\mu\nu}(k,\,g)$ which appear in (58), while every term in the expressions for the transverse components ζ_t and ζ_τ contains such a factor. If instead of $\boldsymbol{\zeta}$ one calculates the expectation value of $\boldsymbol{\delta}$, formulae analogous to (48) and (58) hold with $\Delta_{\mu\nu}$ replaced by $E^{-1}\Delta_{\mu\nu}$. Thus the component in the direction of motion of the expectation value of $\boldsymbol{\delta}$ is equal to ζ_n, while the transverse components of the expectation value of $\boldsymbol{\delta}$ are equal to $(1-v^2/c^2)^{\frac{1}{2}}$ times the corresponding transverse components of $\boldsymbol{\zeta}$. Since $\boldsymbol{\zeta}$ is the expectation value of the electron spin calculated in the rest frame of the electron (Tolhoek 1956), it should not be surprising that the relation between $\boldsymbol{\zeta}$ and $\boldsymbol{\delta}$ just announced is a Lorentz transformation.

The simplification of formula (58) resulting from the specialization to

$R(k0kk0)$ and $R(g0kk1)$ is not sufficient to merit the rewriting of (58) in simplified form. Explicit formulae for allowed transitions are given in Section 8. Certain first-forbidden transitions are treated in Section 9; it is felt that because so much space would be required for a full tabulation, this should be delayed until a better knowledge of the β-interaction permits the leaving out of unnecessary terms.

A general discussion of angular distribution of electrons from an oriented nucleus was given by Spiers and Blin-Stoyle (1952*b*), though calculations were performed for only a few types of matrix elements. In the post parity-nonconservation era, Alder *et al.* (1957) have published a formulation of the problem, but have not carried out enough of the summations to make comparison with our results profitable. No earlier work (except for allowed transitions) on the polarization of electrons from oriented sources seems to be available. Comparison with previous work on allowed and first-forbidden transitions is discussed in Sections 8 and 9.

7. NEUTRINO CORRELATIONS

Following the program outlined in the first paragraph of the preceding section we next examine experiments in which one of the three directions involved is that of the neutrino momentum vector. The angular distributions of neutrinos and of electrons emitted by an oriented source was given brief consideration in Section 6; see relation (81). When the source is randomly oriented, i.e. when $Z(k) = \delta_{k0}$, considerable simplification results. We shall refer to the function $W(\Theta)$ defined in (95) as the electron–neutrino angular-correlation function; Θ is the angle between the directions of emission of the electron and the neutrino.

$$(94) \qquad W(\Theta) \equiv (4\pi)^2 S_0(\theta, \theta', \phi - \phi'),$$
$$= \sum_g R(gg0g0) P_g(\cos\Theta) \quad \text{(for an unoriented nucleus).}$$

The relation of $W(\Theta)$ to the coefficients $R(gg0g0)$, given by formula (58), is thus particularly simple. Because $g' = g$, parity nonconserving terms containing G_{n2n1} or Γ_{n2n1} do not occur. However, combinations of coupling constants of the form Δ_{n2n1}, which must vanish if the β-interaction is invariant under time-reversal, do occur. The existence of such terms in the $W(\Theta)$ for allowed transitions seems to have been pointed out first by Morita (1953); see also Morita and Morita (1957). Our formulae for allowed transitions, given in Section 8, contain the results of Morita (1953); they are also in agreement with the zeroth-order results of Morita and Morita (1957) and of Jackson *et al.* (1957). Formulae for certain cases of first-forbidden transitions have been given by Hamilton (1947), for $Z = 0$, and by Greuling and Meeks (1951). The relation of the present results to those of the latter authors is discussed in Section 9.

The electron polarization will be treated almost exactly as in Section 6. Because the source is now randomly oriented, the Z-axis of Fig. 1 has no special significance. We are free, therefore, to assume that a neutrino is

observed travelling upward along the Z-axis; the unit-vector $\mathbf{j}$ is now parallel to $\mathbf{q}$, the neutrino momentum vector. The derivation of the formulae for the components in the directions of $\mathbf{n}$, $\boldsymbol{\tau}$, and $\mathbf{t}$ of the vector polarization is very similar to that outlined in Section 6.

$$(95a)\quad W(\Theta)\zeta_n = \sum_{g'} Q_n(g')P_{g'}(\cos\Theta),$$

$$(95b)\quad W(\Theta)\zeta_t = -\sum_{g'} Q_t(g')[g'(g'+1)]^{-\frac{1}{2}}P_{g'}{}^{1}(\cos\Theta),$$

$$(95c)\quad W(\Theta)\zeta_\tau = -i\sum_{g'} R(g'g'0g'1)[g'(g'+1)]^{-\frac{1}{2}}P^1_{g'}(\cos\Theta).$$

$$(96a)\quad Q_n(g') = \sum_{g} (1g'00|g0)R(gg'0g'1),$$

$$(96b)\quad Q_t(g') = [6(2g'+1)]^{\frac{1}{2}}\sum_{g} (1g'00|g0)W(11g'g', 1g)R(gg'0g'1).$$

Just as in Section 6 the g-sums in (96) can be carried out. Both $Q_n(g')$ and $Q_t(g')$ can be calculated from formula (58) for $R(gg'0g'1)$, if the quantities of the form

$$(97)\qquad [(1g'00\ g0)X_{\mu\nu}(\zeta\sigma\tau) - \Delta_{\mu\nu}(g', g)X_{\mu\nu}(\zeta+1\sigma\tau)]$$

are suitably replaced. For $Q_n(g')$ the replacement is simply $X_{\mu\nu}(\zeta\sigma\tau)$; for $Q_t(g')$ it is $-\Delta_{\mu\nu}(g', g')X_{\mu\nu}(\zeta+1\sigma\tau)$; the value of g in $R(gg'0g'1)$ can be either of $g'\pm1$. It is easily seen that $Q_n(0) = R(10001)$.

8. FORMULAE FOR ALLOWED TRANSITIONS

Within the limits set in the first paragraph of Section 6 formulae corresponding to all feasible experiments for allowed transitions have been given by Jackson *et al.* (1957). The electron wave-functions are treated by these authors in a manner equivalent to our zeroth-order approximation. In addition the nonrelativistic approximation for nuclear matrix elements was made, i.e., β was set equal to -1. If $|M_F|^2$ and $|M_{GT}|^2$ are used for $|\langle I00\rangle|^2$ and $|\langle\mathfrak{d}10\rangle|^2$ respectively, this approximation gives

$$(98)\qquad |\langle\beta00\rangle|^2 \doteq |M_F|^2, \qquad \langle\beta00\rangle\langle I00\rangle^* \doteq -|M_F|^2.$$

$$(99)\qquad |\langle\beta\mathfrak{d}10\rangle|^2 \doteq |M_{GT}|^2, \qquad \langle\beta\mathfrak{d}10\rangle\langle\mathfrak{d}10\rangle^* \doteq -|M_{GT}|^2.$$

Using the definition (A17) of Jackson *et al.* one can show that

$$(100)\qquad \langle I00\rangle\langle\mathfrak{d}10\rangle^* \doteq -M_F M_{GT};$$

analogous results follow for matrix elements containing β. When the same approximations are made in our formulae, complete agreement is obtained with all the results of Jackson *et al.*

For most purposes the more approximate treatment is probably adequate. However, it is possible that, when more accurate experiments have been performed, it will be desirable to allow for the effects of the finite distribution of nuclear charge. To facilitate the making of such an allowance formulae in which the zeroth-order approximation has not been made are quoted for

the more important cases. First we give the correction-factor for electrons from an unoriented source, $R(00000)$ in the present notation.

$$(101)\quad R(00000) = [D_{SS}|\langle\beta 00\rangle|^2+D_{VV}|\langle I00\rangle|^2+D_{TT}|\langle\beta\delta 10\rangle|^2+D_{AA}|\langle\delta 10\rangle|^2]L_0 -2[D_{SV}\langle\beta 00\rangle\langle I00\rangle^*+D_{TA}\langle\beta\delta 10\rangle\langle\delta 10\rangle^*]L_0(110).$$

To compute the longitudinal polarization of electrons from an unoriented source we need $R(10001)$.

$$(102)\quad R(10001) = [G_{SS}|\langle\beta 00\rangle|^2-G_{VV}|\langle I00\rangle|^2+G_{TT}|\langle\beta\delta 10\rangle|^2-G_{AA}|\langle\delta 10\rangle|^2]L_0(0-11) +2[\Gamma_{SV}\langle\beta 00\rangle\langle I00\rangle^*+\Gamma_{TA}\langle\beta\delta 10\rangle\langle\delta 10\rangle^*]L_0(1-10).$$

The angular distribution from an oriented source requires $R(10110)$.

$$(103)\quad -R(10110) = 2^{\frac{1}{2}}(2J_i+1)^{\frac{1}{2}}W(11J_fJ_i,\,1J_i)\{[G_{TT}|\langle\beta\delta 10\rangle|^2-G_{AA}|\langle\delta 10\rangle|^2]L_0(0-11) +2\Gamma_{TA}\langle\beta\delta 10\rangle\langle\delta 10\rangle^*L_0(1-10)\} +2\times 3^{-\frac{1}{2}}\{[G_{AV}\langle\delta 10\rangle\langle I00\rangle^*-G_{TS}\langle\beta\delta 10\rangle\langle\beta 00\rangle^*]L_0(0-11) +[\Gamma_{VT}\langle\beta\delta 10\rangle\langle I00\rangle^*-\Gamma_{SA}\langle\delta 10\rangle\langle\beta 00\rangle^*]L_0(1-10)\}.$$

Recall that $Z(1)$ is given in relation (50). To find the three components of the polarization of electrons from an oriented source we require:

$$(104a)\quad B_n(1) = -2^{\frac{1}{2}}(2J_i+1)^{\frac{1}{2}}W(11J_fJ_i,\,1J_f)\{[D_{TT}|\langle\beta\delta 10\rangle|^2+D_{AA}|\langle\delta 10\rangle|^2]L_0 -2D_{TA}\langle\beta\delta 10\rangle\langle\delta 10\rangle^*L_0(110)\} +2\times 3^{-\frac{1}{2}}\{[D_{AV}\langle\delta 10\rangle\langle I00\rangle^*+D_{TS}\langle\beta\delta 10\rangle\langle\beta 00\rangle^*]L_0 -[D_{VT}\langle\beta\delta 10\rangle\langle I00\rangle^*+D_{SA}\langle\delta 10\rangle\langle\beta 00\rangle^*]L_0(110)\}.$$

$$(104b)\quad -2^{-\frac{1}{2}}B_t(1) = B_n(1) \text{ with } L_0 \text{ and } L_0(110) \text{ interchanged.}$$

$$(104c)\quad i2^{-\frac{1}{2}}R(10111) = 2^{\frac{1}{2}}(2J_i+1)^{\frac{1}{2}}W(11J_fJ_i,\,1J_i)\{[G_{TT}|\langle\beta\delta 10\rangle|^2-G_{AA}|\langle\delta 10\rangle|^2]L_0(1-10) -2\Gamma_{TA}\langle\beta\delta 10\rangle\langle\delta 10\rangle^*L_0(0-11)\} -2\times 3^{-\frac{1}{2}}\{[G_{TS}\langle\beta\delta 10\rangle\langle\beta 00\rangle^*-G_{AV}\langle\delta 10\rangle\langle I00\rangle^*]L_0(1-10) +[\Gamma_{AS}\langle\delta 10\rangle\langle\beta 00\rangle^*-\Gamma_{TV}\langle\beta\delta 10\rangle\langle I00\rangle^*]L_0(0-11)\}.$$

Now, since $L_0(1-10) \doteqdot -\alpha ZE^{-1}L_0$ and $L_0(0-11) \doteqdot pE^{-1}L_0$, the terms in ζ_τ with relatively large coefficients, at least for nuclei with small values of Z, are those containing Γ_{XY}, which are zero unless time-reversal invariance fails.

The electron–neutrino angular correlation depends upon $R(11010)$.

$$(105)\quad R(11010) = [D_{VV}|\langle I00\rangle|^2-D_{SS}|\langle\beta 00\rangle|^2-\tfrac{1}{3}D_{AA}|\langle\delta 10\rangle|^2+\tfrac{1}{3}D_{TT}|\langle\beta\delta 10\rangle|^2]L_0(0-11) +2[\Delta_{VS}\langle I00\rangle\langle\beta 00\rangle^*-\tfrac{1}{3}\Delta_{AT}\langle\delta 10\rangle\langle\beta\delta 10\rangle^*]L_0(1-10).$$

Note that the dominant terms in (105) contain $L_0(0-11)$, the same combination of electron wave-functions that is important in the longitudinal polarization of electrons from an oriented source. The formula of Morita (1953) after correction according to Morita and Morita (1957) agrees with (105). As suggested by Morita (1953), the different dependences of $L_0(0-11)$ and $L_0(1-10)$ upon electron energies makes it possible in principle to test for failure of time-reversal invariance by measuring allowed electron–neutrino angular correlations.

9. FORMULAE FOR FIRST-FORBIDDEN TRANSITIONS

Expression (106) contains the complete first-forbidden correction-factor; it is divided into paragraphs corresponding to $J = 0$, 1, and 2. The cross-terms between matrix elements belonging to T and A with $J = 0$ are believed to be new. The correction-factor is given in full partly because the original publications are scattered, but mainly to facilitate the description of the calculation of the polarization. As shown in Section 5 the longitudinal polarization is the ratio of $R(10001)$ to $R(00000)$. Each term in (106) produces, under the application of the rules (78) of Section 5, a term of $R(10001)$. Because these rules are very simple the resulting terms of $R(10001)$ will not be given. The rules for the additional terms of $R(10001)$ are sufficiently complicated that we deem it useful to list these terms; they are supplied in (107).

(106)

$$
\begin{aligned}
R(00000) = {} & [D_{AA}|\langle\gamma_5 00\rangle|^2+D_{PP}|\langle\beta\gamma_5 00\rangle|^2]L_0+2D_{AP}\langle\gamma_5 00\rangle\langle\beta\gamma_5 00\rangle^*L_0(110)\\
& +D_{AA}|\langle\delta 01\rangle|^2[M_0-\tfrac{2}{3}qN_0+\tfrac{1}{9}q^2L_0]+D_{TT}|\langle\beta\delta 01\rangle|^2[M_0+\tfrac{2}{3}qN_0+\tfrac{1}{9}q^2L_0]\\
& -2D_{AT}\langle\beta\delta 01\rangle\langle\delta 01\rangle^*[M_0(110)+\tfrac{1}{9}q^2L_0(110)]-2D_{AA}\langle\gamma_5 00\rangle\langle\delta 01\rangle^*\\
& \qquad [N_0-\tfrac{1}{3}qL_0]\\
& -2D_{AP}\langle\beta\gamma_5 00\rangle\langle\delta 01\rangle^*[N_0(110)-\tfrac{1}{3}qL_0(110)]-2D_{AT}\langle\gamma_5 00\rangle\langle\beta\delta 01\rangle^*\\
& \qquad [N_0(110)+\tfrac{1}{3}qL_0(110)]\\
& -2D_{PT}\langle\beta\gamma_5 00\rangle\langle\beta\delta 01\rangle^*[N_0+\tfrac{1}{3}qL_0]\\
& \\
& +D_{SS}|\langle\beta 11\rangle|^2[M_0+\tfrac{2}{3}qN_0+\tfrac{1}{3}q^2L_0+2L_1]+D_{VV}|\langle I11\rangle|^2[M_0-\tfrac{2}{3}qN_0+\tfrac{1}{3}q^2L_0\\
& \qquad +2L_1]\\
& -2D_{SV}\langle I11\rangle\langle\beta 11\rangle^*[M_0(110)+\tfrac{1}{3}q^2L_0(110)+2L_1(110)]-2D_{AT}\langle\delta 11\rangle\\
& \qquad \langle\beta\delta 11\rangle^*[M_0(110)+\tfrac{1}{6}q^2L_0(110)+\tfrac{1}{2}L_1(110)]\\
& +D_{TT}|\langle\beta\delta 11\rangle|^2[M_0-\tfrac{2}{3}qN_0+\tfrac{1}{6}q^2L_0+\tfrac{1}{2}L_1]+D_{AA}|\langle\delta 11\rangle|^2[M_0+\tfrac{2}{3}qN_0\\
& \qquad +\tfrac{1}{6}q^2L_0+\tfrac{1}{2}L_1]\\
& +[D_{TT}|\langle\beta\alpha 10\rangle|^2+D_{VV}|\langle\alpha 10\rangle|^2]L_0+2D_{TV}\langle\beta\alpha 10\rangle\langle\alpha 10\rangle^*L_0(110)\\
& +2[D_{TS}\langle\beta\delta 11\rangle\langle\beta 11\rangle^*+D_{AV}\langle\delta 11\rangle\langle I11\rangle^*][M_0-L_1]\\
& -2D_{AS}\langle\delta 11\rangle\langle\beta 11\rangle^*[M_0(110)-\tfrac{2}{3}qN_0(110)-L_1(110)]-2D_{TV}\langle\beta\delta 11\rangle\langle I11\rangle^*\\
& \qquad [M_0(110)+\tfrac{2}{3}qN_0(110)-L_1(110)]\\
& +2[D_{VV}\langle I11\rangle\langle\alpha 10\rangle^*+D_{TT}\langle\beta\delta 11\rangle\langle\beta\alpha 10\rangle^*][N_0-\tfrac{1}{3}qL_0]\\
& +2[D_{ST}\langle\beta 11\rangle\langle\beta\alpha 10\rangle^*+D_{AV}\langle\delta 11\rangle\langle\alpha 10\rangle^*][N_0+\tfrac{1}{3}qL_0]\\
& +2D_{VT}[\langle I11\rangle\langle\beta\alpha 10\rangle^*+\langle\beta\delta 11\rangle\langle\alpha 10\rangle^*][N_0(110)-\tfrac{1}{3}qL_0(110)]\\
& +2[D_{SV}\langle\beta 11\rangle\langle\alpha 10\rangle^*+D_{AT}\langle\beta\alpha 10\rangle\langle\delta 11\rangle^*][N_0(110)+\tfrac{1}{3}qL_0(110)]\\
& \\
& +[D_{TT}|\langle\beta\delta 21\rangle|^2+D_{AA}|\langle\delta 21\rangle|^2][\tfrac{1}{3}q^2L_0+3L_1]\\
& -2D_{AT}\langle\delta 21\rangle\langle\beta\delta 21\rangle^*[\tfrac{1}{3}q^2L_0(110)+3L_1(110)].
\end{aligned}
$$

$$
\begin{aligned}
(107)\quad & R(10001) = \ldots \\
& +2N_0(1-11)[\tfrac{2}{3}qG_{TA}\langle\beta\delta 01\rangle\langle\delta 01\rangle^*+G_{TA}\langle\beta\delta 01\rangle\langle\gamma_5 00\rangle^* \\
& \quad -G_{PA}\langle\delta 01\rangle\langle\beta\gamma_5 00\rangle^* \\
& \quad -\tfrac{2}{3}qG_{TA}\langle\beta\delta 11\rangle\langle\delta 11\rangle^*+\tfrac{2}{3}qG_{SV}\langle\beta 11\rangle\langle I11\rangle^* \\
& \quad +G_{TV}\langle\beta\alpha 10\rangle\langle I11\rangle^*+G_{TA}\langle\beta\alpha 10\rangle\langle\delta 11\rangle^* \\
& \quad -G_{VS}\langle\alpha 10\rangle\langle\beta 11\rangle^*-G_{VT}\langle\alpha 10\rangle\langle\beta\delta 11\rangle^*] \\
& \quad +2N_0(0-10)[\Gamma_{PT}\langle\beta\gamma_5 00\rangle\langle\beta\delta 01\rangle^* \\
& \quad -\tfrac{2}{3}q\Gamma_{VA}\langle I11\rangle\langle\delta 11\rangle^*-\tfrac{2}{3}q\Gamma_{ST}\langle\beta 11\rangle\langle\beta\delta 11\rangle^* \\
& \quad +\Gamma_{VA}\langle\alpha 10\rangle\langle\delta 11\rangle^*-\Gamma_{TS}\langle\beta\alpha 10\rangle\langle\beta 11\rangle^*].
\end{aligned}
$$

The angular distribution of electrons from an oriented source is calculable in terms of the coefficients $R(k0kk0)$; in first-forbidden transitions k takes the values 0, 1, 2, and 3. Though a complete list of formulae could be generated from (58) with little difficulty, the space required to print it would be considerable. Also, since it is certainly possible that all five types of β-interaction do not occur, many terms in the formulae would probably never be used. Current ideas about the β-interaction suggest *STP* (see Konopinski in Siegbahn 1955), or, more probably, *VA* (Goldhaber *et al.* 1958; Herrmannsfeldt *et al.* 1957). In the remainder of this section results will be presented for *STP* and for *VA*, the cross-terms between the two groups being ignored. Furthermore, if an experiment on a first-forbidden decay is to be interpreted with reasonable ease, a transition should be chosen for which cross-terms containing matrix elements with different values of J do not occur. Thus in considering the emissions from oriented nuclei we exclude ($\Delta J = 0$)-transitions and also those ($\Delta J = 1$)-transitions in which the ($J = 2$)-terms make an appreciable contribution. A convenient abbreviation is defined in (108).

$$
(108)\quad W_k(J) \equiv (-1)^{J_i-J_f}(2J_i+1)^{\frac{1}{2}}W(JJJ_iJ_i, kJ_f).
$$

$$
\begin{aligned}
(109)\quad & R(10110) = \ldots \\
& +2^{\frac{1}{2}}w_1(1)\{-G_{SS}|\langle\beta 11\rangle|^2[M_0(0-11)+\tfrac{2}{3}qN_0(0-11)+L_1(0-11) \\
& \qquad +2N_{01}(011)+\tfrac{2}{3}qL_{01}(011)] \\
& -G_{TT}|\langle\beta\delta 11\rangle|^2[M_0(0-11)-\tfrac{2}{3}qN_0(0-11)+\tfrac{1}{12}q^2L_0(0-11)+\tfrac{1}{4}L_1(0-11) \\
& \qquad -N_{01}(011)+\tfrac{1}{3}qL_{01}(011)] \\
& -2G_{TS}\langle\beta 11\rangle\langle\beta\delta 11\rangle^*[M_0(0-11)-\tfrac{1}{6}q^2L_0(0-11)-\tfrac{1}{2}L_1(0-11)-\tfrac{1}{2}qL_{01}(011) \\
& \qquad +\tfrac{1}{2}N_{01}(011)] \\
& -2\Gamma_{TS}\langle\beta 11\rangle\langle\beta\delta 11\rangle^*[\tfrac{2}{3}qN_0(0-10)-\tfrac{1}{6}qL_{01}(010)+\tfrac{3}{2}N_{01}(010)] \\
& -G_{TT}|\langle\beta\alpha 10\rangle|^2L_0(0-11)-2G_{TT}\langle\beta\delta 11\rangle\langle\beta\alpha 10\rangle^*[N_0(0-11)-\tfrac{1}{3}qL_0(0-11) \\
& \qquad -\tfrac{1}{2}L_{01}(011)] \\
& -2G_{TS}\langle\beta 11\rangle\langle\beta\alpha 10\rangle^*[N_0(0-11)+\tfrac{1}{3}qL_0(0-11)+L_{01}(011)]+2\Gamma_{TS} \\
& \qquad \langle\beta 11\rangle\langle\beta\alpha 10\rangle^*[N_0(0-10)-L_{01}(010)] \\
& +G_{VV}|\langle I11\rangle|^2[M_0(0-11)-\tfrac{2}{3}qN_0(0-11)+L_1(0-11)+2N_{01}(011) \\
& \qquad -\tfrac{2}{3}qL_{01}(011)] \\
& +G_{AA}|\langle\delta 11\rangle|^2[M_0(0-11)+\tfrac{2}{3}qN_0(0-11)+\tfrac{1}{12}q^2L_0(0-11)+\tfrac{1}{4}L_1(0-11) \\
& \qquad -N_{01}(011)-\tfrac{1}{3}qL_{01}(011)] \\
& +2G_{AV}\langle\delta 11\rangle\langle I11\rangle^*[M_0(0-11)-\tfrac{1}{6}q^2L_0(0-11)-\tfrac{1}{2}L_1(0-11) \\
& \qquad +\tfrac{1}{2}qL_{01}(011)+\tfrac{1}{2}N_{01}(011)]
\end{aligned}
$$

$$-2\Gamma_{AV}\langle\delta 11\rangle\langle I11\rangle^*[\tfrac{2}{3}qN_0(0-10)-\tfrac{1}{6}qL_{01}(010)-\tfrac{3}{2}N_{01}(010)]$$
$$+G_{VV}|\langle\alpha 10\rangle|^2L_0(0-11)+2G_{VV}\langle I11\rangle\langle\alpha 10\rangle^*[N_0(0-11)-\tfrac{1}{3}qL_0(0-11)$$
$$+L_{01}(011)]$$
$$+2G_{AV}\langle\delta 11\rangle\langle\alpha 10\rangle^*[N_0(0-11)+\tfrac{1}{3}qL_0(0-11)-\tfrac{1}{2}L_{01}(011)]$$
$$+2\Gamma_{AV}\langle\delta 11\rangle\langle\alpha 10\rangle^*[N_0(0-10)+\tfrac{1}{2}L_{01}(010)]+\ldots\}$$
$$+2^{-\frac{1}{2}}\times 3\times 5^{\frac{1}{2}}w_1(2)[G_{TT}|\langle\beta\delta 21\rangle|^2-G_{AA}|\langle\delta 21\rangle|^2][\tfrac{1}{5}q^2L_0(0-11)$$
$$+\tfrac{3}{5}L_1(0-11)]+\ldots$$

(110) $R(20220)=\ldots$
$$+6^{\frac{1}{2}}w_2(1)\{D_{SS}|\langle\beta 11\rangle|^2[L_1+2N_{01}(0-10)+\tfrac{2}{3}qL_{01}(0-10)]$$
$$+D_{TT}|\langle\beta\delta 11\rangle|^2[\tfrac{1}{4}L_1-N_{01}(0-10)+\tfrac{1}{3}qL_{01}(0-10)]$$
$$-\langle\beta\delta 11\rangle\langle\beta 11\rangle^*(D_{TS}[L_1-N_{01}(0-10)+qL_{01}(0-10)]$$
$$+\Delta_{TS}[3N_{01}(0-11)-\tfrac{1}{3}qL_{01}(0-11)])$$
$$-D_{TT}\langle\beta\delta 11\rangle\langle\beta\alpha 10\rangle^*L_{01}(0-10)$$
$$+2\langle\beta 11\rangle\langle\beta\alpha 10\rangle^*[D_{ST}L_{01}(0-10)+\Delta_{ST}L_{01}(0-11)]$$
$$+D_{VV}|\langle I11\rangle|^2[L_1+2N_{01}(0-10)-\tfrac{2}{3}qL_{01}(0-10)]$$
$$+D_{AA}|\langle\delta 11\rangle|^2[\tfrac{1}{4}L_1-N_{01}(0-10)-\tfrac{1}{3}qL_{01}(0-10)]$$
$$-\langle\delta 11\rangle\langle I11\rangle^*(D_{AV}[L_1-N_{01}(0-10)-qL_{01}(0-10)]+\Delta_{AV}[3N_{01}(0-11)$$
$$+\tfrac{1}{3}qL_{01}(0-11)])$$
$$-\langle\delta 11\rangle\langle\alpha 10\rangle^*[D_{AV}L_{01}(0-10)+\Delta_{AV}L_{01}(0-11)]$$
$$+2D_{VV}\langle I11\rangle\langle\alpha 10\rangle^*L_{01}(0-10)+\ldots\}$$
$$-2^{-\frac{1}{2}}\times 3\times 7^{\frac{1}{2}}w_2(2)[D_{TT}|\langle\beta\delta 21\rangle|^2+D_{AA}|\langle\delta 21\rangle|^2]L_1+\ldots.$$

(111) $R(30330)=-2^{\frac{1}{2}}\times 3^2\times 5^{-\frac{1}{2}}w_3(2)[G_{TT}|\langle\beta\delta 21\rangle|^2-G_{AA}|\langle\delta 21\rangle|^2]$
$$L_1(0-11)+\ldots.$$

The *ST* parts of (109), (110), and (111) may be compared with the approximate results of Alder *et al.* (1957); the approximations involve the retention of only the first three terms in an expansion in powers of ρ and the neglect of $(\alpha Z)^2$ in comparison with unity. With the use of our zeroth-order approximation it is possible to show that, with one exception, the ρ-dominant term in the coefficient of each power of q in our results agrees with the analogous term of Alder *et al.* The exception is in the coefficient of $\langle\beta\delta 11\rangle\langle\beta 11\rangle^*\Delta_{TS}$ in R (20220); instead of the factor 3/4 in the expression for S_2 at the top of the continuation of Alder's Table IV on page 733, we find 3/8.

(112) $iR(10111)=\ldots$
$$+2w_1(1)\{G_{SS}|\langle\beta 11\rangle|^2[M_0(1-10)+\tfrac{2}{3}qN_0(1-10)+2L_1(1-10)-N_{01}(110)$$
$$-\tfrac{1}{3}qL_{01}(110)]$$
$$+G_{TT}|\langle\beta\delta 11\rangle|^2[M_0(1-10)-\tfrac{2}{3}qN_0(1-10)+\tfrac{1}{12}q^2L_0(1-10)+\tfrac{1}{2}L_1(1-10)$$
$$+\tfrac{1}{2}N_{01}(110)-\tfrac{1}{6}qL_{01}(110)]$$
$$+2G_{TS}\langle\beta\delta 11\rangle\langle\beta 11\rangle^*[M_0(1-10)-\tfrac{1}{6}q^2L_0(1-10)-L_1(1-10)-\tfrac{1}{4}N_{01}(110)$$
$$+\tfrac{1}{4}qL_{01}(110)]$$
$$-\Gamma_{TS}\langle\beta\delta 11\rangle\langle\beta 11\rangle^*[\tfrac{4}{3}qN_0(1-11)-\tfrac{3}{2}N_{01}(111)+\tfrac{1}{6}qL_{01}(111)]$$
$$+G_{TT}|\langle\beta\alpha 10\rangle|^2L_0(1-10)$$
$$+G_{TT}\langle\beta\delta 11\rangle\langle\beta\alpha 10\rangle^*[2N_0(1-10)-\tfrac{2}{3}qL_0(1-10)+\tfrac{1}{2}L_{01}(110)]$$
$$+G_{ST}\langle\beta 11\rangle\langle\beta\alpha 10\rangle^*[2N_0(1-10)+\tfrac{2}{3}qL_0(1-10)-L_{01}(110)]$$
$$-\Gamma_{ST}\langle\beta 11\rangle\langle\beta\alpha 10\rangle^*[2N_0(1-11)+L_{01}(111)]$$

$$-G_{VV}|\langle I11\rangle|^2[M_0(1-10)-\tfrac{2}{3}qN_0(1-10)+2L_1(1-10)-N_{01}(110)+ \\ +\tfrac{1}{3}qL_{01}(110)]$$
$$-G_{AA}|\langle\mathfrak{d}11\rangle|^2[M_0(1-10)+\tfrac{2}{3}qN_0(1-10)+\tfrac{1}{12}q^2L_0(1-10)+\tfrac{1}{2}L_1(1-10) \\ +\tfrac{1}{2}N_{01}(110)+\tfrac{1}{6}qL_{01}(110)]$$
$$-2G_{AV}\langle\mathfrak{d}11\rangle\langle I11\rangle^*[M_0(1-10)-\tfrac{1}{6}q^2L_0(1-10)-L_1(1-10)-\tfrac{1}{4}N_{01}(110) \\ -\tfrac{1}{4}qL_{01}(110)]$$
$$-\Gamma_{AV}\langle\mathfrak{d}11\rangle\langle I11\rangle^*[\tfrac{4}{3}qN_0(1-11)+\tfrac{3}{2}N_{01}(111)+\tfrac{1}{6}qL_{01}(111)]$$
$$-G_{VV}|\langle\alpha10\rangle|^2L_0(1-10)$$
$$-G_{AV}\langle\mathfrak{d}11\rangle\langle\alpha10\rangle^*[2N_0(1-10)+\tfrac{2}{3}qL_0(1-10)+\tfrac{1}{2}L_{01}(110)]$$
$$+\Gamma_{AV}\langle\mathfrak{d}11\rangle\langle\alpha10\rangle^*[2N_0(1-11)-\tfrac{1}{2}L_{01}(111)]$$
$$-G_{VV}(I11\rangle\langle\alpha10\rangle^*[2N_0(1-10)-\tfrac{2}{3}qL_0(1-10)-L_{01}(110)]\}+\ldots.$$

Of the components of polarization of electrons emitted by an oriented source, only ζ_τ is likely to be of interest. One might hope to find that in the ($\Delta J = 1$, yes)-transitions ζ_τ could be measured in order to estimate the magnitude of Γ_{ST} or Γ_{VA}, and hence to study the possible failure of time-reversal invariance. In (112) we give the ($J = 1$)-terms in $iR(10111)$ for ST and for VA. From (112) one can calculate, using (106) and (110) also, the value of ζ_τ for electrons emitted perpendicularly to the direction of nuclear orientation. The coefficients of Γ_{TS} and Γ_{AV} are, however, never appreciably greater than those of G_{TS} and G_{AV} respectively. Hence a clear-cut experiment on time-reversal invariance is not feasible in general. For those beta-emitters for which cancellation of matrix elements seems to occur, e.g. RaE, it is possible that a measurement of ζ_τ would be informative.

$$(113)\quad R(11010) = -|\langle\beta\mathfrak{d}01\rangle|^2D_{TT}[M_0(0-11)+\tfrac{2}{3}qN_0(0-11)+\tfrac{1}{9}q^2L_0(0-11)]$$
$$-|\langle\beta\gamma_5 00\rangle|^2D_{PP}L_0(0-11)+2\langle\beta\mathfrak{d}01\rangle\langle\beta\gamma_5 00\rangle^*\{D_{TP}[N_0(0-11) \\ +\tfrac{1}{3}qL_0(0-11)]+\Delta_{TP}N_0(0-10)\}$$
$$+|\langle\mathfrak{d}01\rangle|^2D_{AA}[M_0(0-11)-\tfrac{2}{3}qN_0(0-11)+\tfrac{1}{9}q^2L_0(0-11)]+|\langle\gamma_5 00\rangle|^2 \\ D_{AA}L_0(0-11)$$
$$-2D_{AA}\langle\mathfrak{d}01\rangle\langle\gamma_5 00\rangle^*[N_0(0-11)-\tfrac{1}{3}qL_0(0-11)]+\ldots$$
$$+\tfrac{1}{3}D_{SS}|\langle\beta11\rangle|^2[M_0(0-11)-2qN_0(0-11)-q^2L_0(0-11)-2L_1(0-11) \\ +8N_{01}(011)+4qL_{01}(011)]$$
$$+\tfrac{1}{3}D_{TT}|\langle\beta\mathfrak{d}11\rangle|^2[M_0(0-11)-2qN_0(0-11)+\tfrac{1}{2}q^2L_0(0-11)-\tfrac{1}{2}L_1(0-11) \\ -4N_{01}(011)+qL_{01}(011)]$$
$$+\tfrac{2}{3}\langle\beta\mathfrak{d}11\rangle\langle\beta11\rangle^*\{D_{TS}[M_0(0-11)-2qN_0(0-11)+L_1(0-11)+2N_{01}(011) \\ -2qL_{01}(011)]+6\Delta_{TS}N_{01}(010)\}$$
$$+\tfrac{1}{3}D_{TT}|\langle\beta\alpha10\rangle|^2L_0(0-11)+\tfrac{2}{3}D_{TT}\langle\beta\mathfrak{d}11\rangle\langle\beta\alpha10\rangle^*[N_0(0-11)-qL_0(0-11) \\ -2L_{01}(011)]$$
$$+\tfrac{2}{3}\langle\beta11\rangle\langle\beta\alpha10\rangle^*\{D_{ST}[N_0(0-11)-qL_0(0-11)+4L_{01}(011)] \\ +\Delta_{ST}[N_0(0-10)-4L_{01}(010)]\}$$
$$-\tfrac{1}{3}D_{VV}|\langle I11\rangle|^2[M_0(0-11)+2qN_0(0-11)-q^2L_0(0-11)-2L_1(0-11) \\ +8N_{01}(011)-4qL_{01}(011)]$$
$$-\tfrac{1}{3}D_{AA}|\langle\mathfrak{d}11\rangle|^2[M_0(0-11)+2qN_0(0-11)+\tfrac{1}{2}q^2L_0(0-11)-\tfrac{1}{2}L_1(0-11) \\ -4N_{01}(011)-qL_{01}(011)]$$
$$-\tfrac{2}{3}\langle\mathfrak{d}11\rangle\langle I11\rangle^*\{D_{AV}[M_0(0-11)+2qN_0(0-11)+L_1(0-11)+2N_{01}(011) \\ +2qL_{01}(011)]+6\Delta_{AV}N_{01}(010)\}$$

$$-\tfrac{1}{3}D_{VV}|\langle\alpha 10\rangle|^2L_0(0-11)-\tfrac{2}{3}D_{VV}\langle I11\rangle\langle\alpha 10\rangle^*[N_0(0-11)+qL_0(0-11)+4L_{01}(011)]$$
$$-\tfrac{2}{3}\langle\delta 11\rangle\langle\alpha 10\rangle^*\{D_{AV}[N_0(0-11)+qL_0(0-11)-2L_{01}(011)]+\Delta_{AV}[N_0(0-10)+2L_{01}(010)]\}+\ldots$$
$$+D_{TT}|\langle\beta\delta 21\rangle|^2[\tfrac{1}{15}q^2L_2(0-11)+2qL_{01}(011)+\tfrac{3}{5}L_1(0-11)]$$
$$-D_{AA}|\langle\delta 21\rangle|^2[\tfrac{1}{15}q^2L_2(0-11)-2qL_{01}(011)+\tfrac{3}{5}L_1(0-11)]+\ldots$$

$$\begin{aligned}(114)\quad R(22020) = {}& \tfrac{1}{3}[4D_{SS}|\langle\beta 11\rangle|^2-D_{TT}|\langle\beta\delta 11\rangle|^2]qL_{01}(0-10)\\ & -\tfrac{4}{3}\Delta_{TS}\langle\beta\delta 11\rangle\langle\beta 11\rangle^*qL_{01}(0-11)\\ & -\tfrac{1}{3}[4D_{VV}|\langle I11\rangle|^2-D_{AA}|\langle\delta 11\rangle|^2]qL_{01}(0-10)\\ & +\tfrac{4}{3}\Delta_{AV}\langle\delta 11\rangle\langle I11\rangle^*qL_{01}(0-11)+\ldots\\ & -\tfrac{2}{5}[D_{TT}|\langle\beta\delta 21\rangle|^2-D_{AA}|\langle\delta 21\rangle|^2]qL_{01}(0-10).\end{aligned}$$

Formulae (113) and (114) for $R(11010)$ and $R(22020)$ enable one to calculate the electron–neutrino angular correlation for STP or for VA. Note that $R(33030)$ contains no first-forbidden terms and therefore that $P_3(\cos\Theta)$ does not occur in the angular correlation. Formulae for pure interactions, omitting all cross-terms, have been given by Greuling and Meeks (1951); again only the first three terms in the expansion in powers of ρ are retained and $(\alpha Z)^2$ is neglected in comparison with unity. When the zeroth-order approximation is incorporated into (113) and (114), agreement with Greuling and Meeks for at least the dominant term in the coefficient of each power of q is obtained.

The coefficients of the coupling-constant combinations Δ_{XY}, whose presence would reveal the failure of time-reversal invariance, all contain, in the zeroth-order approximation, the "small" factor (αZ). Beta–neutrino angular correlations are not, therefore, a very promising phenomenon for investigating time-reversal invariance.

If time-reversal invariance holds, then the angular correlation for $(0\rightarrow 0$, yes)-transitions reduces in the zeroth-order approximation to a particularly simple form, namely

$$(115)\qquad 1\mp(v/c)\cos\Theta;$$

the negative sign holds for TP, the positive sign for A. Our formula (115) is more generally valid than the similar result of Greuling and Meeks, because we have considered all cross-terms and because we have not neglected terms in $(\alpha Z)^2$.

APPENDIX

The first purpose of the Appendix is to define the various nine-parameter recoupling coefficients used in this paper and to state, without proof, those properties which have been employed in the manipulations leading to the formula (58). The definition of the X-coefficient is that of Fano (1951); its relationship to other definitions is discussed by Smith and Stevenson (1957) in the introduction to their numerical tables. In writing the first part of the Appendix much use has been made of the report of Kennedy *et al.* (1954).

The generalized LS-to-jj transformation coefficient

$$A\begin{pmatrix} l & s & j \\ l' & s' & j' \\ L & S & J \end{pmatrix}$$

is defined by (A1). In the definition, magnetic quantum numbers have not been written in the vector-addition coefficients; an angular-momentum quantum number is to be accompanied by the same magnetic quantum number each time it occurs.

$$(A1) \qquad (ls|j)(l's'|j')(jj'|J) = \sum_{LS} A\begin{pmatrix} l & s & j \\ l' & s' & j' \\ L & S & J \end{pmatrix}(ll'|L)(ss'|S)(LS|J).$$

The nine parameters occurring in the A-coefficient may take any integral or half-integral values consistent with the existence of the vector-addition coefficients.

To discuss the properties of the A-coefficient it is convenient to introduce the closely related but more symmetric X-coefficient.

$$(A2) \quad A\begin{pmatrix} l & s & j \\ l' & s' & j' \\ L & S & J \end{pmatrix} = [(2j+1)(2j'+1)(2L+1)(2S+1)]^{\frac{1}{2}} X\begin{pmatrix} l & s & j \\ l' & s' & j' \\ L & S & J \end{pmatrix}.$$

The X-coefficient can be expressed as a sum of triple products of Racah coefficients.

$$(A3) \quad X\begin{pmatrix} l & s & j \\ l' & s' & j' \\ L & S & J \end{pmatrix} = \sum_{k} (2k+1)W(lsJj', jk)W(l'j'Ss, s'k)W(ll'JS, Lk).$$

This expansion can be used to compute X-coefficients when simpler methods fail. Reflection of the array of parameters in the main diagonal does not change the value of X. Interchange of any two rows or of any two columns multiplies the X by a factor $(-1)^{l+l'+L+j+j'+J+s+s'+S}$. An X-coefficient with a parameter equal to zero may always be evaluated by means of (A4).

$$(A4) \quad X\begin{pmatrix} l & s & j \\ l' & s' & j' \\ L & S & 0 \end{pmatrix} = (-1)^{j+L-l-s'}[(2j+1)(2L+1)]^{-\frac{1}{2}} W(lsl's', jL)\delta_{jj'}\delta_{LS}.$$

When any two parameters in one row or column are equal to $\frac{1}{2}$, the A-coefficient can be calculated from reasonably simple algebraic formulae, (A5); in this case A is equivalent to the ordinary LS-to-jj transformation matrix for particles of spin $\frac{1}{2}$. The formulae (A5), which we derived directly from the definition (A1) by making use of the relative simplicity of the vector-addition coefficients when $M_J = J$, has already appeared in a report by Kennedy and Cliff (1955), who also give tables of values in both fractional and decimal forms; Racah (1950) and Matsunobu and Takebe (1955) have published formulae for closely related coefficients.

(A5) FORMULAE FOR $A\begin{pmatrix} l & \frac{1}{2} & j \\ l' & \frac{1}{2} & j' \\ L & S & J \end{pmatrix}$

	$S=0, L=J$	$S=1, L=J$	$S=1, L=J-1$	$S=1, L=J+1$
$j=l+\frac{1}{2}$ $j'=l'+\frac{1}{2}$	$\sqrt{\frac{(l+l'+2+J)(l+l'+1-J)}{2(2l+1)(2l'+1)}}$	$\frac{(l-l')}{\sqrt{J(J+1)}}\times$ entry for $S=0$	$\sqrt{\frac{(l+l'+2+J)(l+l'+1+J)(l-l'+J)(l'-l+J)}{2(2l+1)(2l'+1)J(2J+1)}}$	$-\sqrt{\frac{(l+l'+1-J)(l+l'-J)(l-l'+1+J)(l'-l+1+J)}{2(2l+1)(2l'+1)(J+1)(2J+1)}}$
$j=l+\frac{1}{2}$ $j'=l'-\frac{1}{2}$	$\sqrt{\frac{(l'-l+J)(l-l'+1+J)}{2(2l+1)(2l'+1)}}$	$\frac{(l+l'+1)}{\sqrt{J(J+1)}}\times$ entry for $S=0$	$-\sqrt{\frac{(l-l'+1+J)(l-l'+J)(l+l'+1+J)(l+l'+1-J)}{2(2l+1)(2l'+1)J(2J+1)}}$	$-\sqrt{\frac{(l+l'+2+J)(l+l'-J)(l'-l+1+J)(l'-l+J)}{2(2l+1)(2l'+1)(J+1)(2J+1)}}$
$j=l-\frac{1}{2}$ $j'=l'+\frac{1}{2}$	$-\sqrt{\frac{(l-l'+J)(l'-l+1+J)}{2(2l+1)(2l'+1)}}$	$-\frac{(l+l'+1)}{\sqrt{J(J+1)}}\times$ entry for $S=0$	$\sqrt{\frac{(l'-l+1+J)(l'-l+J)(l+l'+1+J)(l+l'+1-J)}{2(2l+1)(2l'+1)J(2J+1)}}$	$\sqrt{\frac{(l+l'+2+J)(l+l'-J)(l-l'+1+J)(l-l'+J)}{2(2l+1)(2l'+1)(J+1)(2J+1)}}$
$j=l-\frac{1}{2}$ $j'=l'-\frac{1}{2}$	$\sqrt{\frac{(l+l'+1+J)(l+l'-J)}{2(2l+1)(2l'+1)}}$	$\frac{(l'-l)}{\sqrt{J(J+1)}}\times$ entry for $S=0$	$-\sqrt{\frac{(l-l'+J)(l'-l+J)(l+l'+1-J)(l+l'-J)}{2(2l+1)(2l'+1)J(2J+1)}}$	$\sqrt{\frac{(l+l'+2+J)(l+l'+1+J)(l-l'+1+J)(l'-l+1+J)}{2(2l+1)(2l'+1)(J+1)(2J+1)}}$

The third nine-parameter coefficient used in this paper, A_0, is merely an A modified by multiplication by a collection of miscellaneous factors, the repetition of which would be very tedious in writing formulae like (58).

$$\text{(A6)}\quad A_0\begin{pmatrix} l & \frac{1}{2} & j \\ l' & \frac{1}{2} & j' \\ L & S & J \end{pmatrix} = [(2l+1)(2l'+1)(2L+1)^{-1}]^{\frac{1}{2}}(ll'00|L0) \times A\begin{pmatrix} l & \frac{1}{2} & j \\ l' & \frac{1}{2} & j' \\ L & S & J \end{pmatrix} G_{l'}(q\rho).$$

Here, of course, l and l' are integers. The presence of the special vector-addition coefficient ensures that A_0 vanishes if $l+l'+L$ is odd. Except when examining spectra which have been measured with the highest precision, it suffices to retain only the first term in the MacLaurin series for the spherical Bessel function contained in the definition of $G_{l'}(q\rho)$; thus

$$\text{(A7)}\quad G_{l'}(q\rho) \equiv (q\rho)^{-l'} j_{l'}(q\rho) \doteq [(2l'+1)!!]^{-1} = [1 \times 3 \times 5 \ldots (2l'+1)]^{-1}.$$

Values of A_0 can therefore be computed using (A7), (A5), and the well-known formula for the special vector-addition coefficient appearing in (A6) (e.g. Rose 1957, page 47). Except when small corrections of order of forbiddenness higher than the dominant order are being considered, it happens, as was seen in Section 2, that $l+l'$ is equal to L. In this case a small amount of simplification, which we shall not give, is possible in the formulae (A5); note, however, that the simplified formulae printed by Banerjee and Saha (1954) contain misprints in

$$A\begin{pmatrix} l & \frac{1}{2} & l+\frac{1}{2} \\ l' & \frac{1}{2} & l'+\frac{1}{2} \\ L & 1 & L \end{pmatrix} \quad \text{and} \quad A\begin{pmatrix} l & \frac{1}{2} & l+\frac{1}{2} \\ l' & \frac{1}{2} & l'+\frac{1}{2} \\ L & 1 & L-1 \end{pmatrix}.$$

A result valid for $l+l' = L$ and useful in discussing the U class transitions is

$$A\begin{pmatrix} l & \frac{1}{2} & j \\ l' & \frac{1}{2} & j' \\ L & 1 & L+1 \end{pmatrix} = 1$$

when $j = l+\frac{1}{2}$ and $j' = l'+\frac{1}{2}$, $= 0$ otherwise. Also for $l+l' = L$ we find

$$\text{(A8)}\qquad (ll'00|L0) = L![l!l'!]^{-1}\{(2l)!(2l')![(2L)!]^{-1}\}^{\frac{1}{2}}.$$

Next we shall derive an identity between vector-addition coefficients and a special class of X-coefficients. From the definitions (A1) and (A2) we find

$$\text{(A9)}\quad (\tfrac{1}{2}\,\tfrac{1}{2}\,\rho\,\sigma|t\,\rho+\sigma)(j\,j'\,-\rho\,-\sigma|k'-\rho-\sigma)(t\,k\,\rho+\sigma\,-\rho-\sigma|g\,0) = \sum_{ll'} [(2t+1)(2k'+1)(2l+1)(2l'+1)]^{\frac{1}{2}} X\begin{pmatrix} \frac{1}{2} & \frac{1}{2} & t \\ j & j' & k' \\ l & l' & g \end{pmatrix} \times (\tfrac{1}{2}\,j\,\rho\,-\rho|l\,0)(\tfrac{1}{2}\,j'\,\sigma\,-\sigma|l'\,0)(ll'00|g\,0).$$

Multiply both sides of (A9) by $(\frac{1}{2}\, j\, \rho\, -\rho|l\, 0)(\frac{1}{2}\, j'\, \sigma\, -\sigma|l'\, 0)$ and sum over ρ and σ. Then the use of the relation

$$(\text{A10}) \qquad (\tfrac{1}{2}\, j\, \tfrac{1}{2}\, -\tfrac{1}{2}|l\, 0) = 2^{-\frac{1}{2}} \quad \text{for } l = j \pm \tfrac{1}{2},$$

the correctness of which is made evident by inspection of the algebraic formulae for vector-addition coefficients, permits us to transform (A9) into (A11).

$$\begin{aligned}(\text{A11}) \quad & [(2t+1)(2k'+1)(2l+1)(2l'+1)]^{\frac{1}{2}}(ll'00|g0)\, X\begin{pmatrix} \frac{1}{2} & j & l \\ \frac{1}{2} & j' & l' \\ t & k' & g \end{pmatrix} \\ & = \tfrac{1}{2}(-1)^{j+j'-k'}[1+(-1)^{l+l'+g}] \\ & \times\{2^{-\frac{1}{2}}(-1)^{j'+\frac{1}{2}-l'}(jj'\tfrac{1}{2}-\tfrac{1}{2}|k'0)(tk'00|g0) \\ & +\delta_{t1}(jj'\tfrac{1}{2}\tfrac{1}{2}|k'1)(1\, k'\, 1\, -1|g\, 0)\}.\end{aligned}$$

Now from a recurrence relation for vector-addition coefficients given by Condon and Shortley (1935, page 74) it follows that

$$\begin{aligned}(\text{A12}) \quad & (jj'\tfrac{1}{2}\tfrac{1}{2}|k'1) = \\ & [k'(k'+1)]^{-\frac{1}{2}}[(j'+\tfrac{1}{2})+(-1)^{j+j'+k'}(j+\tfrac{1}{2})](j\, j'\, \tfrac{1}{2}\, -\tfrac{1}{2}|k'\, 0).\end{aligned}$$

Using (A12) one can rewrite (A11) in the form

$$\begin{aligned}(\text{A13}) \quad & [(2l+1)(2l'+1)]^{\frac{1}{2}}(ll'00|g0)\, X\begin{pmatrix} j & \frac{1}{2} & l \\ j' & \frac{1}{2} & l' \\ k' & t & g \end{pmatrix} = \\ & (-1)^t 2^{-3/2}[(2t+1)(2k'+1)]^{-\frac{1}{2}}[1+(-1)^{l+l'+g}](j\, j'\, \tfrac{1}{2}\, -\tfrac{1}{2}|k'\, 0) \\ & [(-1)^{j'-\frac{1}{2}+l'}(tk'00|g0)-\delta_{t1}\Delta_{j'-\frac{1}{2},j-\frac{1}{2}}(k', g)].\end{aligned}$$

$$\begin{aligned}(\text{A14}) \quad & \Delta_{j'-\frac{1}{2},j-\frac{1}{2}}(k', g) = \\ & 2^{\frac{1}{2}}[k'(k'+1)]^{-\frac{1}{2}}(1k'1-1|g0)[(j'+\tfrac{1}{2})+(-1)^{j+j'-k'}(j+\tfrac{1}{2})].\end{aligned}$$

Of course $\Delta_{j'-\frac{1}{2},j-\frac{1}{2}}(0, g) = 0$. The equation (46) used in Section 3 is equivalent to (A13). By putting $t = 0$ in (A13) one obtains

$$\begin{aligned}(\text{A15}) \quad & [(2l+1)(2l'+1)]^{\frac{1}{2}}(ll'00|g0)W(ljl'j', \tfrac{1}{2}g) = \\ & \tfrac{1}{2}[1+(-1)^{g+l+l'}](j\, j'\, \tfrac{1}{2}\, -\tfrac{1}{2}|g\, 0),\end{aligned}$$

of which relation (25) of Section 2 is a special case. Note also that (A15) is equivalent to

$$(\text{A16}) \quad Z(ljl'j', \tfrac{1}{2}g) = i^{g-l+l'}[(2j+1)(2j'+1)]^{\frac{1}{2}}(j\, j'\, \tfrac{1}{2}\, -\tfrac{1}{2}|g\, 0),$$

valid for even values of $l+l'+g$. The Z-coefficient in (A16) is that discussed by Biedenharn *et al.* (1952); relation (A16) may be used to calculate $(jj'\frac{1}{2}-\frac{1}{2}|g0)$ from the tables of Z.

REFERENCES

ALDER, K., STECH, B., and WINTHER, A. 1957. Phys. Rev. **107**, 723.
BANERJEE, M. K. and SAHA, A. K. 1954. Proc. Roy. Soc. A**224**, 472.
BERESTETSKY, V. B., IOFFE, B. L., RUDIK, A. P., and TER-MARTIROSYAN, K. A. 1958. Nuclear Phys. **5**, 464.
BETHE, H. A. 1930. Ann. Physik, **4**, 443.
——— 1948. Z. Naturforsch. **3a**, 470.
BIEDENHARN, L. C., BLATT, J. M., and ROSE, M. E. 1952. Revs. Modern Phys. **24**, 249.
BLATT, J. M. and WEISSKOPF, V. F. 1952. Theoretical nuclear physics (John Wiley & Sons, Inc., New York).
CONDON, E. U. and SHORTLEY, G. H. 1953. Theory of atomic spectra (Cambridge University Press, London).
CURTIS, R. B. and LEWIS, R. R. 1957. Phys. Rev. **107**, 543.
DE-SHALIT, A. 1953. Phys. Rev. **91**, 1479.
DOLGINOV, A. Z. 1958. Nuclear Phys. **5**, 512.
FANO, U. 1951. Nat. Bureau of Standards Report No. 1214.
——— 1952. Nat. Bureau of Standards Report, Applied Math. Ser. 13.
FERMI, E. 1934. Z. Physik, **88**, 161.
GOLDHABER, M., GRODZINS, L., and SUNYAR, A. W. 1958. Phys. Rev. **109**, 1015.
GREULING, E. 1942. Phys. Rev. **61**, 568.
GREULING, E. and MEEKS, M. L. 1951. Phys. Rev. **82**, 531.
HAMILTON, D. R. 1947. Phys. Rev. **71**, 456.
HERRMANNSFELDT, W. B., MAXSON, D. R., STÄHELIN, P., and ALLEN, J. S. 1957. Phys. Rev. **107**, 641.
JACKSON, J. D., TREIMAN, S. B., and WYLD, H. W. 1957. Nuclear Phys. **4**, 206.
JAHNKE, E. and EMDE, F. 1945. Tables of functions (Dover Publications, New York).
KENNEDY, J. M., SEARS, B. J., and SHARP, W. T. 1954. Atomic Energy of Canada Limited Report, CRT-569.
KENNEDY, J. M. and CLIFF, M. J. 1955. Atomic Energy of Canada Limited Report, CRT-609.
KONOPINSKI, E. J. and UHLENBECK, G. E. 1941. Phys. Rev. **60**, 308.
LEE, T. D. and YANG, C. N. 1956. Phys. Rev. **104**, 254.
——— 1957. Phys. Rev. **105**, 1671.
LEE-WHITING, G. E. 1958. Can. J. Phys. **36**, 252.
LONGMIRE, C. L. and MESSIAH, A. M. L. 1951. Phys. Rev. **83**, 464.
LÜDERS, G. 1958. Nuovo Cimento, **7**, 171.
MATSUNOBU, H. and TAKEBE, H. 1955. Progr. Theoret. Phys. **14**, 589.
MORITA, M. 1953. Progr. Theoret. Phys. **10**, 364.
MORITA, M. and MORITA, R. S. 1957. Phys. Rev. **107**, 1316.
PAULI, W. 1936. Ann. inst. Henri Poincaré **6**, 109.
——— 1957. Nuovo Cimento, **6**, 204.
PURSEY, D. L. 1951. Phil. Mag. **42**, 1193.
RACAH, G. 1950. Physica, **16**, 651.
ROSE, M. E. 1937. Phys. Rev. **51**, 484.
ROSE, M. E., PERRY, C. L., and DISMUKE, N. M. 1953. Oak Ridge National Laboratory Report, ORNL-1459.
ROSE, M. E. 1955. Multipole fields (John Wiley & Sons, Inc., New York).
——— 1957. Elementary theory of angular momentum (John Wiley & Sons, Inc., New York).
SCHIFF, L. I. 1955. Quantum mechanics (McGraw-Hill Book Company Inc., New York).
SHARP, W. T., KENNEDY, J. M., SEARS, B. J., and HOYLE, M. G. 1953. Atomic Energy of Canada Limited Report, CRT-556.
SHARP, W. T. 1957. Atomic Energy of Canada Limited Report, CRL-43.
SIEGBAHN, K. 1955. Beta- and gamma-ray spectroscopy (North-Holland Pub. Co., Amsterdam).
SLIV, L. A. and VOLCHOK, B. A. 1956. Tables of coulomb phases etc., Publication of the Academy of Sciences, U.S.S.R., Moscow. A translation has been made by R. V. Jermain for the United States Atomic Energy Comm., as AEC-tr-2875.
SMITH, A. M. 1951. Phys. Rev. **82**, 955.
SMITH, K. and STEVENSON, J. W. 1957. Argonne National Laboratory Report, ANL-5776.
SPIERS, J. A. and BLIN-STOYLE, R. J. 1952*a*. Proc. Phys. Soc. A, **65**, 891.
——— 1952*b*. Proc. Phys. Soc. A, **65**, 809.
TOLHOEK, H. A. 1956. Revs. Modern Phys. **28**, 277.
WU, C. S., AMBLER, E., HAYWARD, R. W., HOPPES, D. D., and HUDSON, R. P. 1957. Phys. Rev. **105**, 1413.
ZWEIFEL, P. F. 1954. Phys. Rev. **95**, 112.

THE EFFECT OF ELONGATION ON THE ELECTRICAL RESISTIVITY OF POLYCRYSTALLINE ZINC

H. R. PEIFFER*

In recent years there have been many investigations of the changes in electrical resistivity introduced upon cold-working face-centered cubic metals (Broom 1954). These changes have been correlated to changes in the defect structures of the material. Very recently experiments have been performed on a body-centered cubic metal such as molybdenum (Martin 1957; Peiffer 1958). A further experiment concerning these changes in a hexagonal metal such as zinc would be most interesting. The research described in this note is concerned with changes in the electrical resistivity of zinc produced by tensile elongations.

The zinc used in these experiments was 99.999% pure. The specimens were first annealed at 150° C for 1 hour and then were elongated at room temperature up to approximately nine per cent. The specimens were transferred

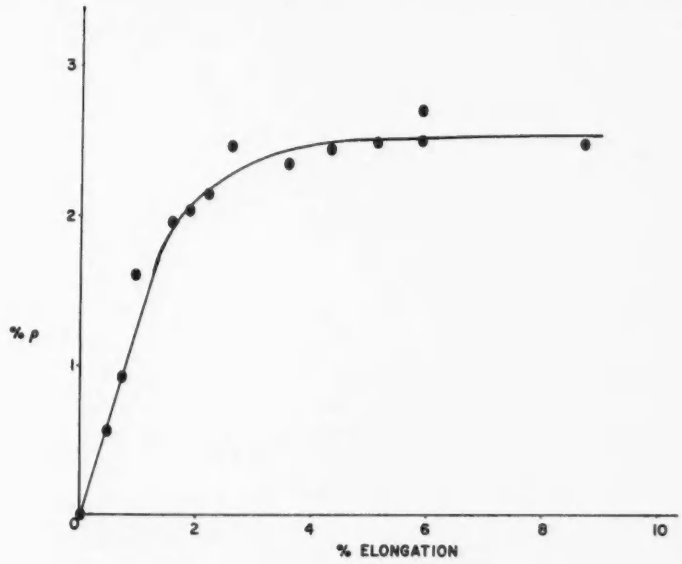

FIG. 1.

*Work performed at RIAS Inc., 7212 Bellona Ave., Baltimore 12, Md.

immediately after elongation to a Dewar flask containing liquid nitrogen. The resistivity of the zinc was measured in this container by means of an L & N Precision Kelvin Double Bridge. The specimens were periodically warmed to room temperature and were allowed to remain at this temperature for long periods. They were then again immersed in liquid nitrogen and the resistivity was subsequently measured to determine whether any recovery had occurred. None was observed even after the zinc was held at room temperature a few days.

The resistivity increase as a function of strain is shown in Fig. 1. The rate of change of the resistivity with elongation decreases as the elongation increases. Furthermore, the total resistivity increase anneals out in the region of 90° C to 120° C, which is around the temperature range of recrystallization for zinc. It appears, then, that the total increase in the resistivity is caused by dislocations.

Since no recovery of the resistivity is noted at room temperature, one is led to believe that few or no point defects are formed. However, there is a likely possibility that the point defects are formed and diffuse so very rapidly that their contribution disappears before the specimen is immersed in liquid nitrogen.

1. Broom, T. 1954. Advances in Physics, **3**, 9.
2. Martin, D. G. 1957. Acta Met. **5**, 371.
3. Peiffer, H. R. 1958. J. Appl. Phys. In press.

Received June 4, 1958.

LETTERS TO THE EDITOR

Under this heading brief reports of important discoveries in physics may be published. These reports should not exceed 600 words and, for any issue, should be submitted not later than six weeks previous to the first day of the month of issue. No proof will be sent to the authors.

Decay of Heavy Hyperfragment

The study of heavier hyperfragments can give very useful results regarding the interaction of the Λ^0 particle with different nuclei. Looking through the literature one finds hardly any report on hyperfragments heavier than Be. The reason is that the study of such events is difficult because the decay mode for elements heavier than helium is predominantly non-mesonic, which leads to a high nuclear excitation. From such a disintegration, emission of more than one neutron is quite common, which does not help to analyze the event completely. But even an incomplete analysis of such events can help in the understanding of the interaction of the Λ^0 hyperon with nuclear matter by providing information about the stimulated decay processes of the Λ^0 hyperon in different nuclei, about which we know very little at the present time.

We are presenting here a partial analysis of an event which is interpreted as a non-mesonic decay of either a boron or carbon hyperfragment. This event was observed during the normal scanning of G-5 6-in.×4-in. stripped emulsions of 400 μ thickness which were exposed near Guam (Marian Island 6° N. geomagnetic latitude) at an altitude of 102,000 ft.

A slow, unstable, and heavily ionizing nuclear fragment (Track 1) is ejected from a primary star A, of type $7+0n$, comes to rest and disintegrates, producing a secondary star B with four prongs which are not coplanar. (The projection drawing of the event is shown in Fig. 1.) In the primary star two prongs were due to doubly charged particles and the rest were due to singly charged particles. All these tracks were followed to the end of their range or until they left the stack. No evidence for the coproduction of a heavy meson or hyperon was found.

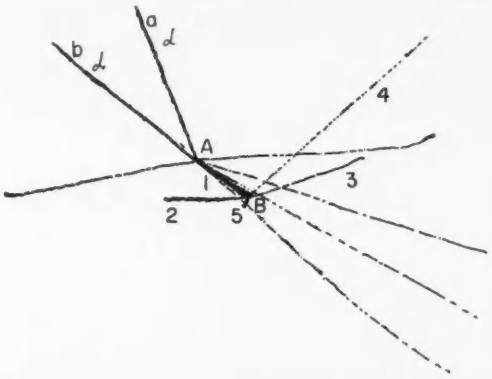

FIG. 1. A nuclear fragment 1 from a primary star A stops in emulsion and produces a secondary star B which has four prongs. Both tracks 3 and 4 were produced by a proton, and track 5 by a proton or an He nucleus. Track 2 was produced by an alpha particle.

Data relating to the secondary star are given in Table I. Tracks 2 and 3, when compared with other similar tracks in the emulsion, appear to be due to doubly and singly charged particles, respectively. Both of them stop in the emulsion and on account of their short length no direct measurement can be made for mass determination. The mean width of track 2 is about 0.76 μ and this agrees fairly well with 0.75 μ obtained from the width of number of alpha particle tracks from thorium stars contained in the emulsion, which confirms that the charge of particle 2 is two. Track 4 is steep and leaves the stack after traveling a total distance of 550 μ in two plates. It appears to arise from a singly charged particle. The delta-ray count on this

TABLE I

MEASUREMENT ON BORON OR CARBON HYPERFRAGMENT

Track	Identity	Range, μ	Energy, Mev	Momentum, Mev/c
a	α	805		
b	α	202		
1	^{5}B or ^{6}C	18.5		
2	^{3}He or ^{4}He	15.4	4.0 (^{4}He)	172.7
3	p,d,t	21.9	1.3 (p)	49.89
4	p*		98.0	439.81
5	p, α	3.5	0.35 (p)	25.6 (p)
			1.0 (α)	86.4 (α)

*Energy was calculated from ionization density.

track was 0.42 delta rays per 100 μ, which indicates that the particle may be a proton. Its ionization density was 3.8 times minimum so its energy calculated from ionization density is 98 Mev. Since these tracks are not coplanar, the identity of the short track 5 cannot be inferred from momentum imbalance. The general appearance of this track indicates a charge of one or two.

Since the secondary star has four nuclear tracks, one of which is due to charge two and none of which is due to a negative meson, the total charge of the second star must be at least five. So charge conservation requires that the primary track 1 may be due to a hyperfragment of an isotope of boron or carbon, depending upon whether the recoil track 5 is due to a singly charged or a doubly charged particle.

In order to conserve momentum, one or more neutrons may also be emitted, so that the visible energy released from the secondary star is greater than 104 Mev. The energy released from non-mesonic decay of Λ^0 hyperon is 175 Mev while for mesonic decay it is 37 Mev. As the energy released in the present event (neglecting even the energy taken up by neutrons) is much greater than 37 Mev, we consider the present decay of the hyperfragment as non-mesonic; the large energy of the proton track 4 indicates that the initial stimulation of the Λ^0 hyperon was caused by a proton. Unfortunately the shortness of the track 4 puts limitation on its identification. One cannot rule out the alternative possibility of track 4 being a π-meson. In that case its energy calculated from ionization density is about 16 Mev. Thus an alternative interpretation of the event is that it may be due to mesonic decay of Li or Be hyperfragment. The total energy released in the latter case is about 22 Mev. The non-coplanarity of four tracks indicates that one or more neutrons are still involved in the mesonic decay of Li or Be hyperfragment. As we do not know, in either case, the energy of the neutron, we can only put a lower limit on Q and so it is not possible to say anything about the binding energy of the particle.

We would like to thank Drs. K. E. Davis, N. M. Duller, and C. A. Randall for sharing with us their plates which were exposed near Guam. We would also like to thank Professor Marcel Schein for our stimulating introduction to this field in his laboratory during the summer 1956.

RECEIVED MAY 27, 1958.
PHYSICS DEPARTMENT,
UNIVERSITY OF BUFFALO,
BUFFALO, NEW YORK.

P. L. JAIN

The Influence of the Martensitic Transformation on the Electrical Resistance of Sodium*

Although Barrett (1948, 1955, 1956) has reported the discovery of a martensitic transformation in sodium, there has hitherto been no direct evidence of the effects of this transformation on the transport properties of sodium. Recent experiments in this laboratory have shown that the martensitic transformation can influence many of the thermodynamic,† mechanical,‡ and electrical properties of sodium and lithium. Consequently a more careful study of the low-temperature electrical resistance of sodium was made and some results of this study are reported here.

*Issued as N.R.C. No. 4855.
†See Martin (1958).
‡L. Verdini (private communication).

The electrical resistance of three specimens of very pure sodium was measured between about 100° K and 4° K as a function of both decreasing and increasing temperature. Two of the specimens (Nos. 1 and 3) were bare sodium wires about 1 meter in length and about 0.5 mm in diameter. The third specimen (No. 2) consisted of a glass capillary tube about 40 cm long and about 0.2 mm diameter§ filled with sodium. The residual resistance ratios ($R_{4\cdot2}/R_{273}$) of the three specimens were as follows: No. 1, 4×10^{-4}; No. 2, 2×10^{-4}; and No. 3, 3×10^{-4}.

The phase of sodium stable at high temperature is body-centered cubic and, according to Barrett, no spontaneous change to the low-temperature hexagonal close-packed phase occurs until the specimen is cooled to 36° K. By 4° K, about 5% of the specimen may transform spontaneously to the h.c.p. phase, the exact amount depending on the purity, grain size, and surface condition of the specimen. On the warming up of the specimen, spontaneous reconversion should begin at about 45° K and be complete in the temperature region between 80° and 110° K, according to the state of the specimen. By temperature-cycling each specimen and measuring its resistance at a suitable fixed temperature (40° K) we were able to show that all the specimens began to transform and to revert at approximately these temperatures. We had no method of determining the actual fraction transformed at any temperature but by assuming that the measured resistance at 40° K was linearly related to the proportion of each phase present we could estimate the approximate relative amounts transformed. A transformation curve obtained in this way is shown for specimen No. 3 in Fig. 1. The excellent definition of this curve suggests that this would be a useful method of investigating other properties of the martensitic transition in sodium.

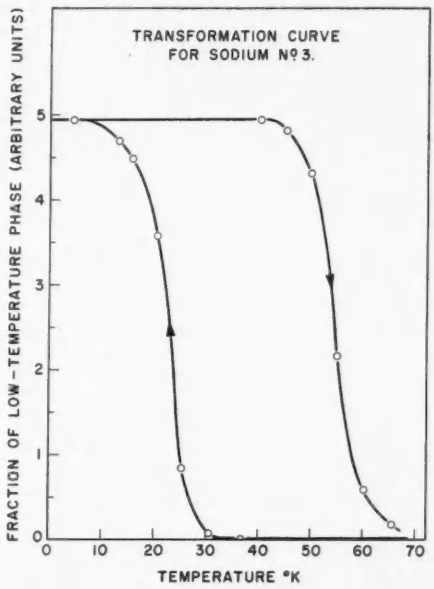

FIG. 1. The transformation curve for sodium specimen No. 3.

The measurements showed that at a given temperature conversion to the low-temperature phase *reduced* the resistance of the specimen. The maximum reduction amounted to about 11%; this was found in specimen 1 and occurred at about 28° K. The capillary specimen, No. 2, showed the least change, the maximum reduction being approximately 5%, which also occurred at about 28° K. The percentage difference between the resistance of specimen No. 3 measured with decreasing and increasing temperatures is shown as a function of the temperature in Fig. 2. The specimen was annealed at 170° K between the two runs shown in the figure; the tail at the high temperature end of the diagram appeared to extend up to about 120° K.

§We are grateful to Dr. S. B. Woods for the loan of this specimen.

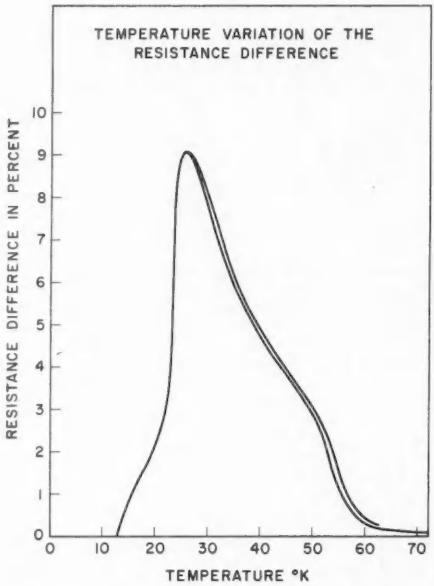

FIG. 2. The percentage difference between the resistance of specimen No. 3 measured with decreasing and increasing temperatures plotted as a function of the temperature.

We draw the following conclusions from the results.

Firstly, the fact that the transition is *not* inhibited in specimens cast in glass capillary tubes suggests that many of the existing measurements of the transport properties of sodium at low temperatures should be used with caution in any comparison with theoretical predictions.

Secondly, if we accept, following Barrett, that the maximum spontaneous conversion to the h.c.p. phase even at the lowest temperature is only about 5%, then the resistivity of this phase at 28° K must be at least three times smaller than that of the b.c.c. phase at the same temperature. Indeed, a rough estimate of the temperature dependence of the resistance of the h.c.p. phase in the range from 25 to 60° K can be made from these results, and it appears that this can be approximately represented by a Bloch-Grüneisen function with a characteristic temperature $\theta_R \sim 280°$ K as compared with $\theta_R \sim 200°$ K for the b.c.c. phase.

We hope to test this conclusion further by measuring the resistance of specimens whose composition is more completely changed by suitable straining.

BARRETT, C. S. 1948. Am. Mineralogist, **33**, 749.
——— 1955. J. Inst. Metals, **84**, 43.
——— 1956. Acta Cryst. **9**, 671.
MARTIN, D. L. 1958. Phys. Rev. Letters, **1**, 4.

RECEIVED JUNE 27, 1958.
DIVISION OF PURE PHYSICS,
NATIONAL RESEARCH COUNCIL,
OTTAWA, CANADA.

D. GUGAN*
J. S. DUGDALE

*National Research Council Postdoctorate Fellow.

Spontaneous Magnetization of a Thin Film Measured by Electron Diffraction

An electron beam is deflected by a magnetic field (the Lorentz effect). This effect is observable in a diffraction pattern obtained from a ferromagnetic substance. In this letter, we describe how the spontaneous magnetization of a thin film of nickel and nickel oxide was estimated by means of electron diffraction. A thin crystalline film of thickness 50–500 Å can give a distinct interference diagram; this is convenient for magnetic analysis. Magnetic analysis of a thin film is usually carried out by means of the Faraday effect (Daniels and Wesemeyer 1958).

A double-exposure technique was used to measure the deflection of the incident beam by a magnetic field. The diffraction pattern of a non-ferromagnetic film was first photographed, then that of the ferromagnetic specimen was photographed on the same film. It was noticed that the two diffraction patterns were not concentric, on account of the Lorentz effect.

A thin film of nickel was prepared by vacuum evaporation and then was heated in air at 250° C for 10 hours. This film was used for the diffraction experiment. Figures 1 and 2 are double exposures of this film and of a gold foil. In each case the incident beam was almost perpendicular to the film. In Fig. 1 the incident beam grazed the boundary of the film; in Fig. 2 it penetrated the center of the film. We notice that in Fig. 1 the rings from the specimen and the gold are eccentric, while in Fig. 2 they are concentric. In both figures we can detect only nickel oxide (NiO, NaCl type lattice, lattice constant 4.17 Å). No diffraction pattern from nickel is visible. Since pure nickel oxide is not ferromagnetic, the observed Lorentz effect means that the specimen contains amorphous nickel.

From Fig. 1 we can estimate the spontaneous magnetization H of the film. We have an equation

$$H = (h/elL\lambda)\Delta Z,$$

where e = electron charge (1.6×10^{-20} e.m.u.), L = camera length (495 mm), λ = the wavelength of the electrons (0.0304 Å), h = Planck's constant (6.6×10^{-27} erg-sec), ΔZ = the deflection of the incident beam measurable from the ring eccentricity found in Fig. 1 (0.18 mm), and l = the effective range of the magnetic field (about 0.1 mm). Therefore, we obtain $H \simeq 50$ gauss.

DANIELS, J. M. and WESEMEYER, H. 1958. Can. J. Phys. **36**, 405.

RECEIVED MAY 20, 1958.
INSTITUTE OF PHYSICAL AND CHEMICAL RESEARCH,
31 KAMIFUJI (HONGO),
TOKYO, JAPAN.

S. YAMAGUCHI

Can. J. Phys. Vol. 36 (1958)

NOTE: Figures 1 and 2 follow.

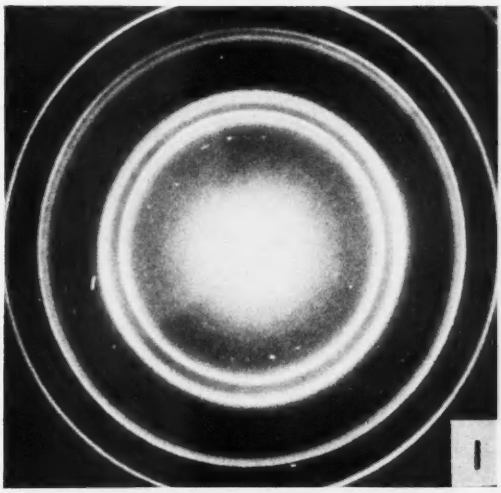

FIG. 1. Diffraction pattern of a NiO–Ni film and that of gold are superposed. Incident beam grazed the boundary of the film. There is recognizable the ring eccentricity as the result of magnetic effect. Wavelength, 0.0304 Å. Camera length, 495 mm. Positive enlarged 3.3 times.

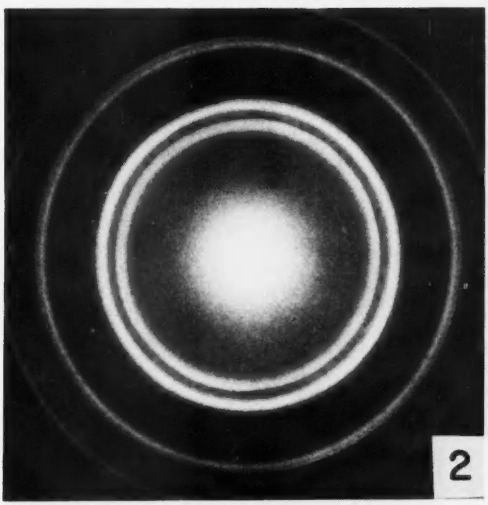

FIG. 2. Incident beam passed through the center of the film. Magnetic effect is quite faint.

CANADIAN JOURNAL OF PHYSICS

Notes to Contributors

Manuscripts

(i) General. Manuscripts, in English or French, should be typewritten, double spaced, on paper 8½×11 in. **The original and one copy are to be submitted.** Tables and captions for the figures should be placed at the end of the manuscript. Every sheet of the manuscript should be numbered.

Style, arrangement, spelling, and abbreviations should conform to the usage of recent numbers of this journal. Names of all simple compounds, rather than their formulas, should be used in the text. Greek letters or unusual signs should be written plainly or explained by marginal notes. Superscripts and subscripts must be legible and carefully placed.

Manuscripts and illustrations should be carefully checked before they are submitted. Authors will be charged for unnecessary deviations from the usual format and for changes made in the proof that are considered excessive or unnecessary.

(ii) Abstract. An abstract of not more than about 200 words, indicating the scope of the work and the principal findings, is required, except in Notes.

(iii) References. References should be listed **alphabetically by authors' names,** unnumbered, and typed after the text. The form of the citations should be that used in current issues of this journal; in references to papers in periodicals, titles should not be given and only initial page numbers are required. The names of periodicals should be abbreviated in the form given in the most recent *List of Periodicals Abstracted by Chemical Abstracts.* All citations should be checked with the original articles and each one referred to in the text by the authors' names and the year.

(iv) Tables. Tables should be numbered in roman numerals and each table referred to in the text. Titles should always be given but should be brief; column headings should be brief and descriptive matter in the tables confined to a minimum. Vertical rules should not be used. Numerous small tables should be avoided.

Illustrations

(i) General. All figures (including each figure of the plates) should be numbered consecutively from 1 up, in arabic numerals, and each figure referred to in the text. The author's name, title of the paper, and figure number should be written in the lower left corner of the sheets on which the illustrations appear. Captions should not be written on the illustrations (see Manuscripts (i)).

(ii) Line Drawings. Drawings should be carefully made with India ink on white drawing paper, blue tracing linen, or co-ordinate paper ruled in blue only; any co-ordinate lines that are to appear in the reproduction should be ruled in black ink. Paper ruled in green, yellow, or red should not be used. All lines should be of sufficient thickness to reproduce well. Decimal points, periods, and stippled dots should be solid black circles large enough to be reduced if necessary. Letters and numerals should be neatly made, preferably with a stencil (**do NOT use typewriting**) and be of such size that the smallest lettering will be not less than 1 mm high when reproduced in a cut 3 in wide.

Many drawings are made too large; originals should not be more than 2 or 3 times the size of the desired reproduction. Whenever possible two or more drawings should be grouped to reduce the number of cuts required. In such groups of drawings, or in large drawings, full use of the space available should be made; the ratio of height to width should conform to that of a journal page (4¾×7½ in), but allowance must be made for the captions.

The original drawings and one set of clear copies (e.g. small photographs) are to be submitted.

(iii) Photographs. Prints should be made on glossy paper, with strong contrasts. They should be trimmed so that essential features only are shown and mounted carefully, with rubber cement, on white cardboard, with no space between them. In mounting, full use of the space available should be made to reduce the number of cuts required (see Illustrations (ii)). Photographs or groups of photographs should not be more than 2 or 3 times the size of the desired reproduction.

Photographs are to be submitted in duplicate; if they are to be reproduced in groups one set should be mounted, the duplicate set unmounted.

Reprints

A total of 50 reprints of each paper, without covers, are supplied free. Additional reprints, with or without covers, may be purchased at the time of publication.

Charges for reprints are based on the number of printed pages, which may be calculated approximately by multiplying by 0.6 the number of manuscript pages (double-spaced typewritten sheets, 8½×11 in) and including the space occupied by illustrations. An additional charge is made for illustrations that appear as coated inserts. Prices and instructions for ordinary reprints are sent out with the galley proof.

Any reprints required in addition to those requested on the author's reprint requisition form must be ordered officially as soon as the paper has been accepted for publication.

Contents

Printed in Canada *by* University of Toronto Press